



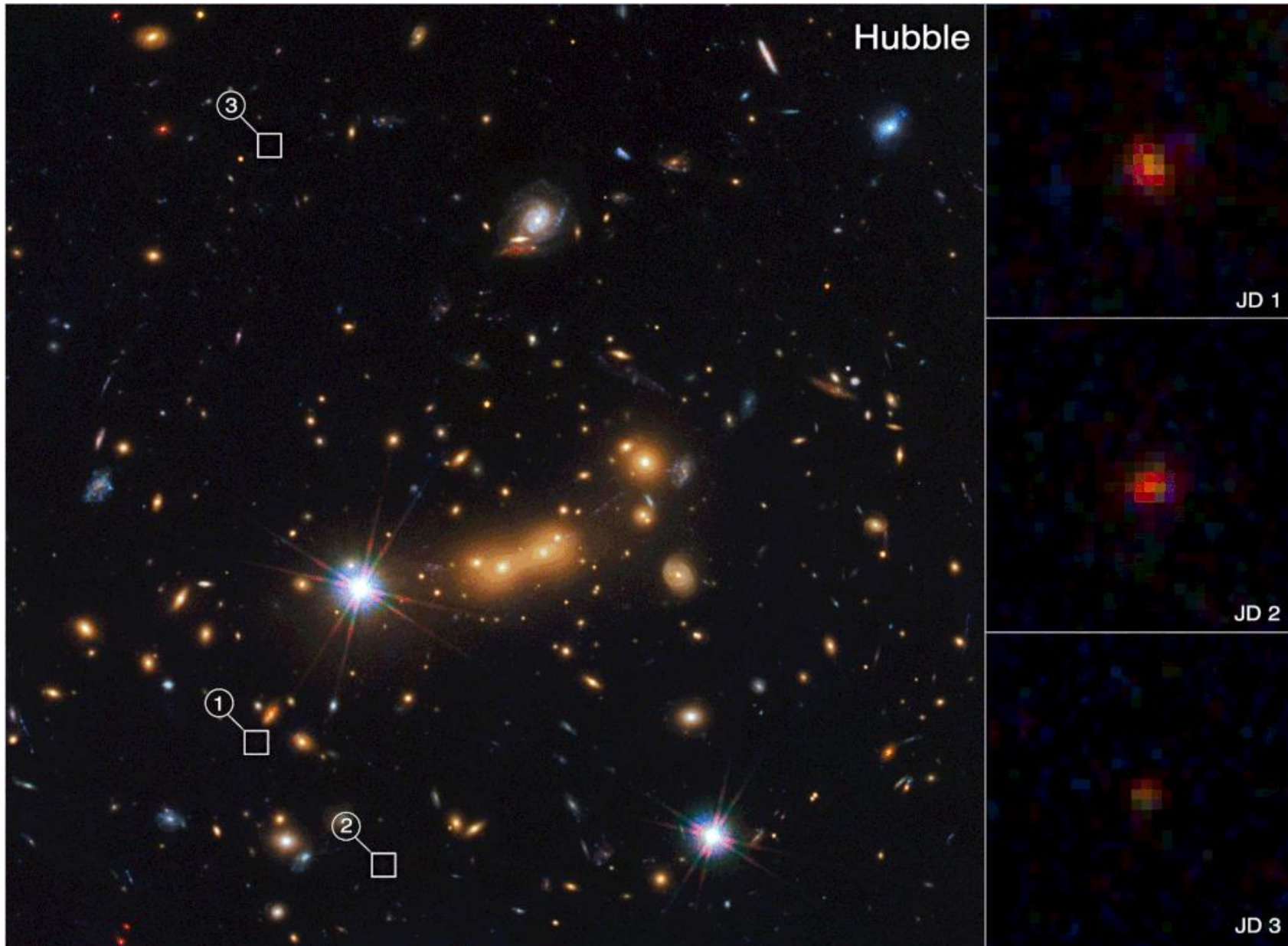
# Gravitational Lensing and dark matter characterization

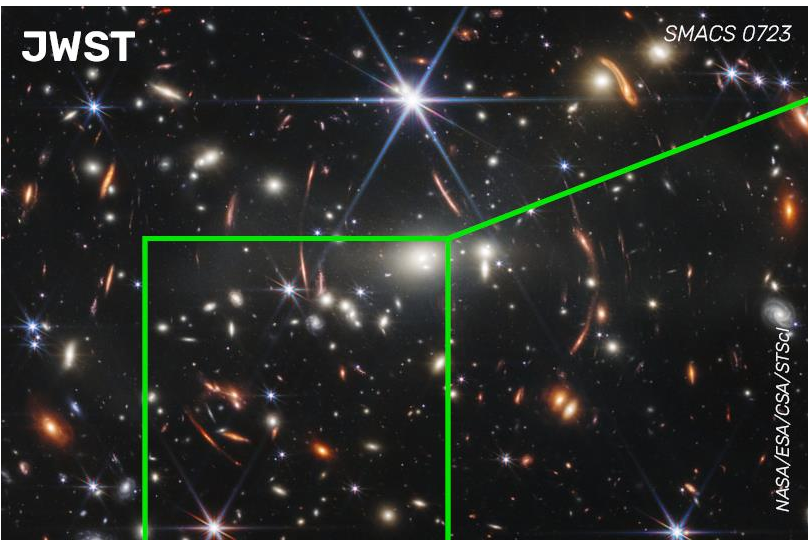
Eric Jullo

Aix-Marseille Université / Laboratoire d'Astrophysique de Marseille



# James Webb Space Telescope (JWST) vs Hubble



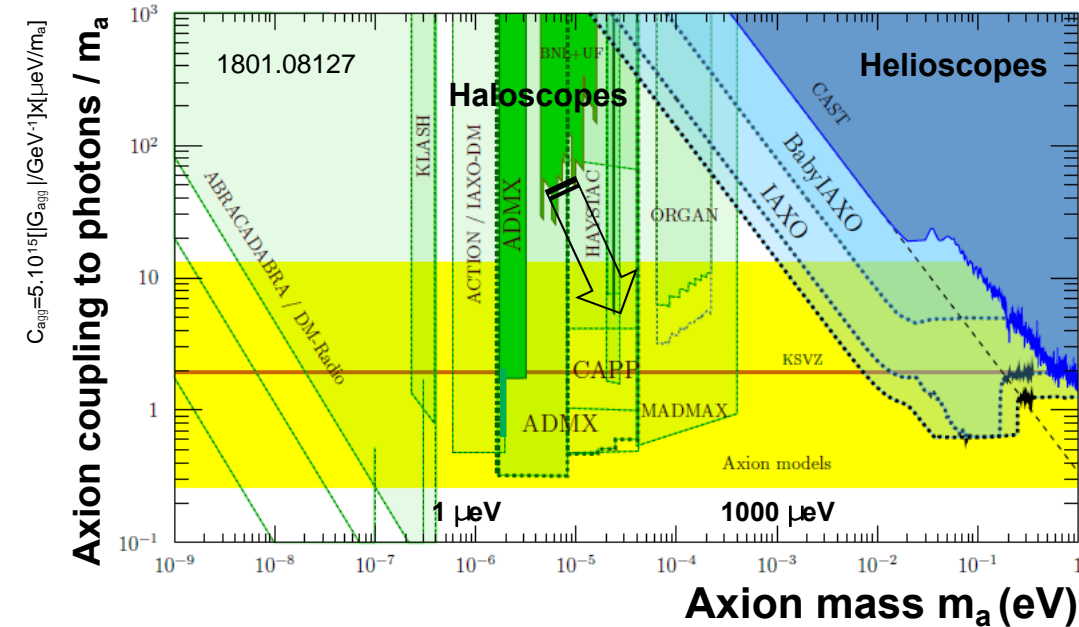
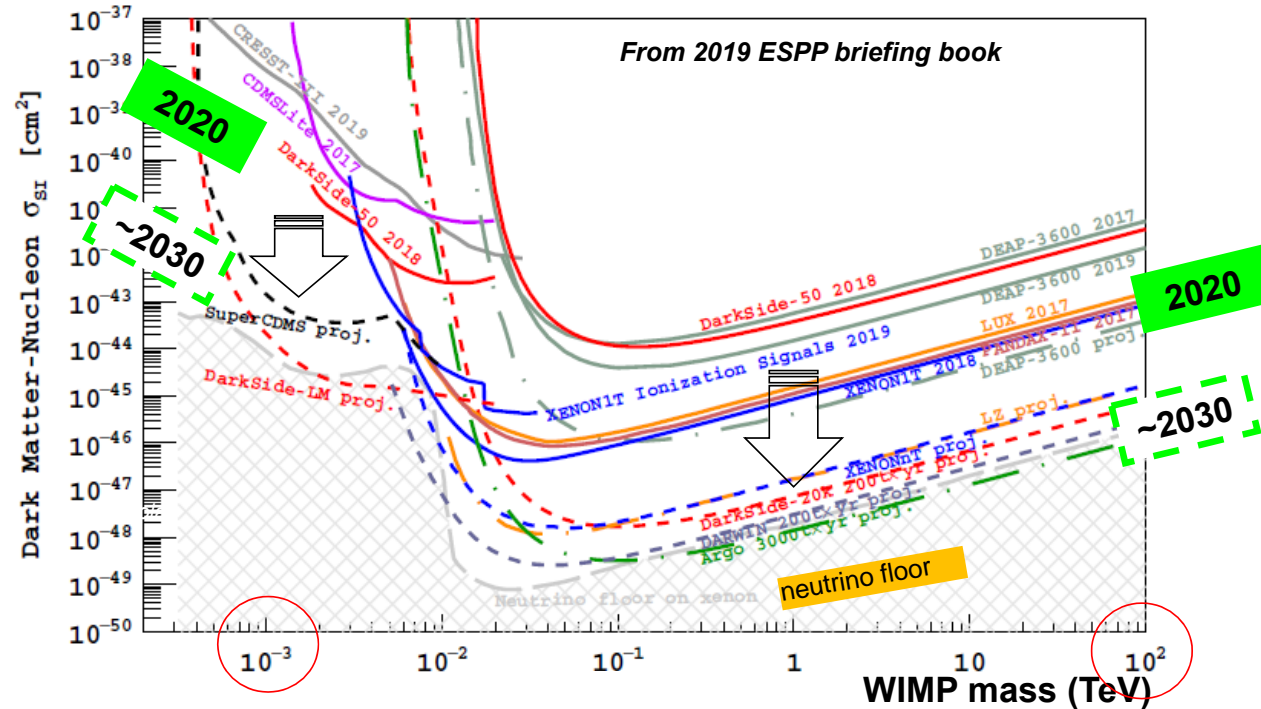


<https://www.iflscience.com/what-are-we-actually-seeing-in-jwsts-first-deep-field-image-64410>



# Dark Matter direct detection sensitivities

Experiments / prototypes in preparation at CPPM:



## DarkSide-20k

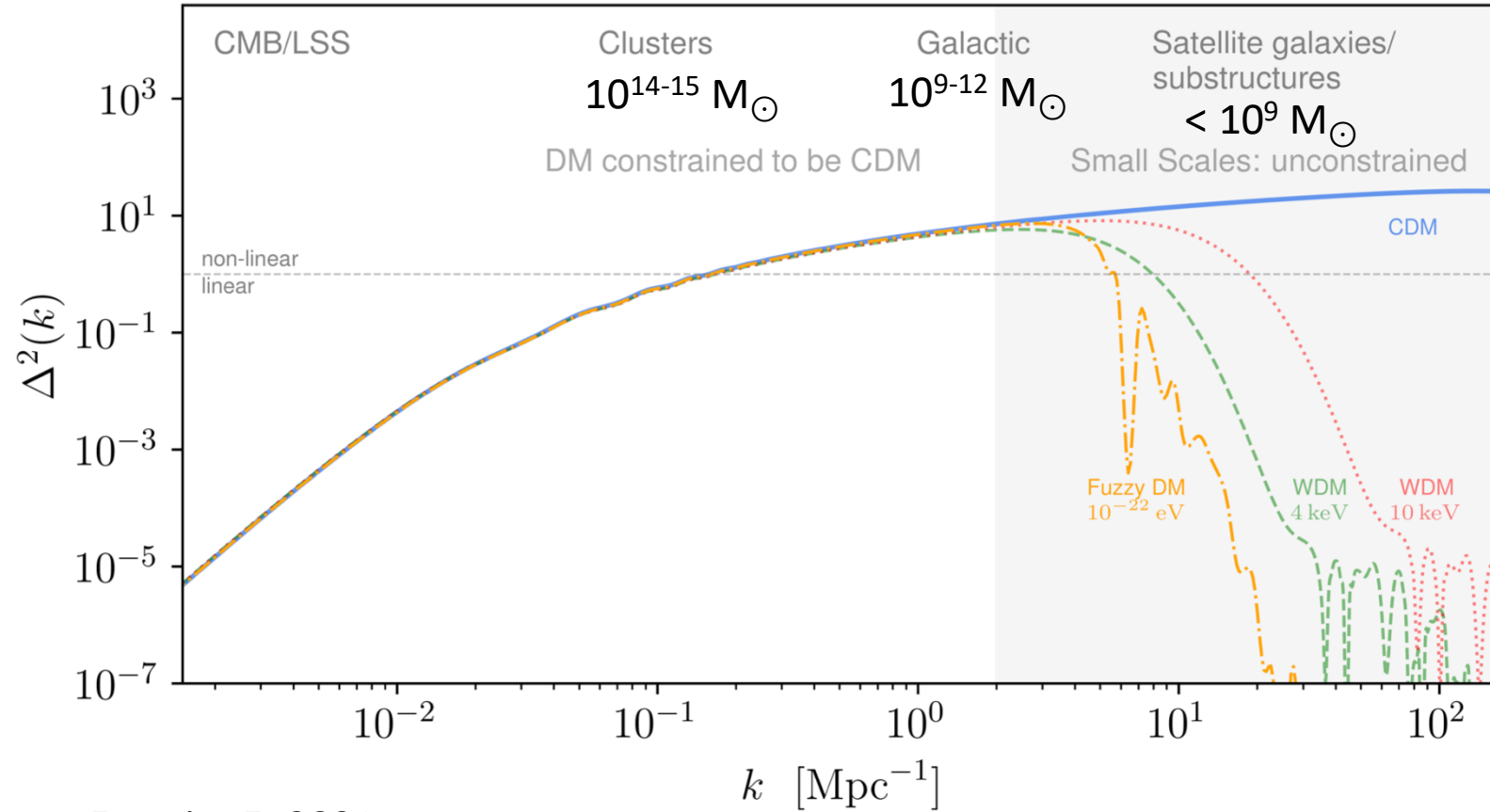
- TPC with noble liquid (Xe, Ar): best limits 1 GeV - 100 TeV
- Next decade decisive to probe WIMPs down to neutrino floor

## MADMAX

- Targets “high mass” DM axions:  $m_a \sim 40-400 \mu\text{eV}$
- R&D program to improve signal sensitivity



# Dark matter in large scale structure context

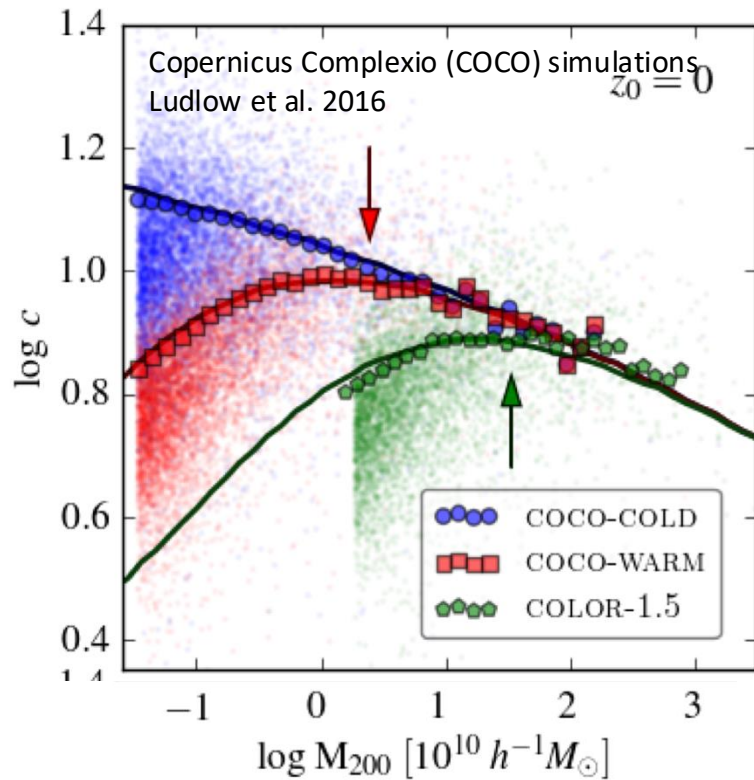


Ferreira E. 2021

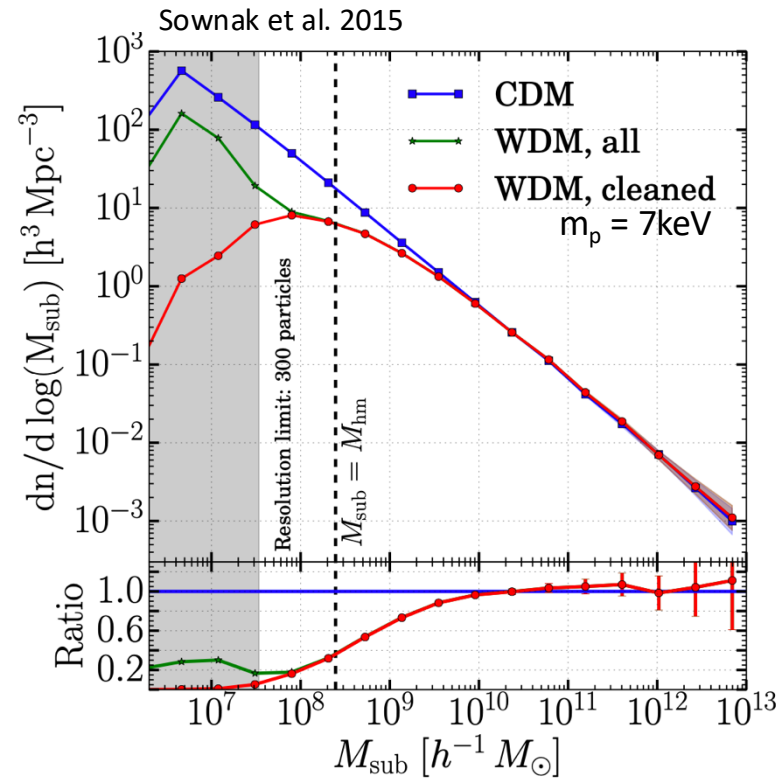


# Cold vs Warm dark matter observables

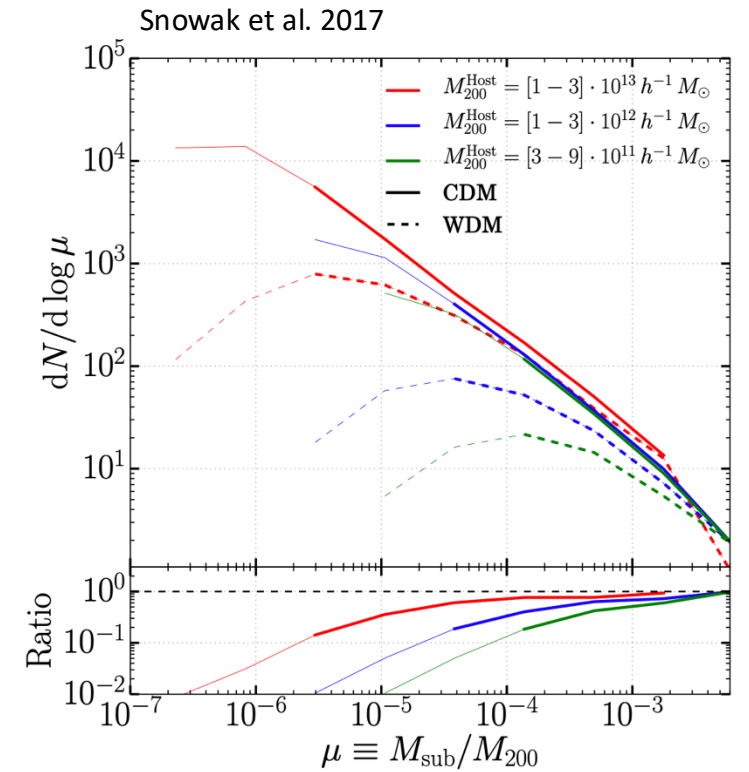
## Mass-Concentration relation



## Halo mass function



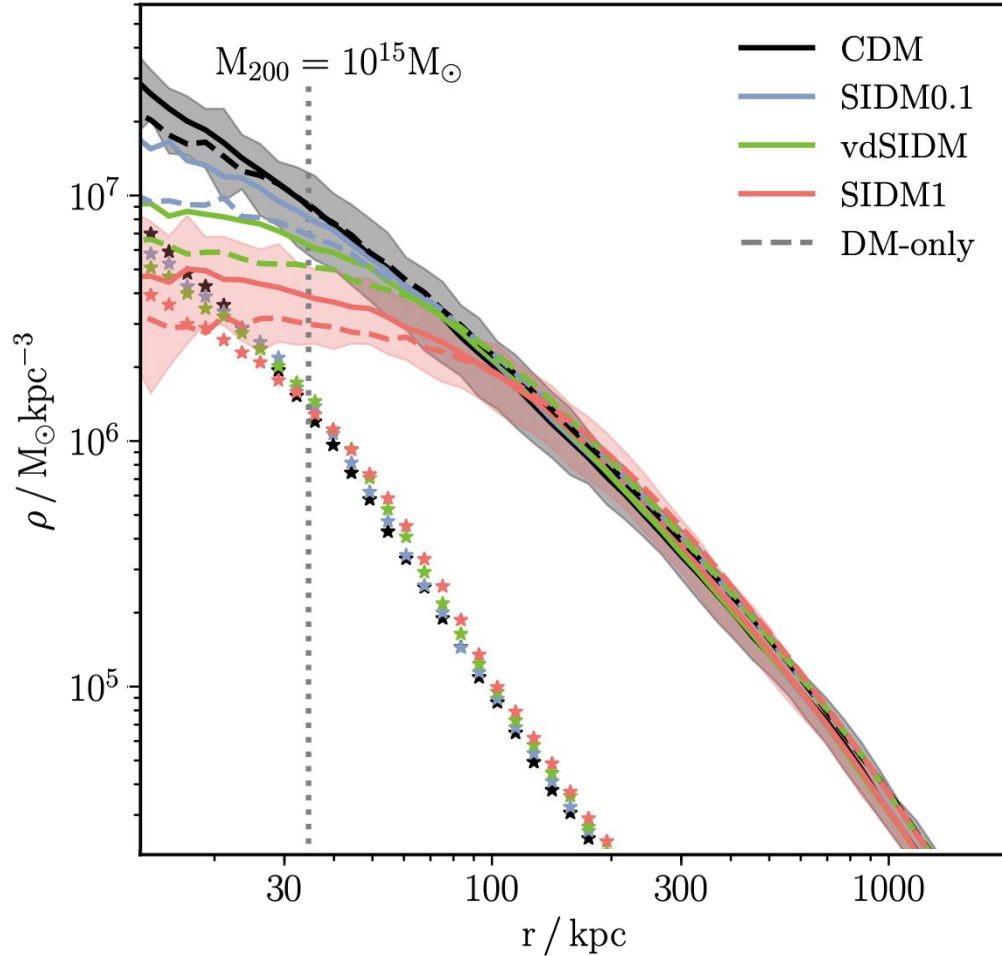
## Sub-Halo mass function



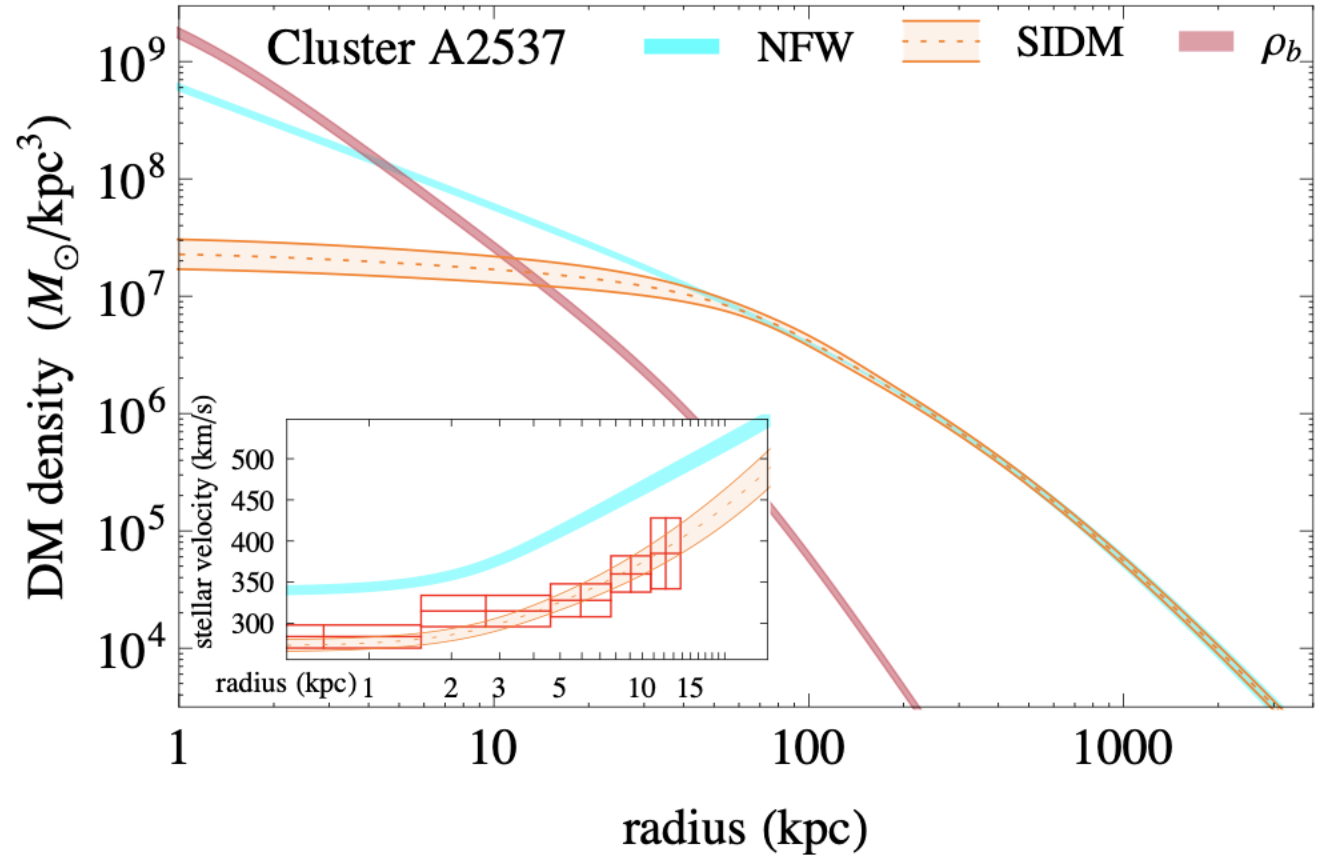


# Galaxy cluster profile in SIDM

Robertson et al. 2019



Kaplinghat et al. 2016



In simulations, dark matter can partially be distinguished from baryons at scales  $R < 20 \text{ kpc}$



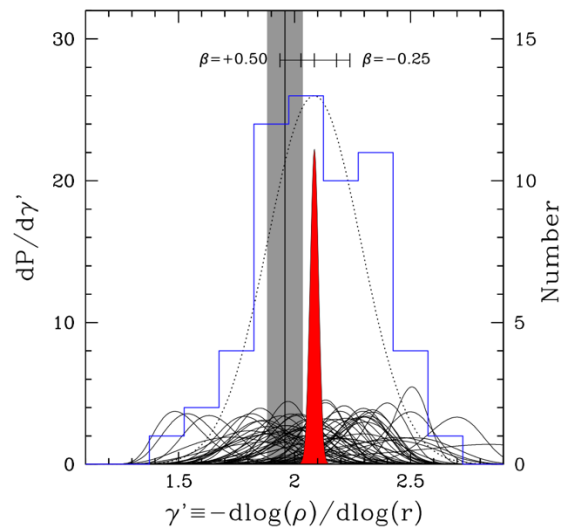
# The central density profile slope of ETG

Bolton et al. 2008

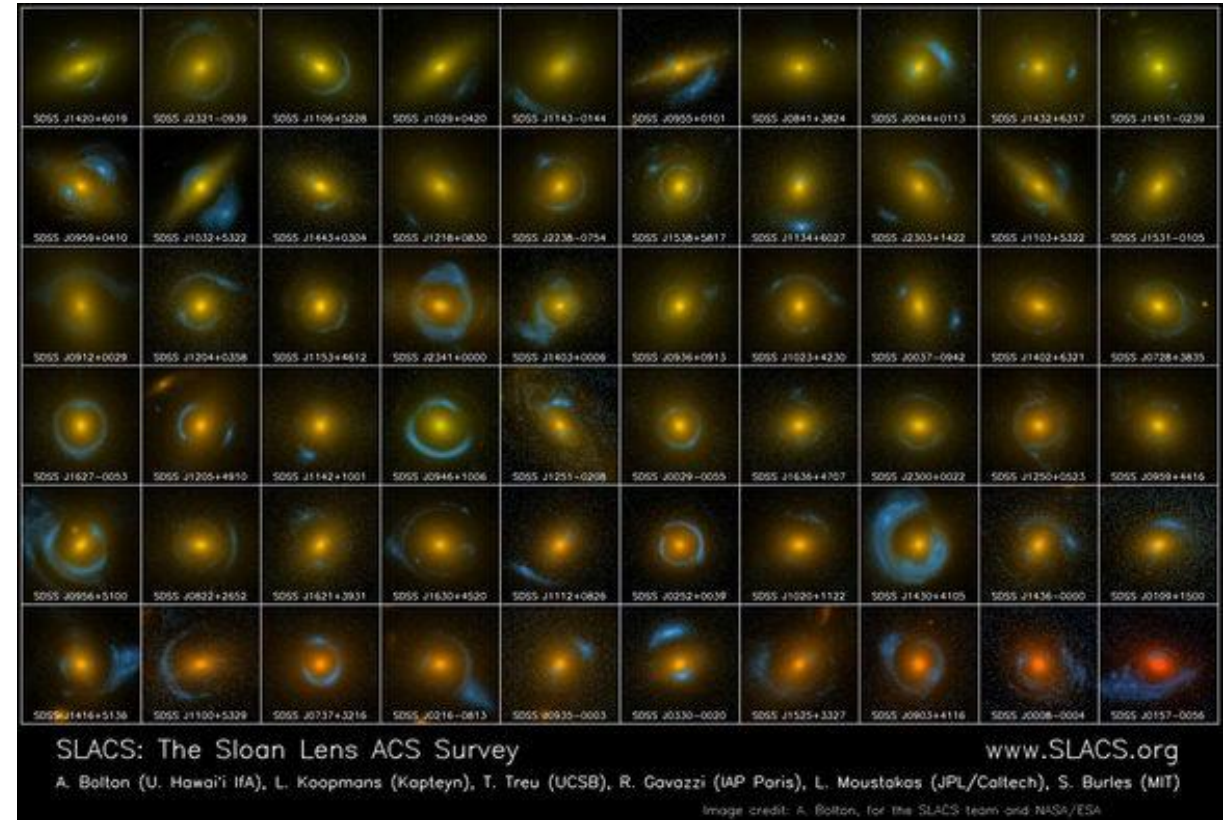
SLACS: 58 elliptical galaxies with gravitational arcs detected in SDSS spectra

Combination of SL mass in Einstein radius, and velocity dispersion of the stars  $\sigma_0$  in SDSS spectra ( $R_{\text{fiber}} = 3''$ )

Confirmation that Early Type Galaxies (ETG) follow isothermal density profile  $\gamma = 2$  **on average**



Koopmans et al. 2009



# The Strong Lensing Legacy Survey (SL2S)

Combination of 25 lenses from SL2S, 53 from SLACS and 4 from Lenses Structure and Dynamics (LSD)

- Redshift range :  $0.2 < z < 0.8$
- Stellar mass range:  $\log M^* / M_{\odot} = 11 - 12$
- Galaxy size range:  $R_{\text{eff}} = 1 - 20 \text{ kpc}$

=> Understand the DM profile slope  $\gamma'$  variation

$$\frac{\partial \gamma'}{\partial z} = \alpha = -0.31 \pm 0.10,$$

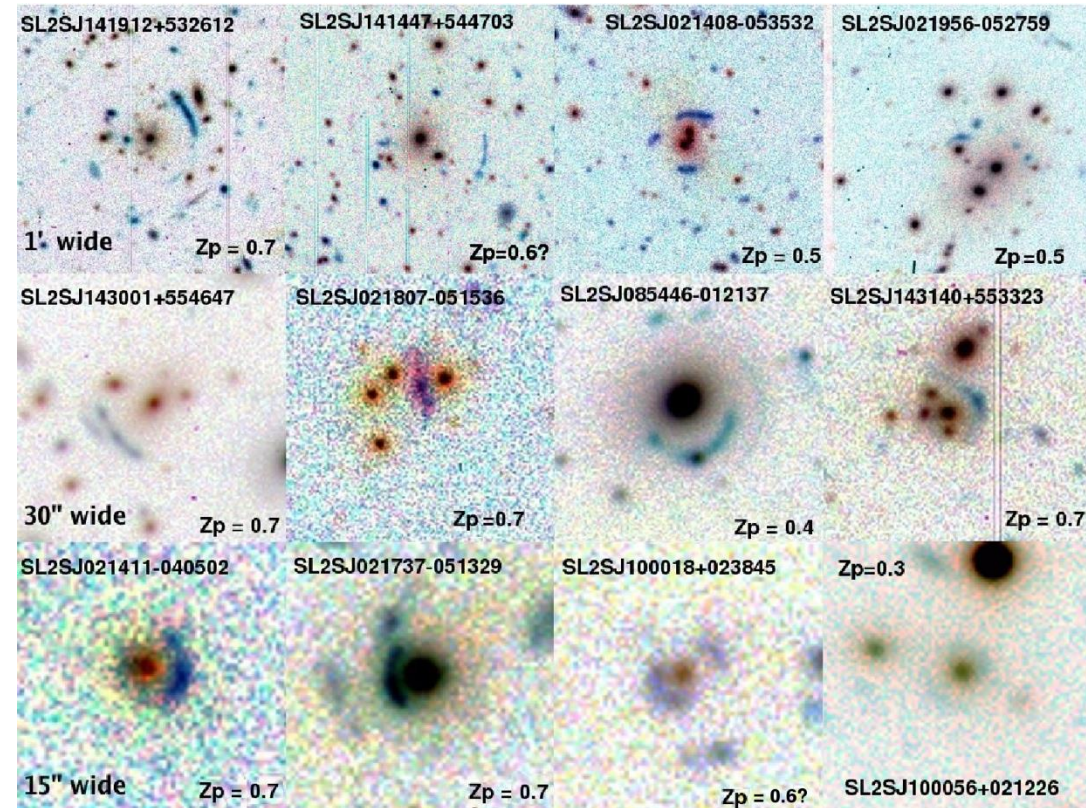
$$\frac{\partial \gamma'}{\partial \log \Sigma_*} = 0.38 \pm 0.07$$

Sonnenfeld et al. 2013

=> The slope is rather constant  $\langle \gamma' \rangle = 2$ , but this hides degeneracies:

- Stellar mass increases on the edges
  - DM infall in the center (+contraction)
- } Slope  $\gamma'$  unchanged

Cabanac et al. 2007, Gavazzi et al. 2012

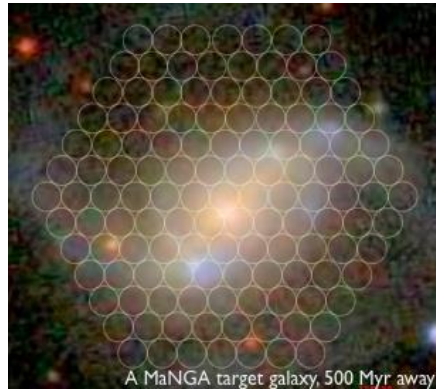


Same results found in Li, Shu & Wang 2018

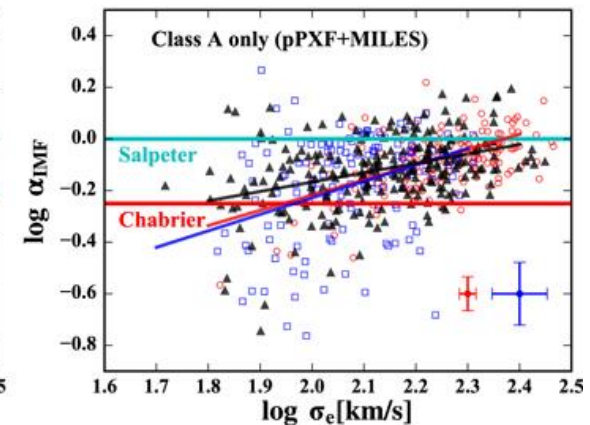
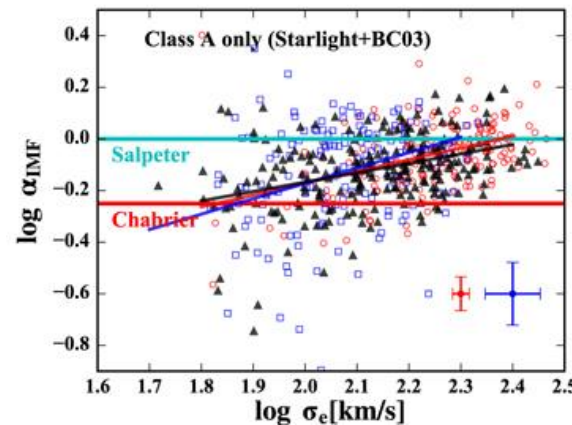
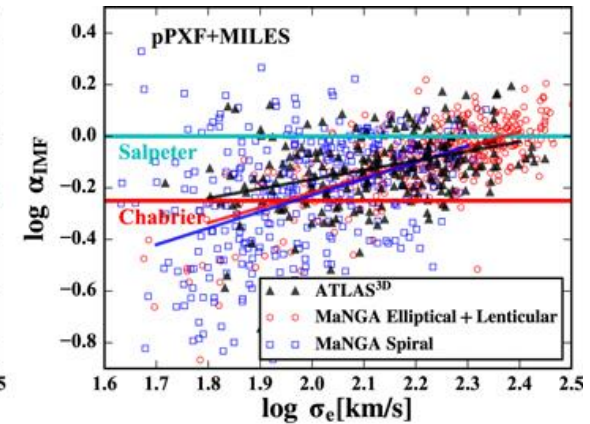
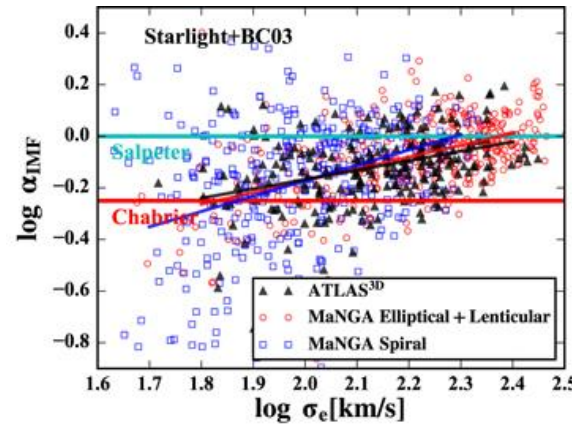


# Stellar Initial Mass Function with MANGA

MANGA observed in IFU mode 17 galaxies on 7deg<sup>2</sup> of sky (1423 fibers total, Bundy et al. 2015)



Li, Ge, Mao et al. 2017



Measurement of IMF mismatch

$$\alpha_{\text{IMF}} \equiv (M^*/L)_{\text{JAM}}^{\text{nogas}} / (M^*/L)_{\text{SPS}}$$

=>  $\alpha_{\text{IMF}}$  increases with  $\sigma_e$  ( $\pm 50\%$  uncertainty)

# Strong-lensing, dynamics & weak-lensing

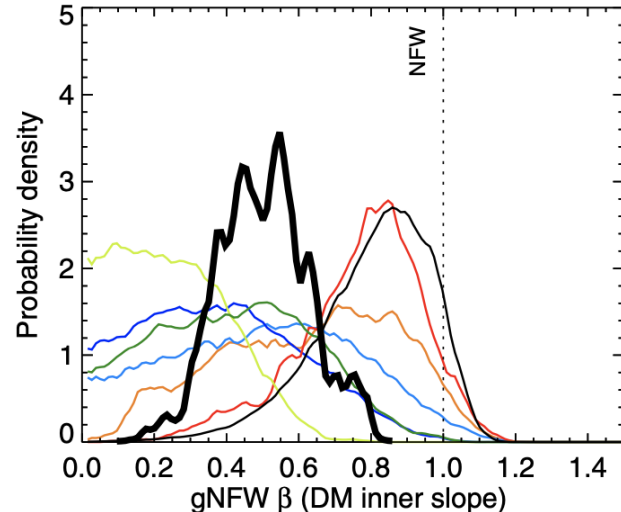
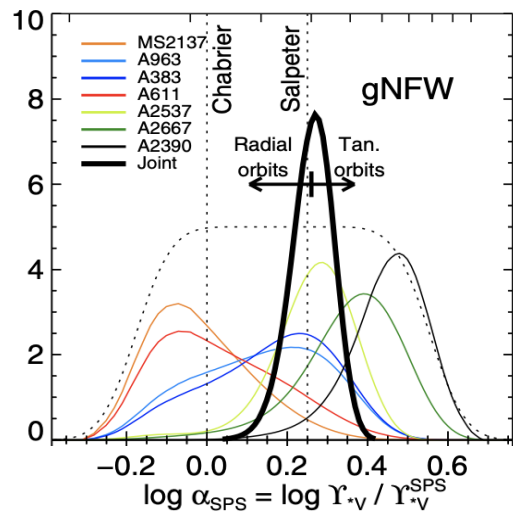
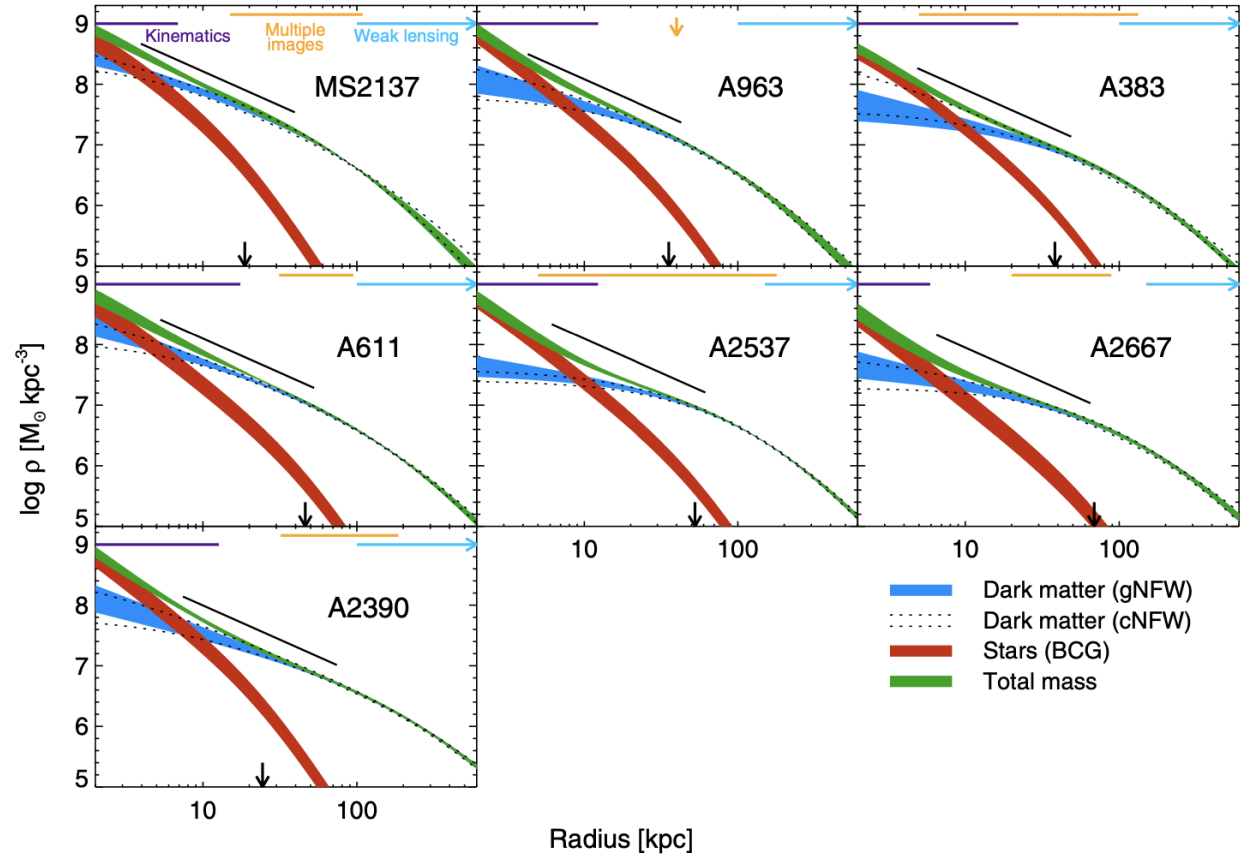
7 galaxy clusters selected w/ SL arcs

DM density profile gNFW: free inner slope  $\beta$  to account for adiabatic contraction

Stellar mass  $M^*$  derived from Stellar Population Synthesis => IMF assumption (quoted factor  $\sim 2$  uncertainty)

Stellar density profile adjusted to Surface Brightness of central BCG, and scaled to  $\alpha_{\text{SPS}} \times M^*$

Newman et al. 2014



=> Galaxy clusters have a flat cored DM profile  $\beta = 0.5 \pm 0.13$



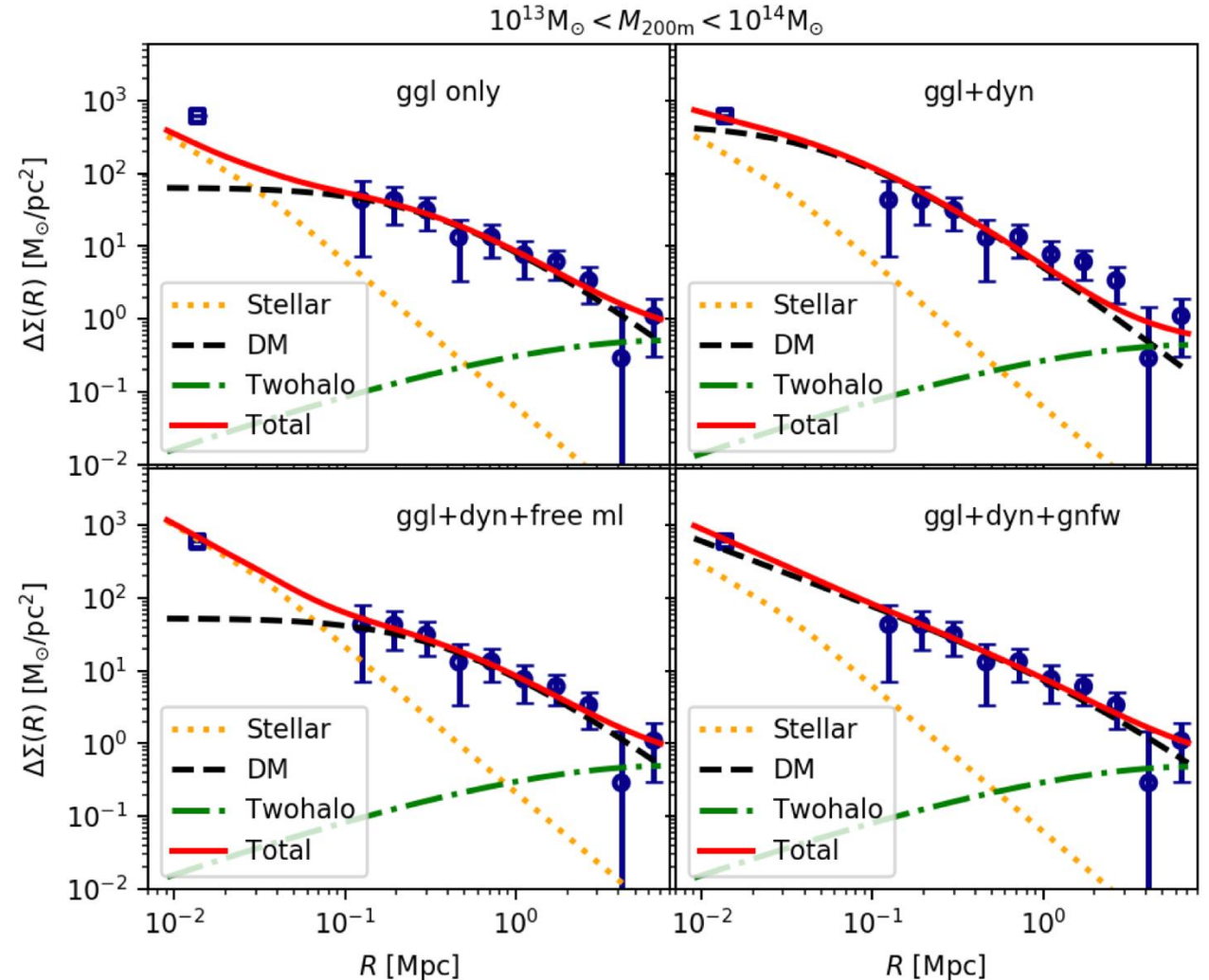
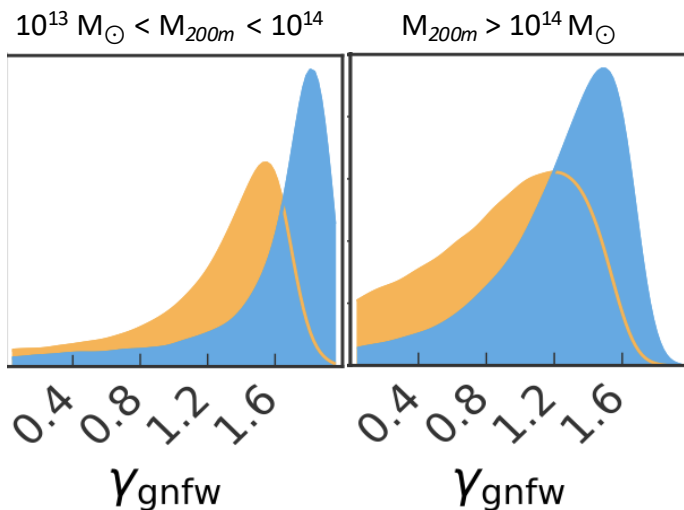
# Averaging over more clusters and groups

Chunxiang Wang et al. 2024

Weak Lensing for the larger scales and stellar kinematics in the center with MANGA (IFU) data

Stellar density profile adjusted on r-band SB distribution scaled to  $\alpha_{\text{SPS}} \times M^*$

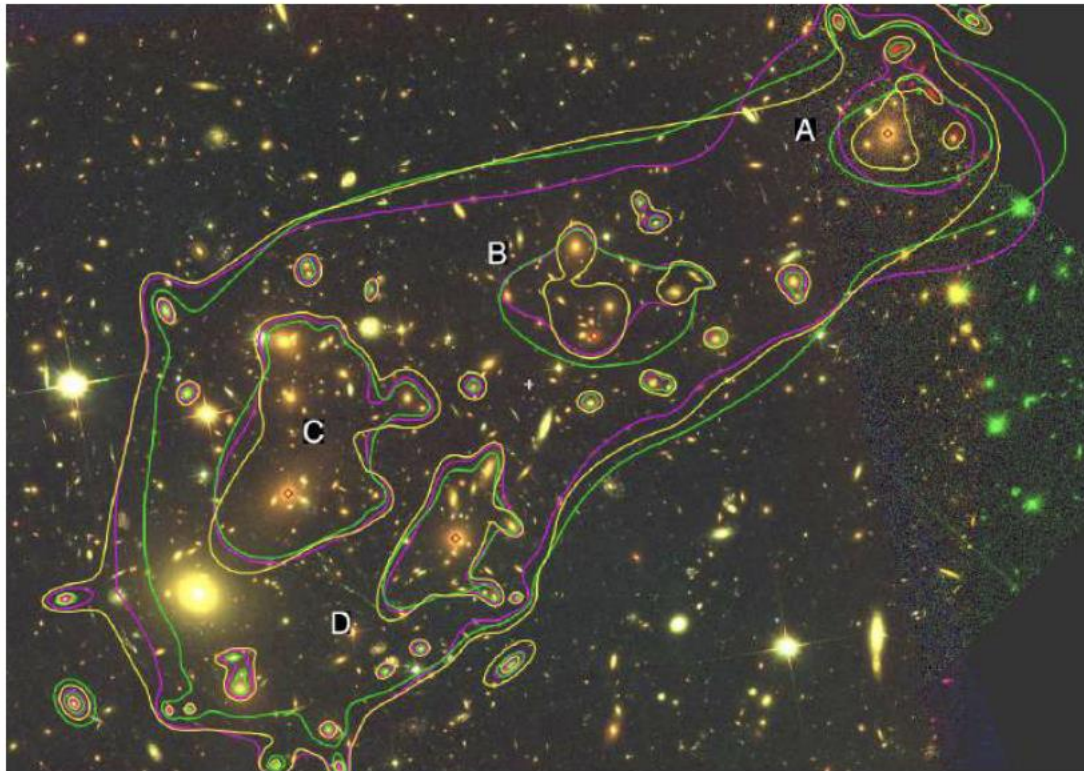
=> The DM profile inner slope is  $\gamma > 1$



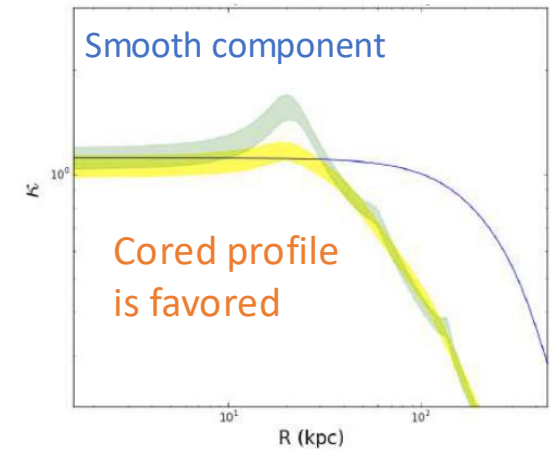
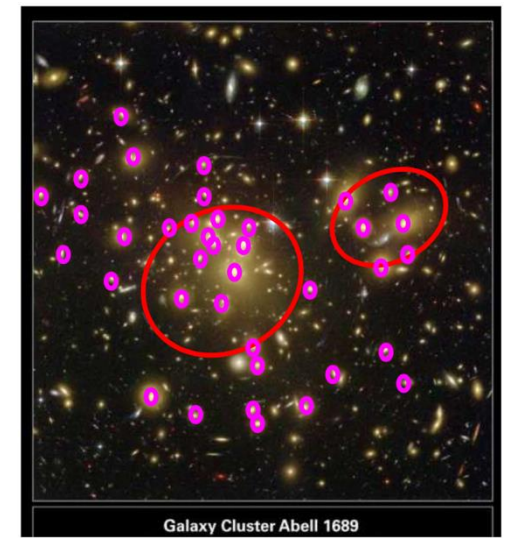
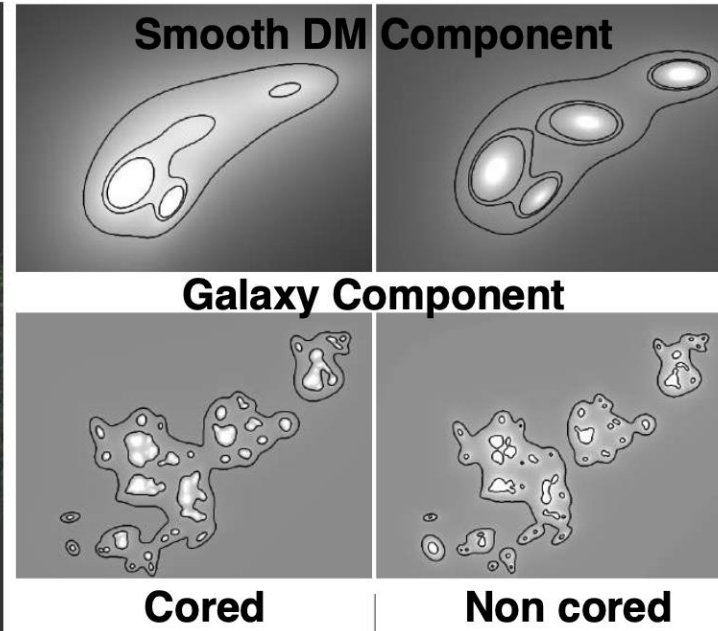
# Strong lensing in galaxy clusters

Better modelling thanks to

- More multiple images constraints with deep HST observations (HFF program, JWST)
- Integral field spectroscopy data to constrain galaxy kinematics (MUSE)
- Dark matter and stellar content decoupled from the cluster DM component



Limousin et al. 2017



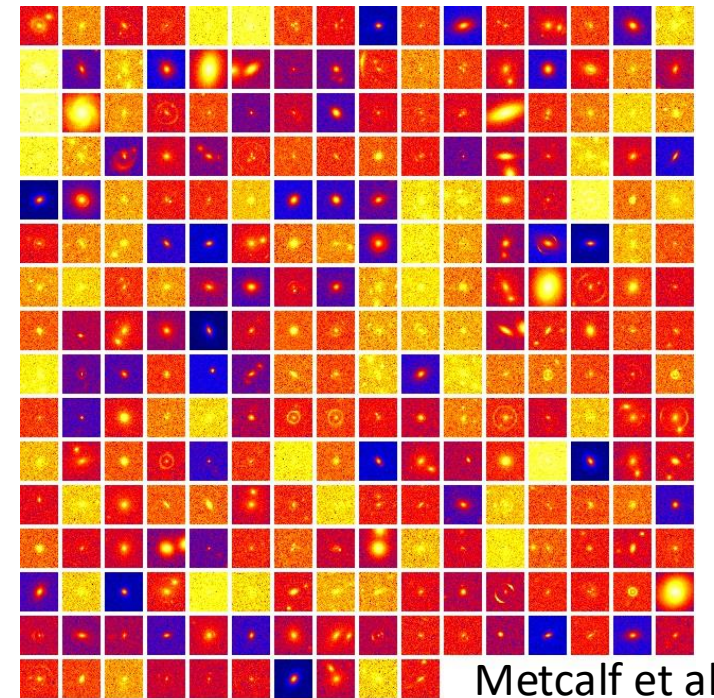
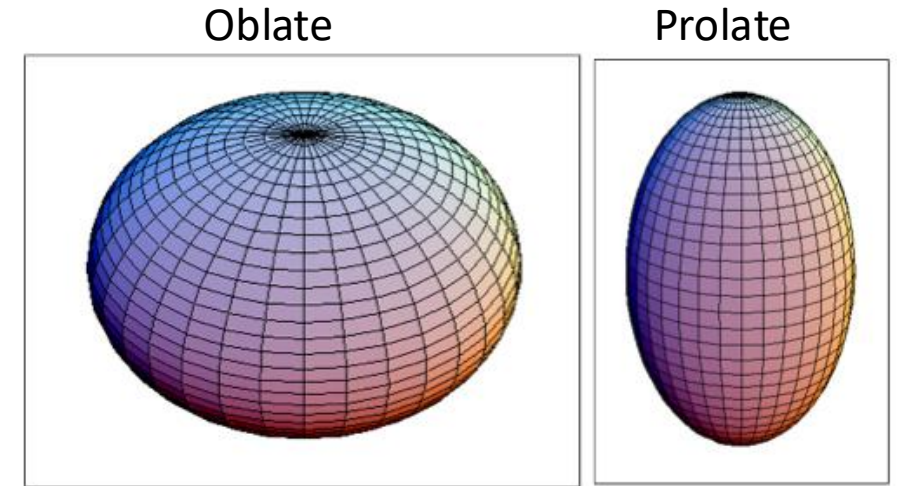
Limousin et al. 2022

=> Hint for self-Interacting DM? Or systematic bias? => need bigger sample



# Selection effect?

- Strong lensing lenses are biased objects (Foex et al. 2014, Sonnenfeld et al. 2024)
  - SL lenses are triaxial objects
  - Elongated halos along the line of sight
- Big efforts to characterize the selection function
  - Analytic predictions : including instrumental effects, e.g. Euclid, LSST, etc
  - Full hydro-simulations (e.g. Xu, Springel et al. 2017, Despali et al. 2021)
  - Spectroscopic observations : characterize redshift distribution of lenses and arcs (e.g. VLT-Xshooter program, PI: Jullo; 4MOST proposal PI: Collett; DESI secondary program Huang et al. in prep)



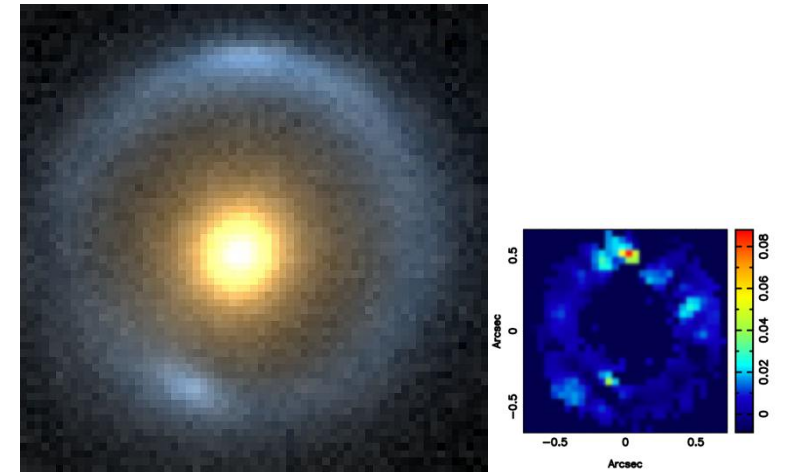
Metcalf et al. 2016

# Einstein rings by galaxies

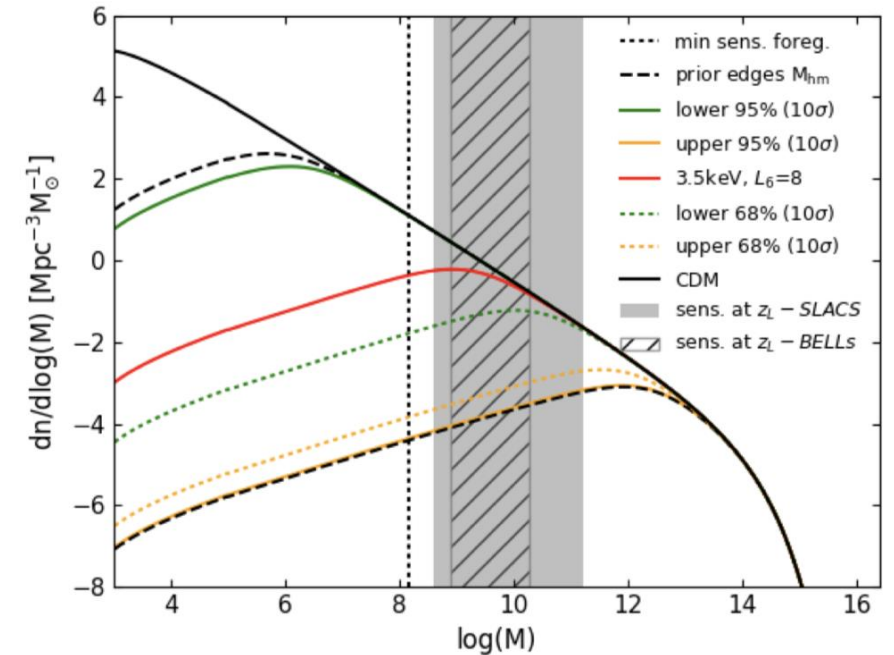
- Flux or position perturbation in Einstein rings reveals low mass subhalos (see also Chan et al. 2020 with axion part.)
- With optical/NIR observations in spectroscopy ( $\sim 4h$  K-band/Keck, 3h NICMOS)  $\Rightarrow \sim 10^8 M_\odot/h$
- Around  $10^5$  Einstein rings to be discovered with Euclid  $\Rightarrow$  good sample of « jackpot » candidates

Combined constraints Lya, lensing, MW satellites :

$\Rightarrow$  Lepton with asymmetries  $L6 > 10$  and 7.1 keV sterile neutrinos are ruled out



Constraints with 17 ER



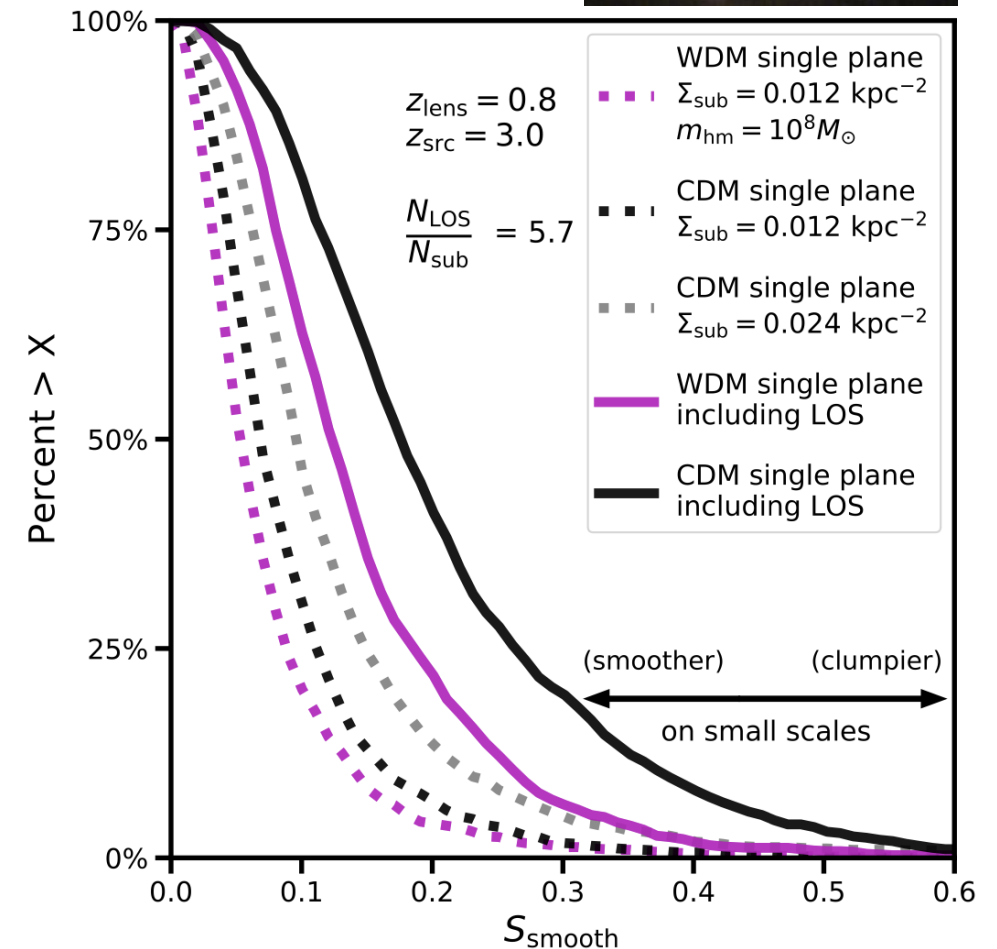




# Quadruply imaged quasars : flux anomalies

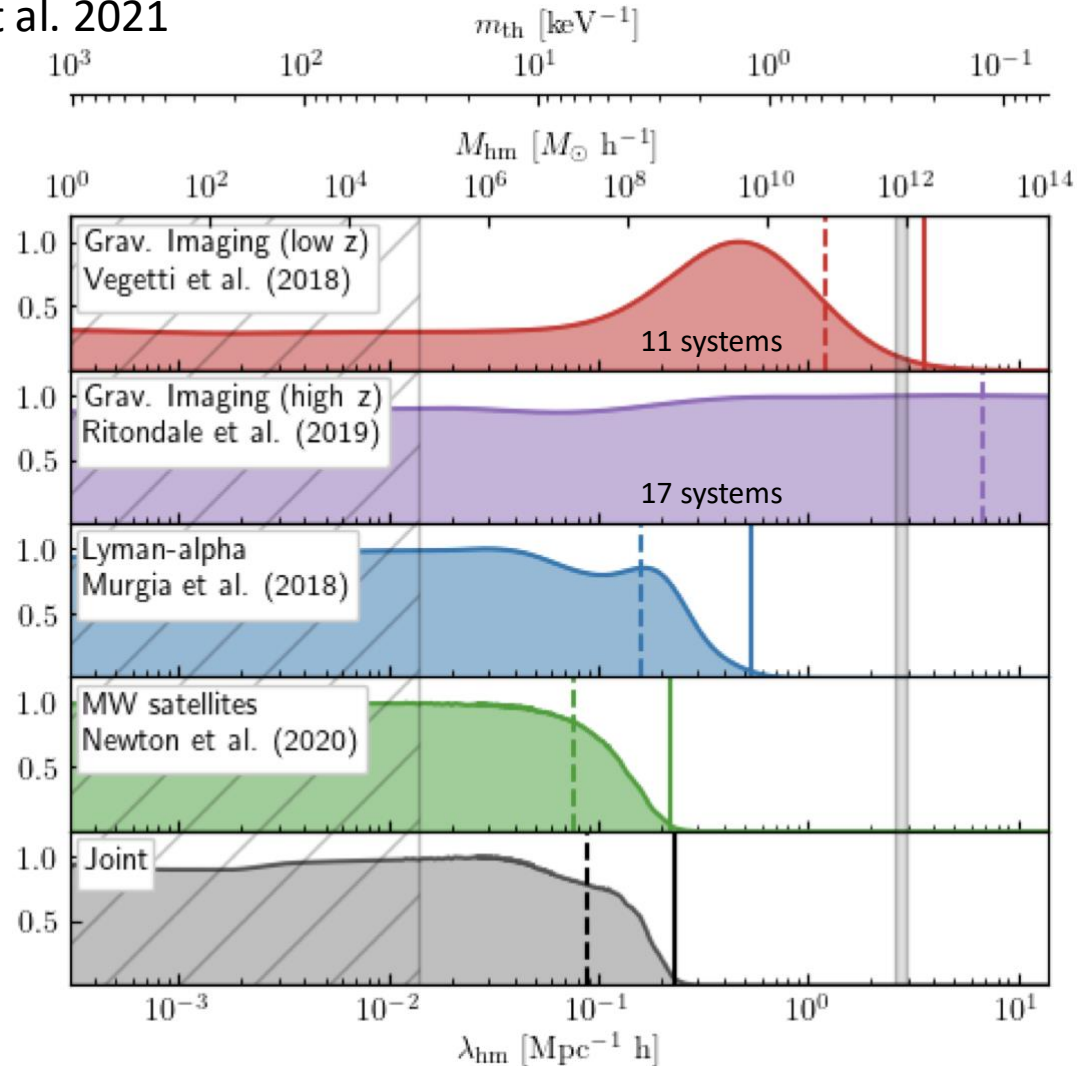
- More small-scale substructures produce more frequent **flux ratio anomalies**
- Require long term monitoring of QSO flux variations
- Impact of Line of Sight structures (He, Li et al. 2021)
- Dependence on the simulation details (e.g. tidal destruction severity)

=> Move from standard modeling to summary statistics techniques to simplify the analyses



# Combined constraints: Lya, SL, MW sat.

Enzi et al. 2021



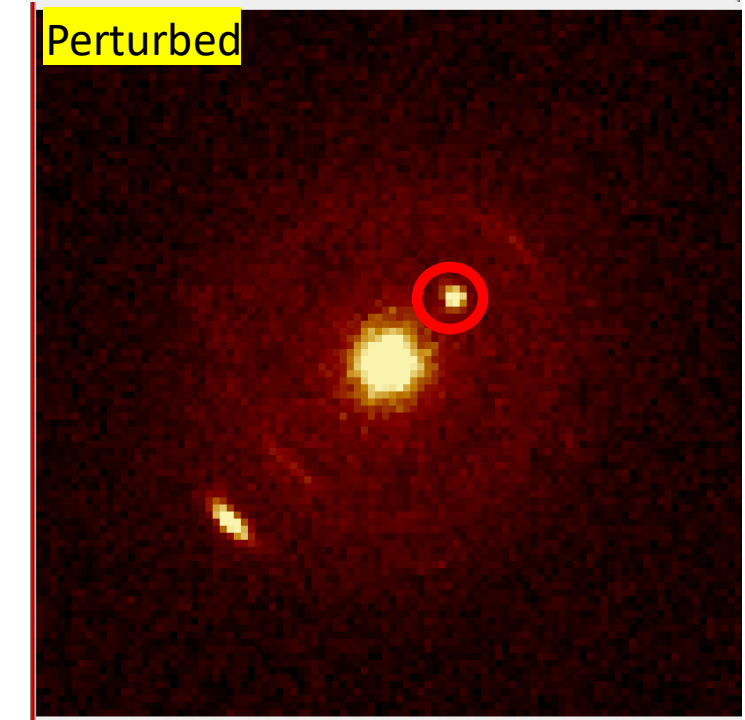
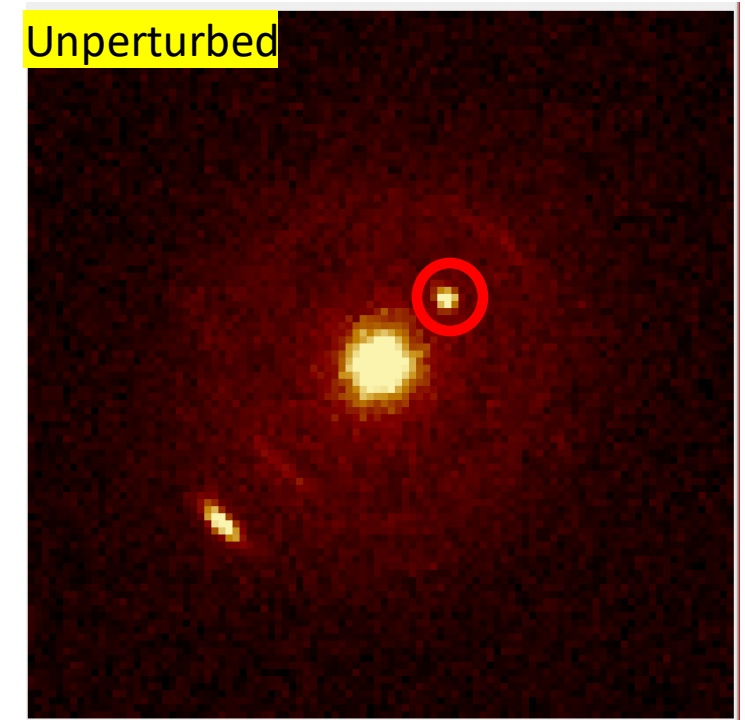
- VLBI + ELT will reach 0.2 to 5 mas resolution to probe halos  $10^6 M_{\odot}$  (Spingola et al. 2018 for VLBI)
- JWST will allow to maximize contribution from LOS haloes for High-z sources => tighter constraints
- Euclid & LSST will bring many candidates ( $\sim 10^5$ )
- High-resolution, realistic hydro simulations will yield better dark matter models

=> For lepton asymmetries  $L6 > 10$ , 7.1 keV sterile neutrinos are ruled out



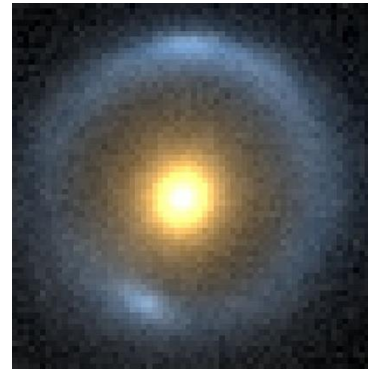
# Preparing the future: ELT-HARMONI simulations

- ELT-HARMONI expected first light  $\sim 2030$ 
  - 42m telescope with Laser Guide Stars Adaptive Optics
  - IFU in NIR with 4mas spaxel resolution
- Simulated observations
  - Background galaxy at  $z = 2$  with star formation clumps
  - Lens galaxy in  $10^{13} M_{\odot}$  halo
  - Perturbation  $10^8 M_{\odot}$
  - Observational setup: Total exptime 5h, K grism,  $30 \times 60$ mas spaxels, LTAO, no moon, airmass 1.3
- Perturbation on the arc :  $0.2 \pm 2$  pixels  $\Rightarrow$  detection limit



# How to join effort?

Vegetti et al. 2012



## 1) Gravitational lenses

=> WIMP & axion: galactic scale CDM behavior => unable to distinguish WIMP & axion?

## 2) Detection of DM particles

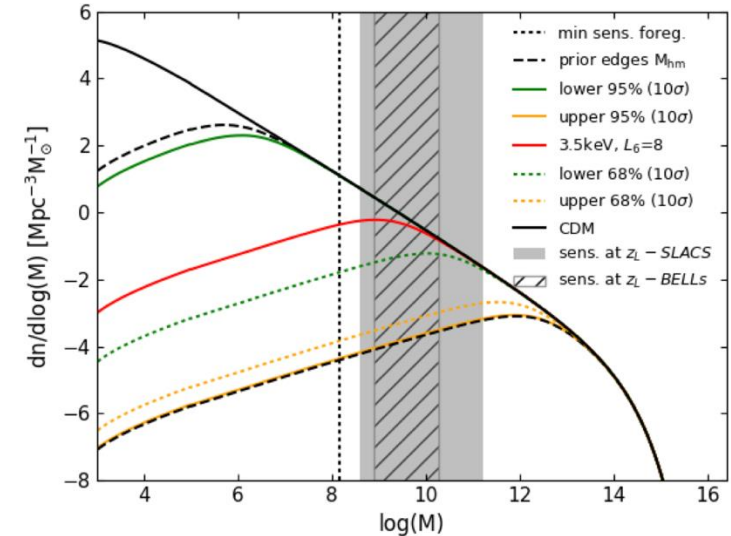
=> Sensitivity depends on the density model of the Galaxy and subhalos  
=> use of simulations, observations (lensing, galaxy rotation curves, etc.)

In the 2 cases

- Use of hydrodynamical simulations

Much to gain by exchanging/joining efforts between communities 1) and 2), especially at the level of simulations

## SL current constraints

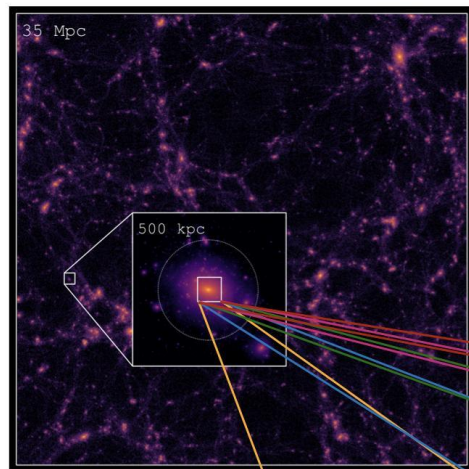


Simulation (Springel et al. 2008)

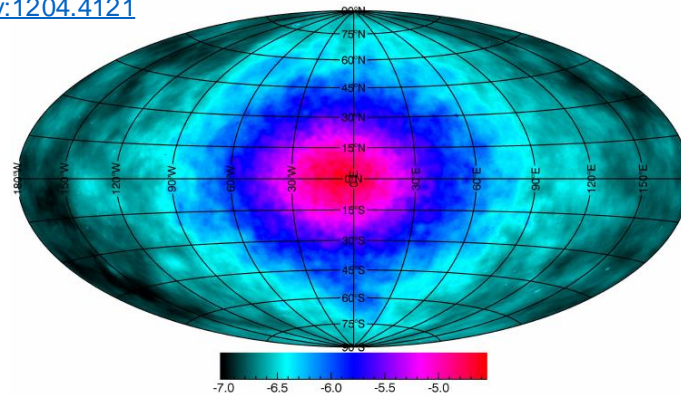


# Milky Way modelling for direct detection

1. Hydrodynamical N-body (zoom-in) simulations including subhalos
2. Connecting cosmo simulations with astroparticles and dark matter detection
3. Phase space distribution beyond the Maxwellian distribution of the Standard Halo Model

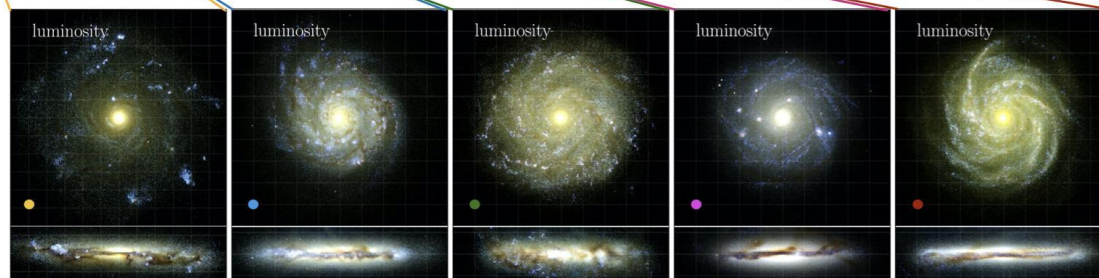


[Nezri et al. 2012](#)  
[arXiv:1204.4121](#)

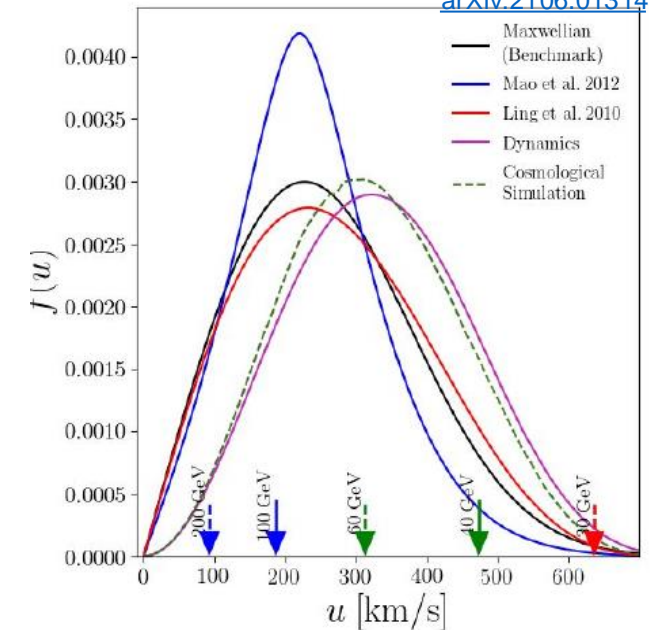


[arXiv:1405.4318](#)

[Nuñez et al. 2022](#)  
[arXiv:2004.06008](#)



[Petač et al. 2021](#)  
[arXiv:2106.01314](#)



- Velocity distribution is more complex than analytical models => need simulations  
=> Observations with gravitational lenses can constrain halo models and simulation

# Dark Matter direct detection sensitivities

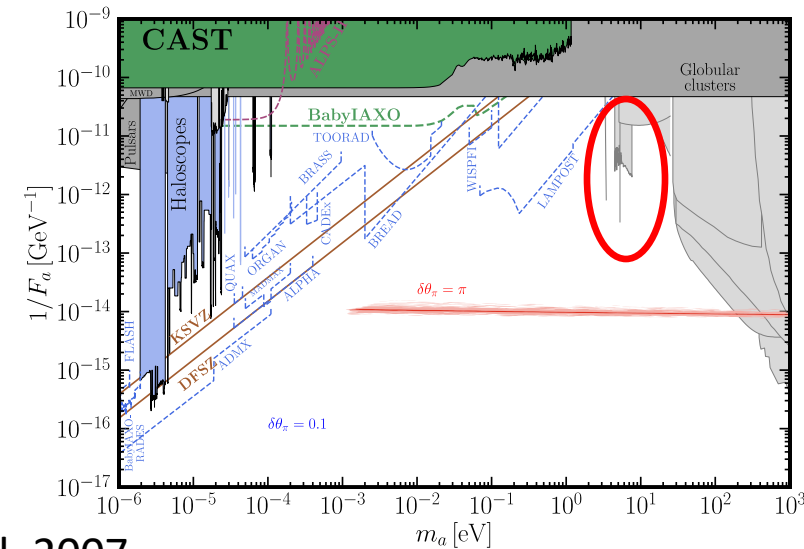
We assume a two-photon coupling to the axion (Ressell 1991, Bershadsky et al. 1991)

Two-photon coupling leads to monochromatic emission line

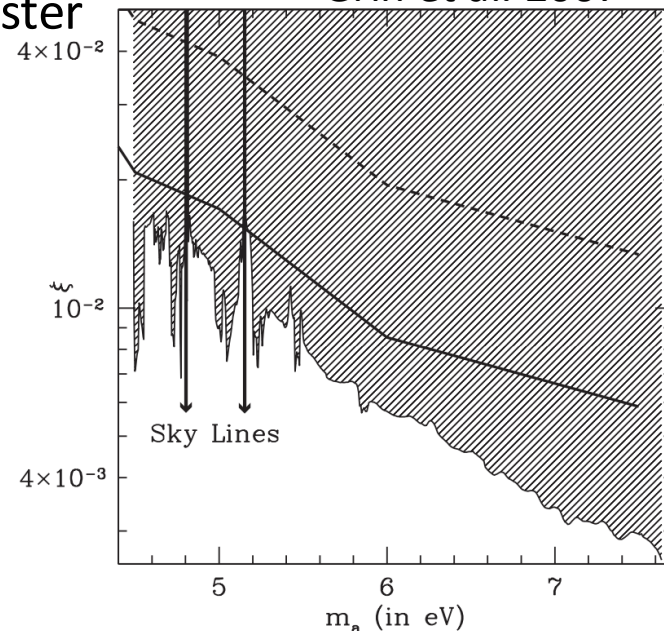
Gravitational lensing is used to determine the cluster density profile, and apply optimal weighting for emission line detection

VLT-VIMOS IFU observations image the core of the cluster

$$I_{\lambda_o} = 2.68 \times 10^{-18} \times \frac{m_{a,eV}^7 \xi^2 \Sigma_{12} \exp[-(\lambda_r - \lambda_a)^2 c^2 / (2\lambda_a^2 \sigma^2)]}{\lambda_a = 24\,800 \text{ \AA} / m_{a,eV} \text{ }^{000} (1 + z_{cl})^4 S^2(z_{cl})} \text{ cgs,} \quad (4)$$

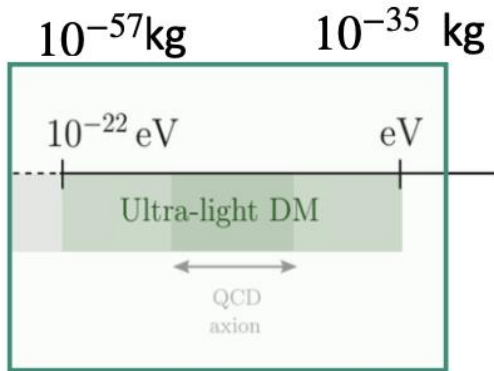


Grin et al. 2007



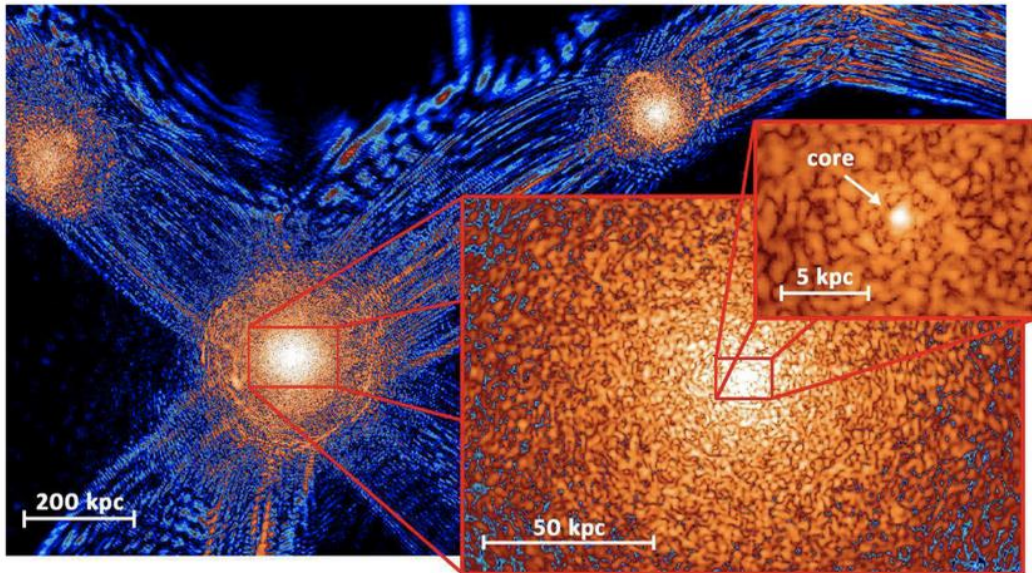


# Scalar Field Dark Matter (SFDM) at small scales



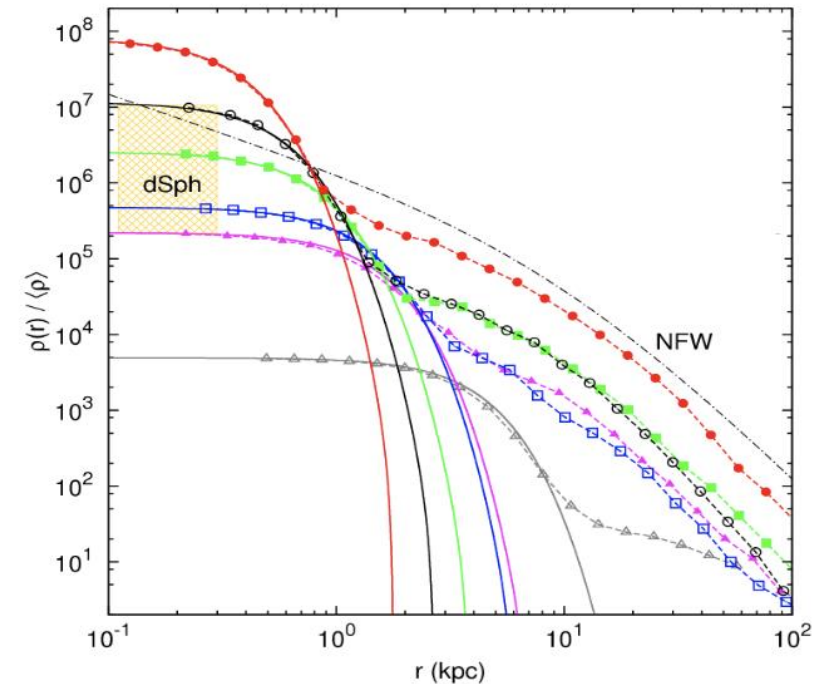
Because of its ultra-light mass  $\rightarrow$  Large de Broglie wavelength,  $\lambda_{dB} \sim 1/mv$

- $\lambda_{dB} \sim \text{pc} - \text{kpc}$
- Small scales: wavelike behaviour.
- **Solitons**: stable equilibrium configurations  $\rightarrow$  **Flat density profile at the center of the halos.**



A slice of density field of  $\psi$ DM simulation on various scales at  $z=0.1$

Schive, Chiueh, and Broadhurst (2014)



Radial density profiles of haloes formed in the  $\psi$ DM model

# SFDM model

DM is represented by a **scalar field minimally coupled to gravity** given by the Lagrangian:

$$\mathcal{L}_\phi = -\frac{1}{2}g^{\mu\nu}\partial_\mu\phi\partial_\nu\phi - V(\phi),$$

The scalar field potential  $V(\phi)$  must have a **parabolic minimum**  $V(\phi) = \frac{m^2}{2}\phi^2 + V_I(\phi)$ ,

## Fuzzy DM (FDM)

$$V_I(\phi) = 0.$$

$m$

## Quartic model

$$V_I(\phi) = \frac{\lambda_4}{4}\phi^4,$$

$m, \lambda_4$

Repulsive  $\rightarrow \lambda_4 > 0$

# Self-interacting soliton

**Soliton: Hydrostatic equilibrium**

$$\Phi_N + \Phi_I + \Phi_Q = \alpha,$$

**Thomas-Fermi regime**  $\rightarrow \Phi_Q \ll \Phi_I$

**Soliton TF limit**

$$\Phi_N + \Phi_I = \alpha,$$

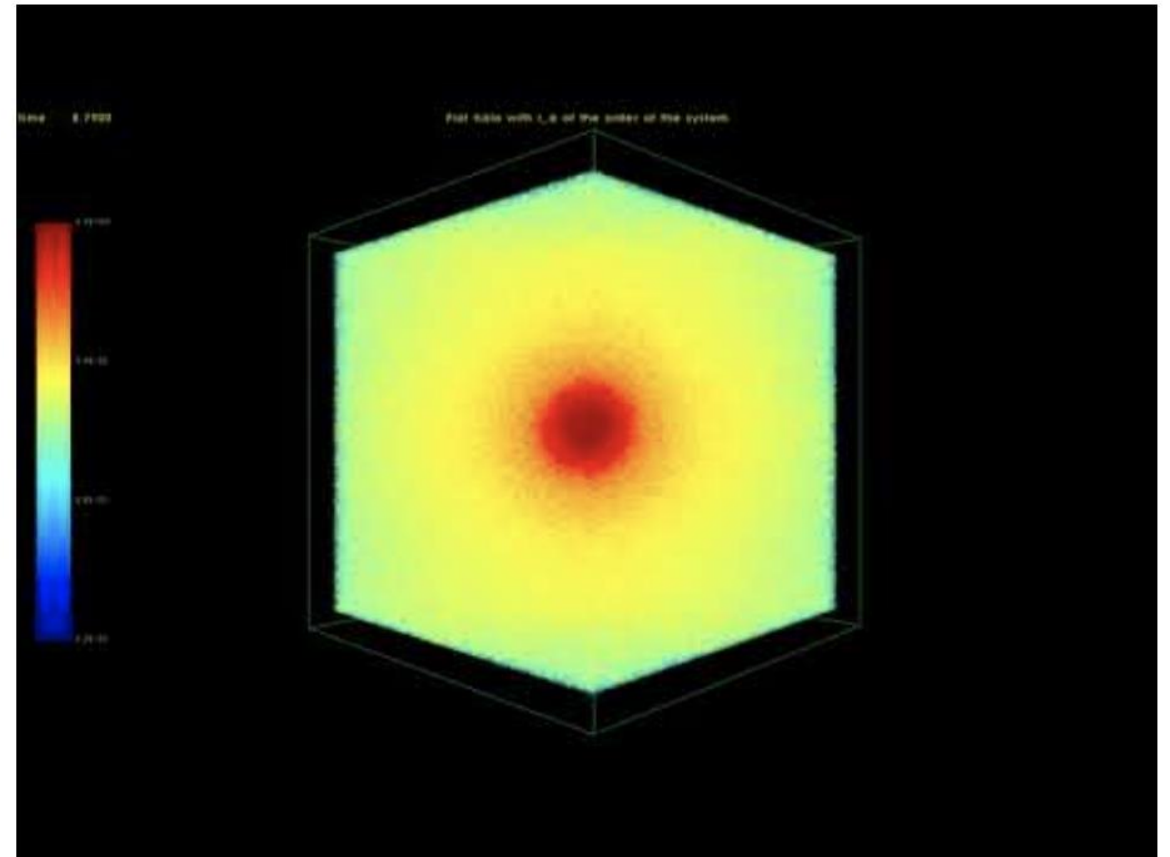
**In this approximation, the soliton density profile :**

$$\rho_{\text{sol}}(r) = \rho_{0\text{sol}} \frac{\sin(\pi r / R_{\text{sol}})}{\pi r / R_{\text{sol}}},$$

$$R_{\text{sol}} = \pi r_a, \text{ with } r_a^2 = \frac{3\lambda_4}{16\pi\mathcal{G}_N m^4}.$$

$r_a$  sets Jeans length !

We consider the semi-classical limit, where  $\lambda_{\text{dB}}$  is smaller than both the core and halo radii.



Flat halo with  $r_a$  of the order of the system

*R.Galazo-García et al. (2024)  
acknowledgements to Jean Charles Lambert*



# Total profile

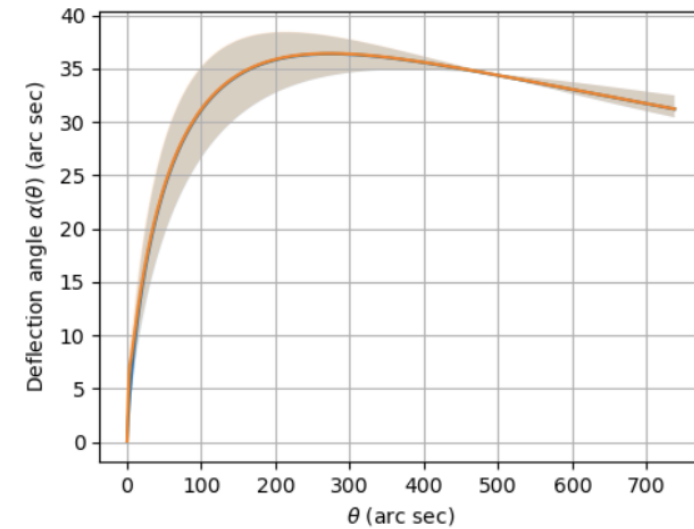
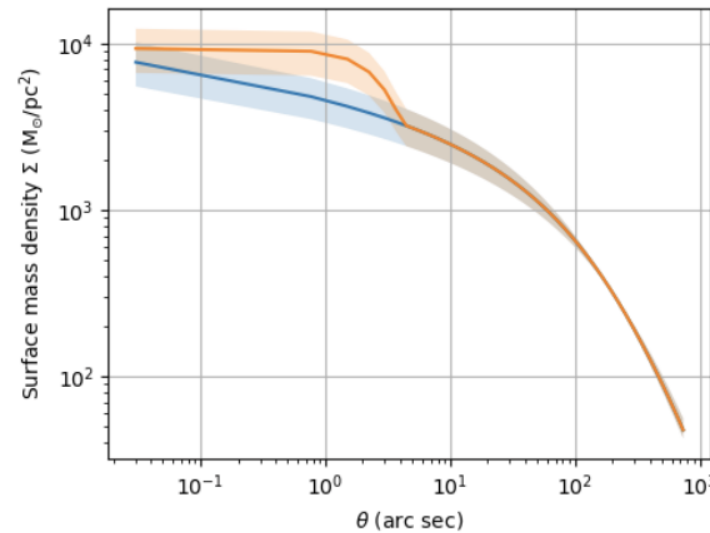
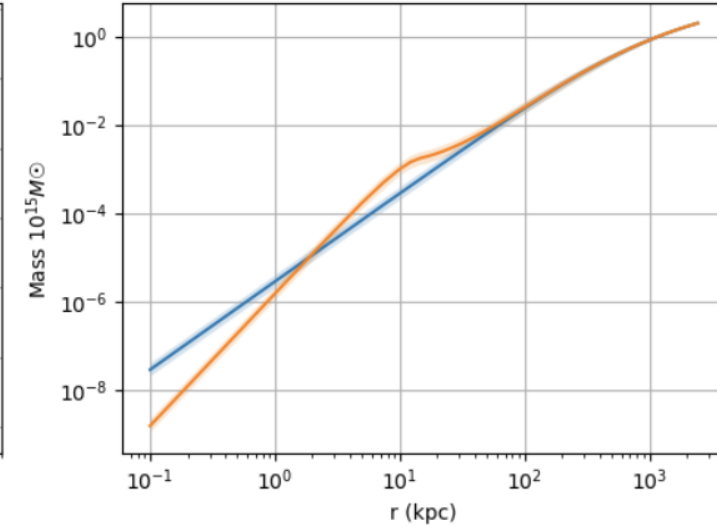
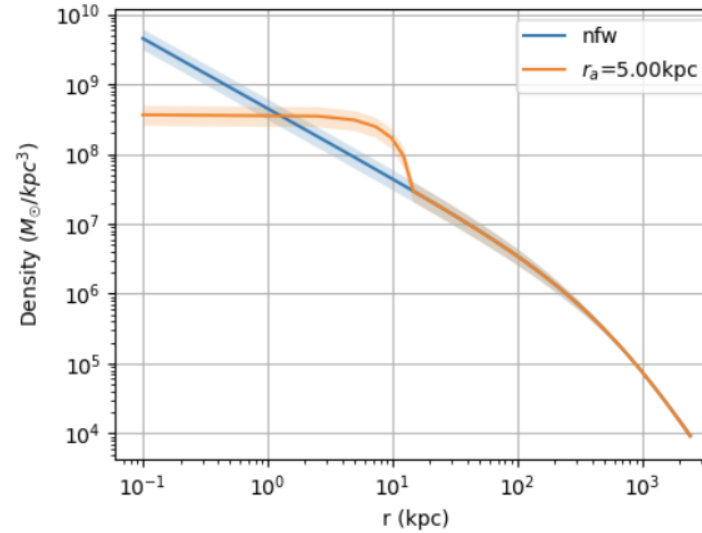
- We choose the model to study  $\rightarrow R_{sol} = \pi r_a$

$$r < r_t: \quad \rho(r) = \rho_{0sol} \frac{\sin(\pi r/R_{sol})}{\pi r/R_{sol}},$$

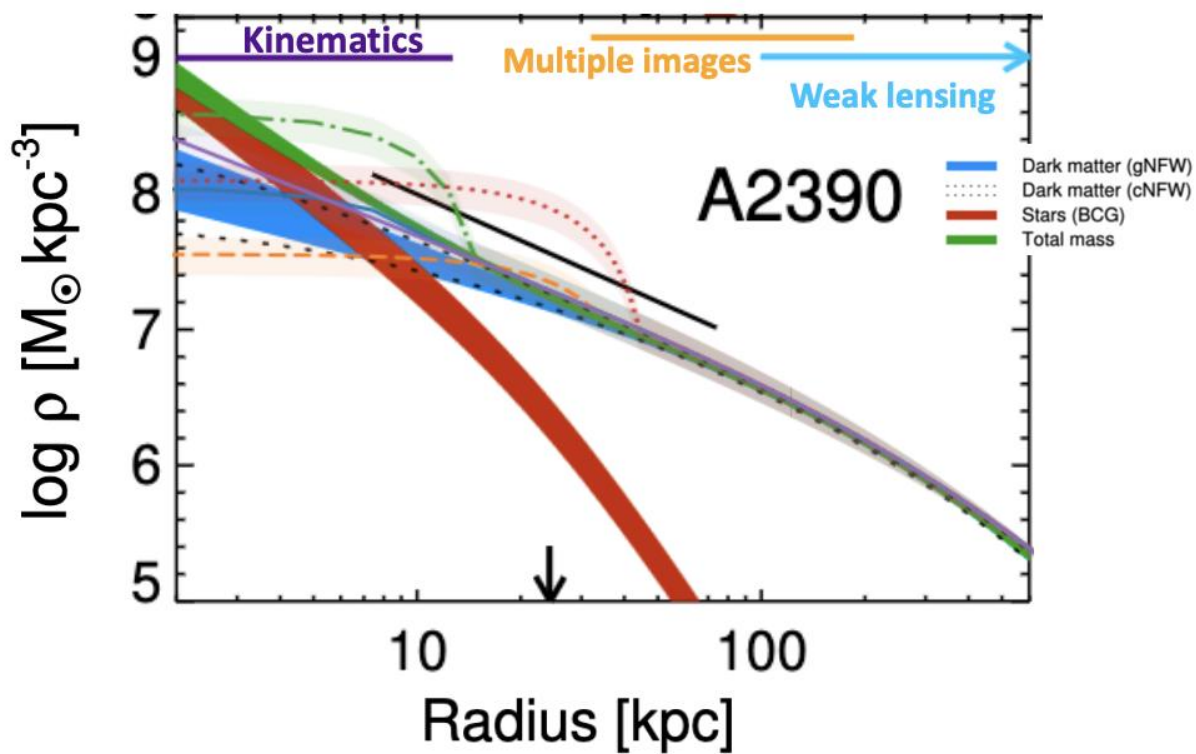
$$r_t < r < R: \quad \rho(r) = \frac{\rho_s}{\left(\frac{r}{r_s} \left(1 + \frac{r}{r_s}\right)\right)^2}.$$

- We calculate the value of  $r_t$  and  $\rho_{0sol}$  such that  $M_{sol}(< r_t) = \alpha M_{NFW}(< r_t)$  and the total mass of the system is conserved.
- We have slight flexibility in the choice of  $\alpha$  as long as we are in the Newtonian regime ( $M \sim 10^{17} M_\odot$ ) and the mass of the system varies minimally.

Soliton + nfw,  $M = 2e+15 M_\odot$ ,  $\rho_c = 3.64e+08 M_\odot/kpc^3$ ,  $r_t = 15$  kpc,  $\alpha = 3$

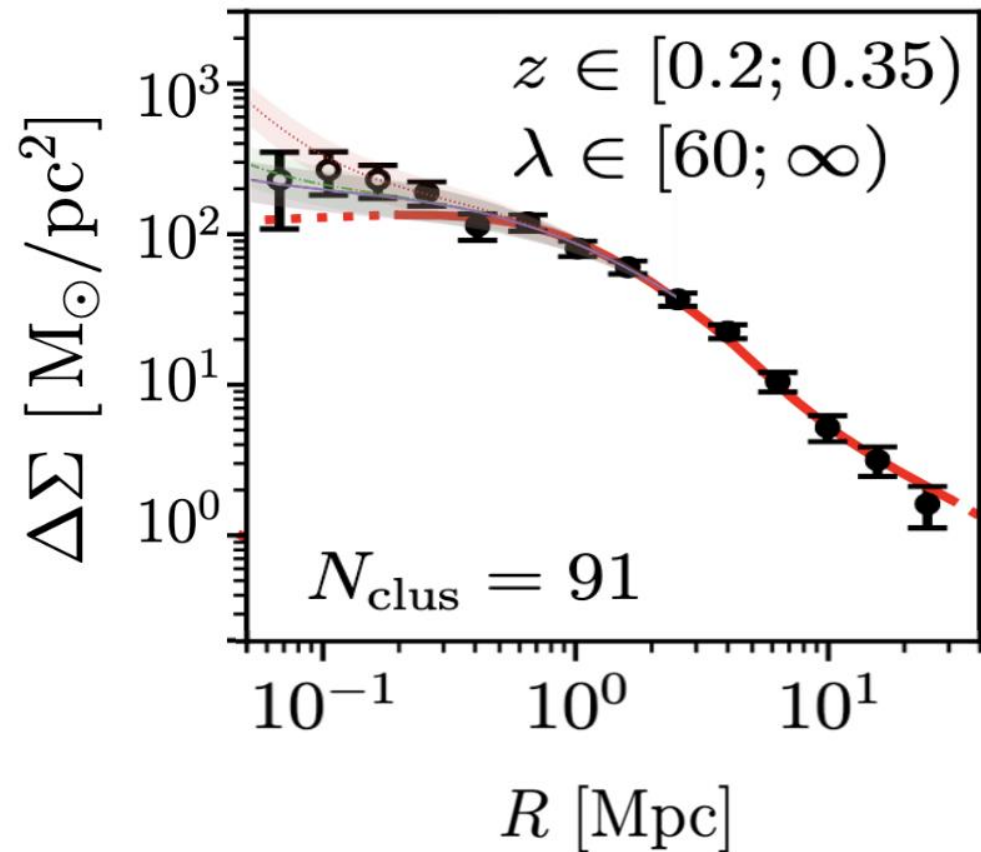


# Study case: Halo $M \sim 10^{15} M_{\odot}$



- $\alpha=1, r_a=5.00\text{kpc}$
- $\alpha=1, r_a=15.00\text{kpc}$
- $\alpha=3, r_a=5.00\text{kpc}$
- $\alpha=3, r_a=15.00\text{kpc}$
- nfw

Halo $M = 2 \cdot 10^{15} M_{\odot}$						
$\alpha$	$r_a$ (kpc)	$r_t$ (kpc)	$\rho_c$ ( $M_{\odot}/\text{kpc}^3$ )	$M_{sol}$ ( $M_{\odot}$ )	$f_{sol}$ (%)	$\Delta M_h$ %
1	5	10.90	$1.02 \cdot 10^8$	$3.31 \cdot 10^{11}$	0.016	$8.28 \cdot 10^{-8}$
1	15	32.06	$3.26 \cdot 10^7$	$2.75 \cdot 10^{12}$	0.137	$6.15 \cdot 10^{-8}$
3	5	14.50	$3.64 \cdot 10^8$	$1.75 \cdot 10^{12}$	0.087	0.058
3	15	43.36	$1.14 \cdot 10^8$	$1.48 \cdot 10^{13}$	0.74	0.49



Comparison with Andrew B. Newman, Tommaso Treu, Richard S. Ellis, and David J. Sand, 2013

Comparison with Dark Energy Survey Year 1 Results: Weak Lensing Mass Calibration of redMaPPer Galaxy Clusters 2018

# Another approach: FDM granules

In  $\psi$ DM simulations ( $\sim$ Mpc size boxes, Schive et al. 2014)

Small halos have large granule size  $l_\sigma \propto M^{-1/3}$

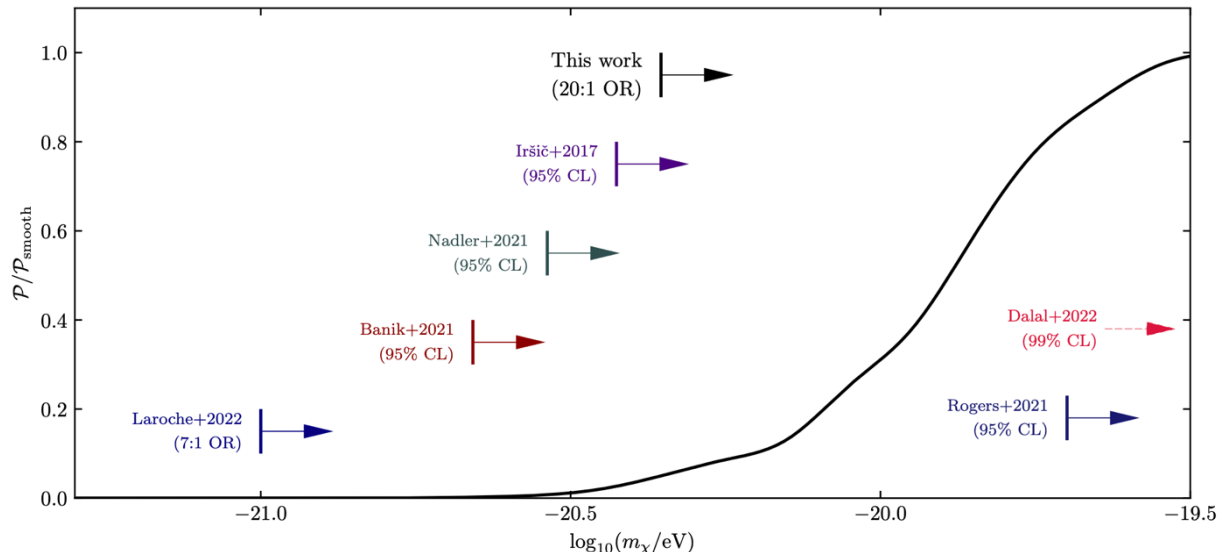
e.g. central soliton core  $r_c \sim 300$  pc and mass  $\sim 10^{8.5} M_\odot$ , granules of mass  $10^6 M_\odot$

Model granule size:  $l_\sigma = \hbar/m_a \sigma_v$

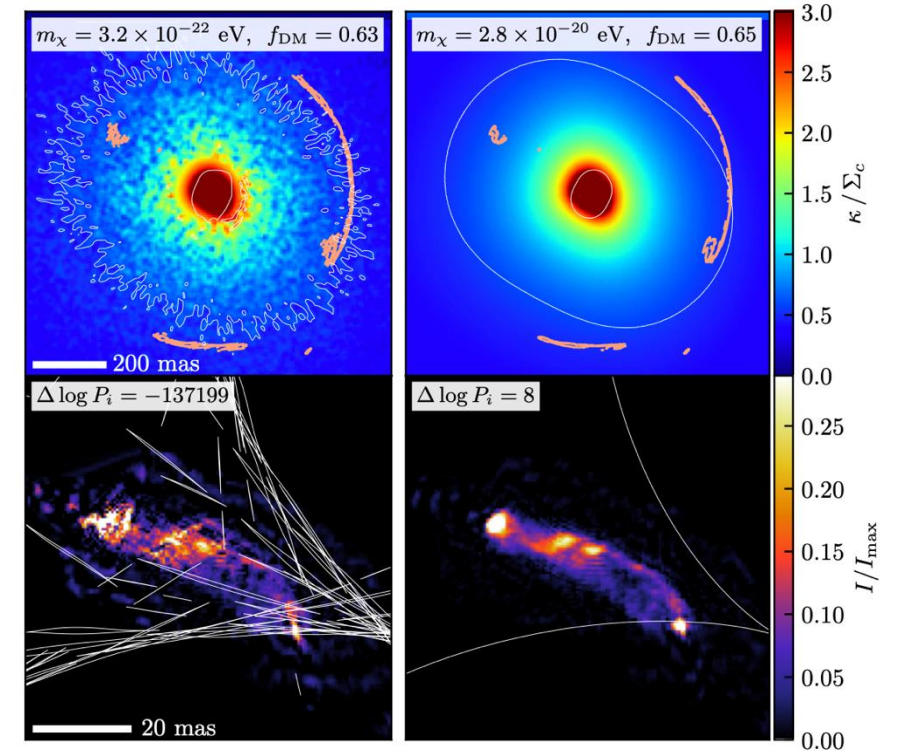
Variance of the granule density field:  $\langle \delta \Sigma^2(r_\perp) \rangle = \sqrt{\pi} \langle l_\sigma \rangle \int dz \langle \rho_\psi(r) \rangle$

Observations with VLBI interferometer in radio (Powell et al. 2023)

=> undistinguishable from CDM at  $m_\chi > 4.4 \times 10^{-21}$  eV



Chan et al. 2020, Powell et al. 2023





# Take home messages

1. Combination of WL+SL+Kinematics is used to measure the slope  $\gamma$  of the dark matter density profile from galaxies to clusters
2. Uncertain stellar masses still impede firm conclusions on  $\gamma$
3. Wide imaging surveys (eg. Euclid, LSST) will provide large samples of galaxies and clusters for stacking => selection function!
4. Future observations (ELT) will constrain the subhalo mass function
5. Axion model is promising and compatible with cluster constraints so far

# Some Definitions

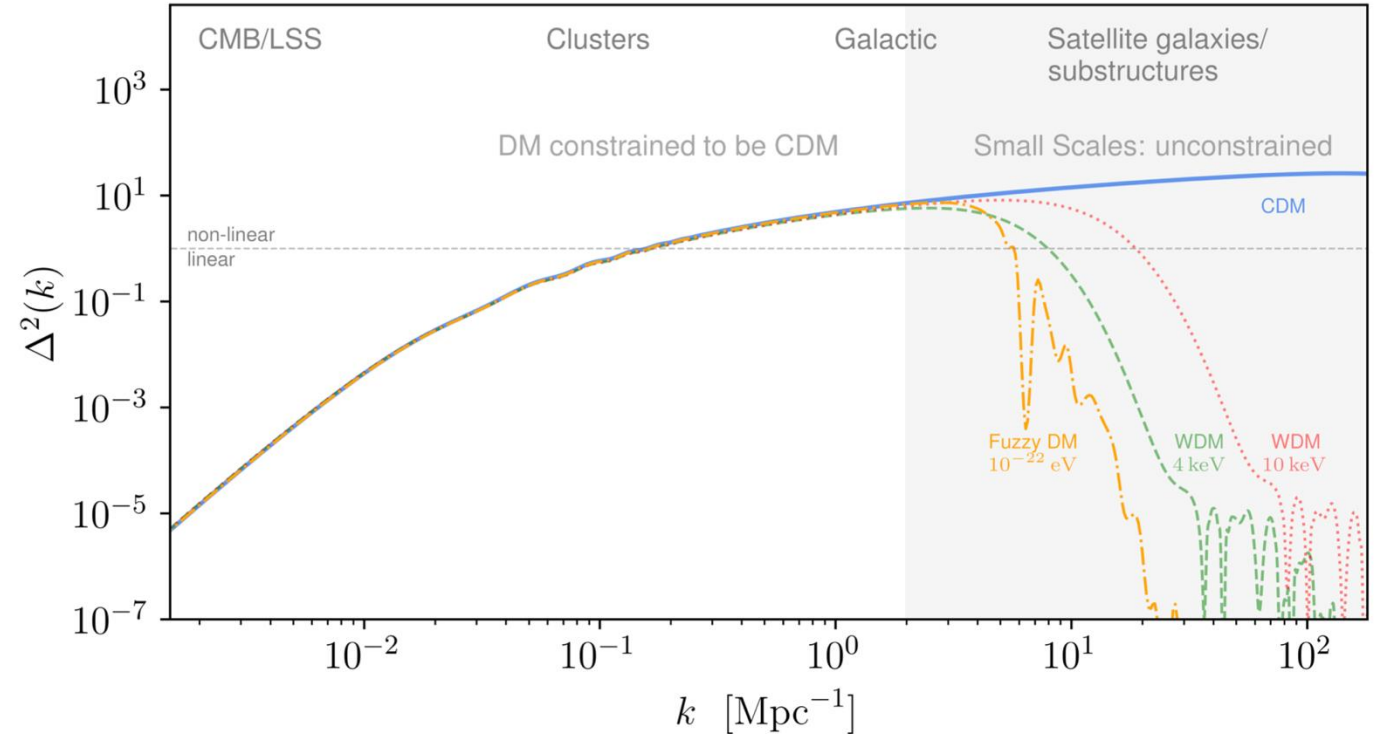
Ferreira E. 2021

- Transfer function

$$T_{\text{matter}}(k)^2 = \frac{P_{\text{WDM}}(k)}{P_{\text{CDM}}(k)}$$

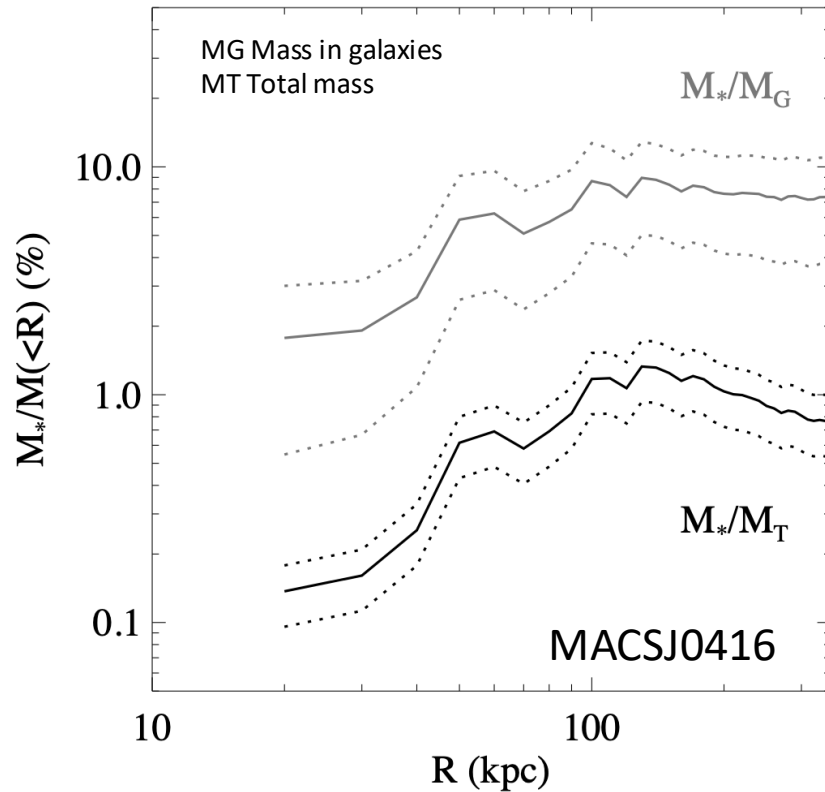
- Half-mode scale  $\lambda_{\text{hm}}$   
=> where the TF = 1/2

- Half-mode mass  $M_{\text{hm}}$   
=> the mass in a halo of scale  $\lambda_{\text{hm}}$   
=>  $M_{\text{hm}} = 0$  means CDM model

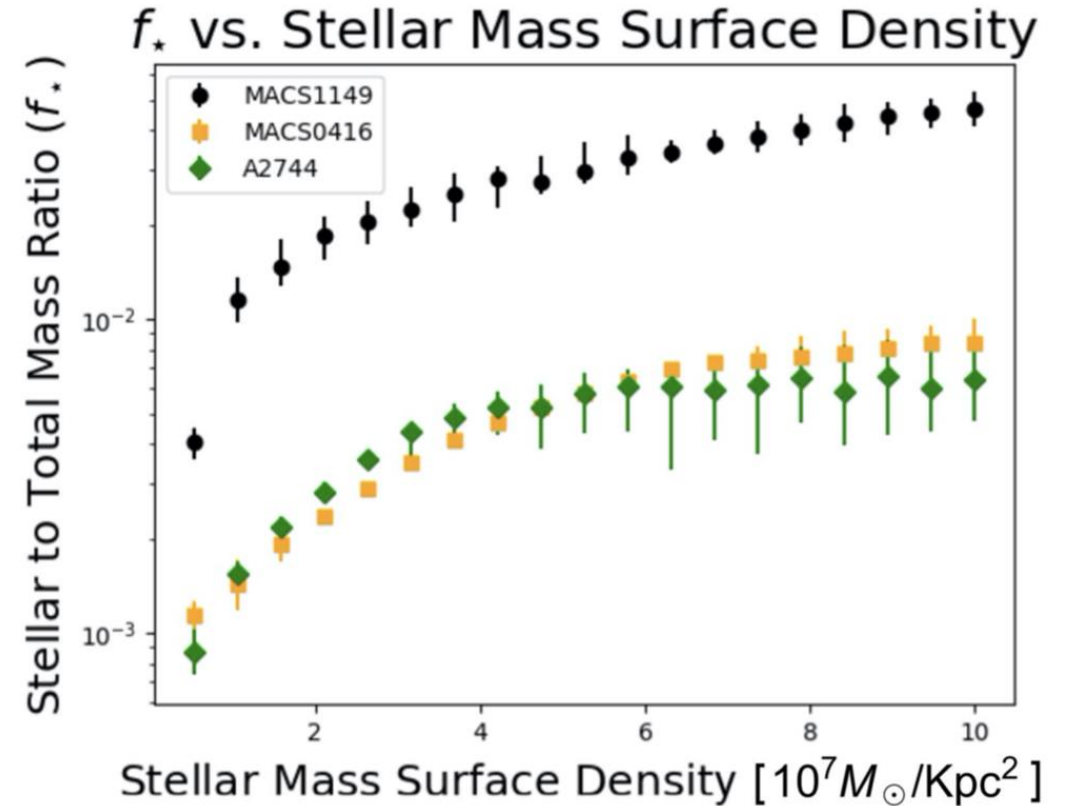


# Cluster profile ...

Grillo et al. 2015



Finney, E.Q. et al. 2018



=> Forward modeling can give insight on 1) DM smooth component, 2) substructures and 3) baryon components

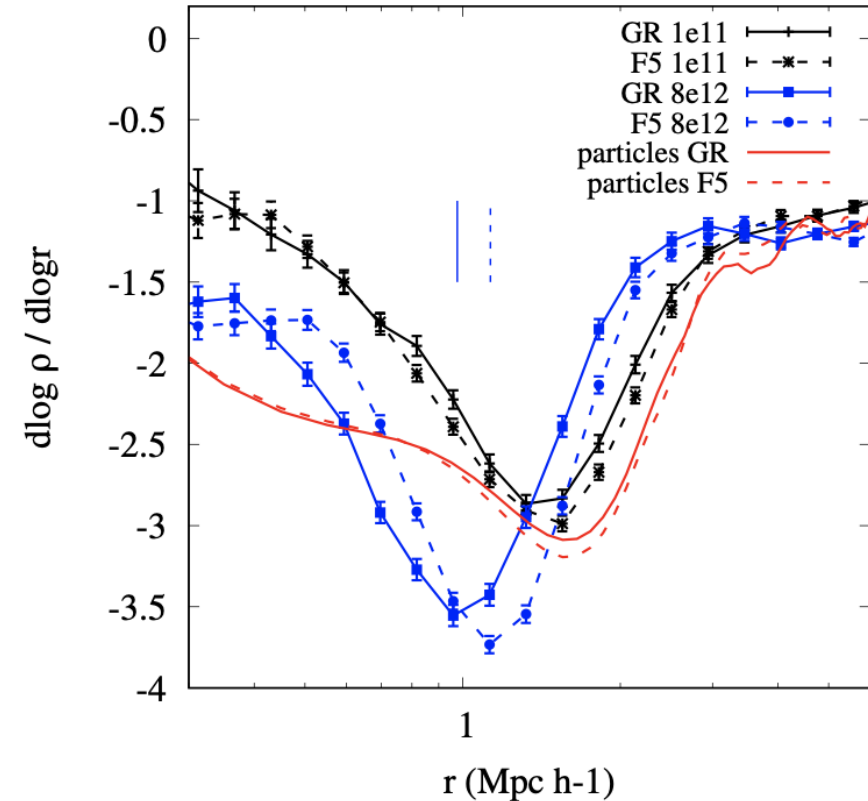
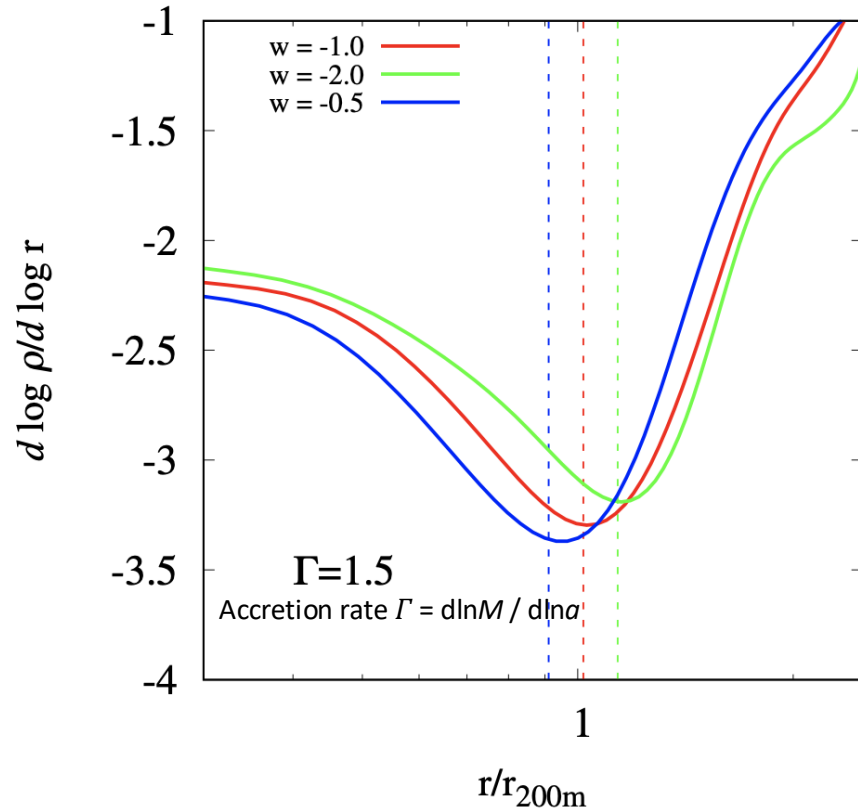


# Splashback radius in simulations

Stacked clusters at  $z=0$  with  $M_{\text{vir}} = 1 - 4 \times 10^{14} M_{\odot}/h$

ECOSMOG-V & ECOSMOG-fR N-body code (Li B., et al. 2011, 2013)

Adhikari et al. 2018



Equation of motion of a shell at radius  $r$

$$\ddot{r} = -\frac{GM(r)}{r^2} - \frac{H_0^2}{2} \Omega_{DE} (1 + 3w) r^{-2-3w}$$

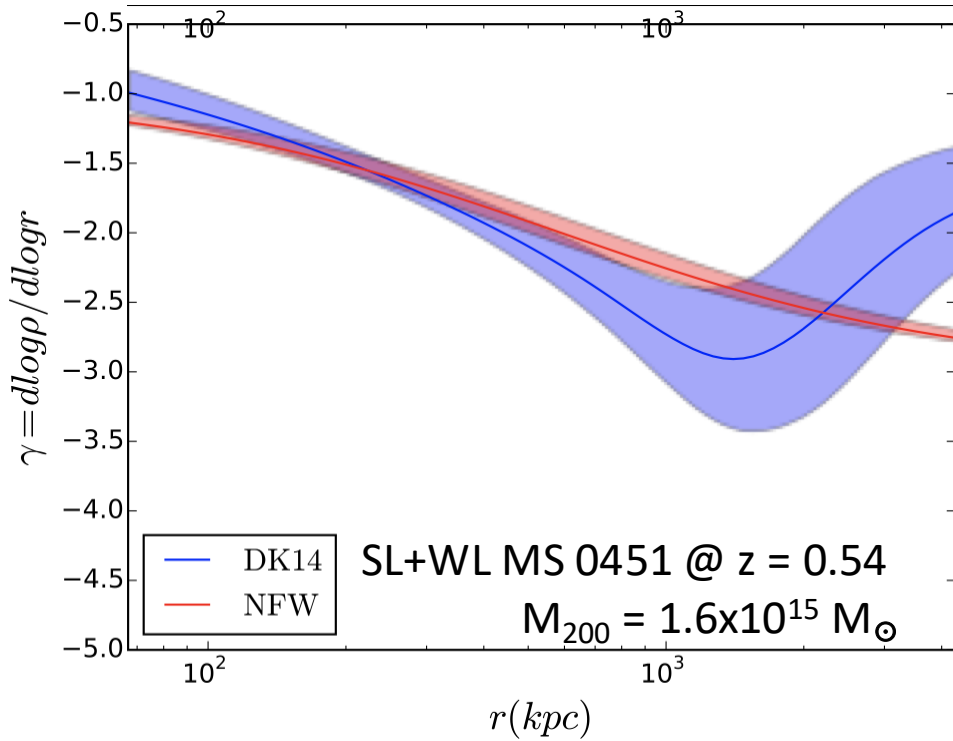
⇒ SB radius sensitive <10%

⇒ Dependency on concentration, galaxy bias... (More et al. 2016)

⇒ Precision achievable with Euclid / Roman / CSST?

# Splashback radius in observations

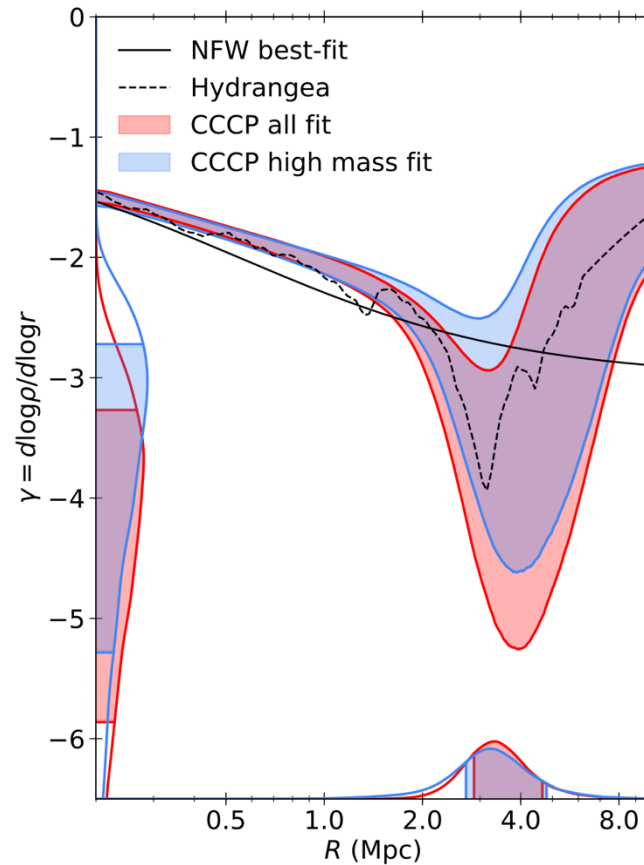
Tam et al. 2020



⇒ WL measurements not yet at the required precision compared to GC

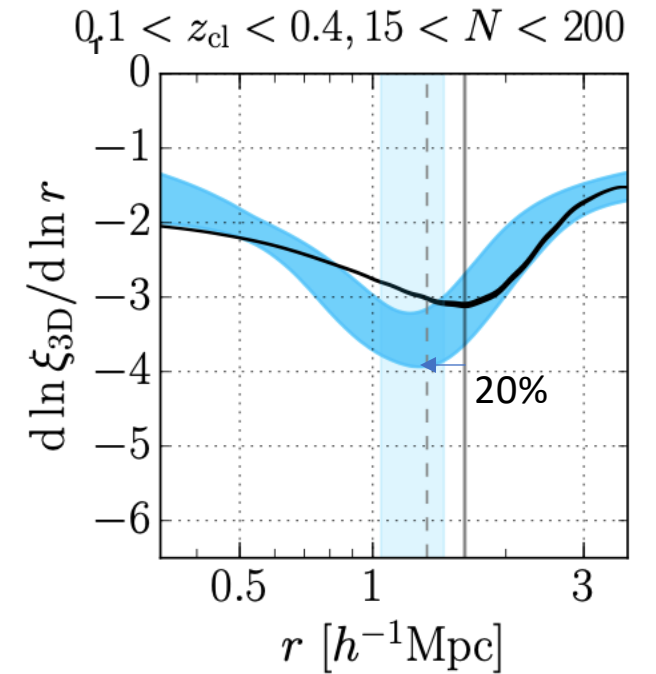
⇒ WL stacking in Euclid / Roman / CSST?

Contigiani et al. 2019



WL stack of 13 clusters @  $z \sim 0.3$   
 $M_{200} > 1.6 \times 10^{14} M_{\odot}$

Murata et al. 2020



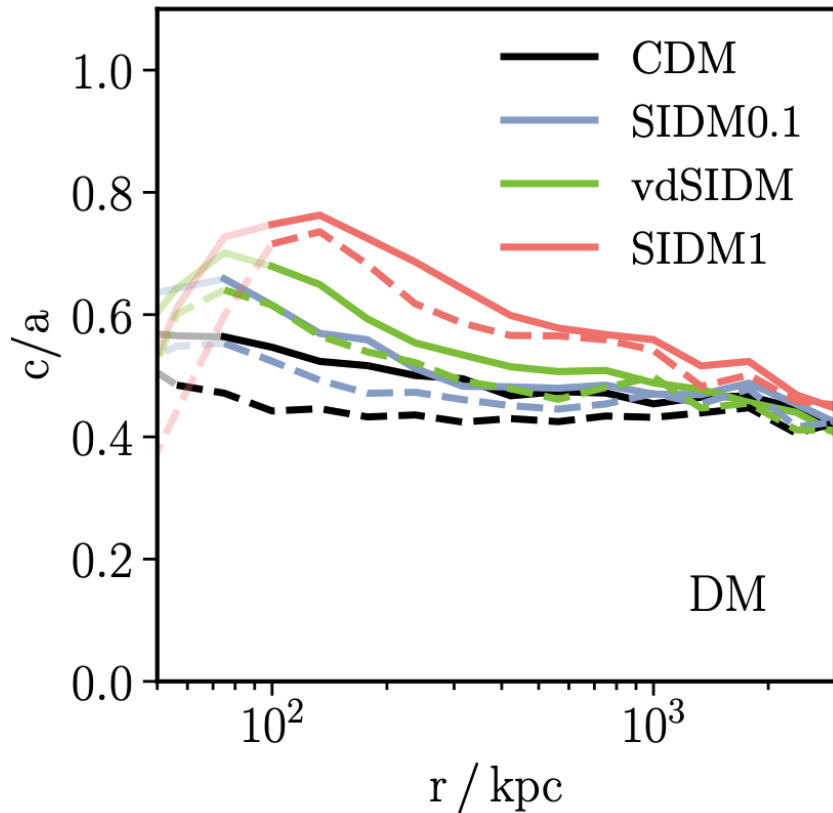
Cluster-galaxies xcorr in HSC  
3000 clusters

# ...And cluster shape

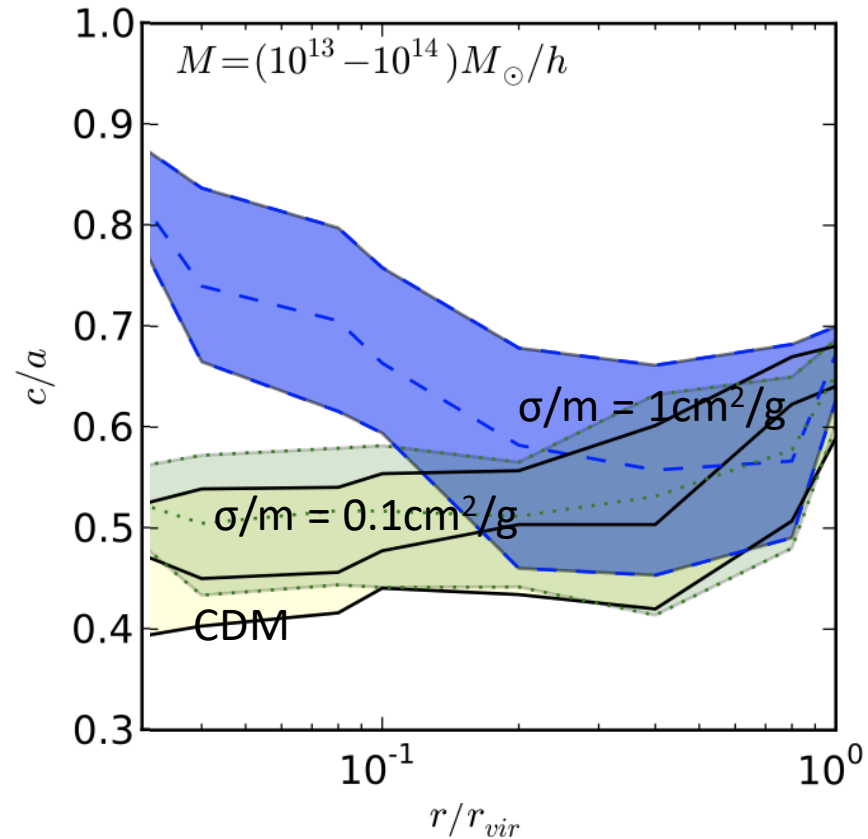
Self-interacting dark matter tends to produce rounder clusters

Simulations

Robertson et al. 2019



Peter et al. 2013





# Cluster ellipticity

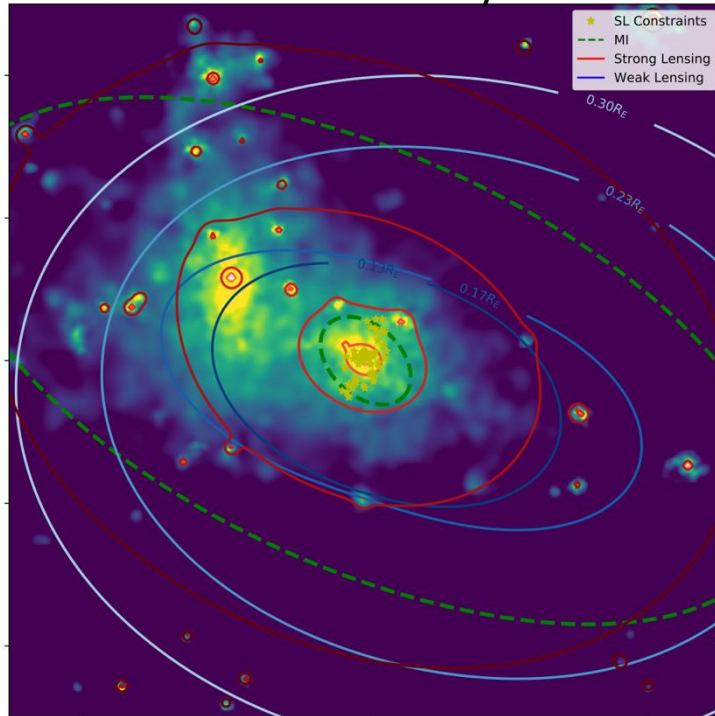
But strong and weak lensing observations can be biased

⇒ WL shape noise and LSS contribute to make lensing estimates rounder

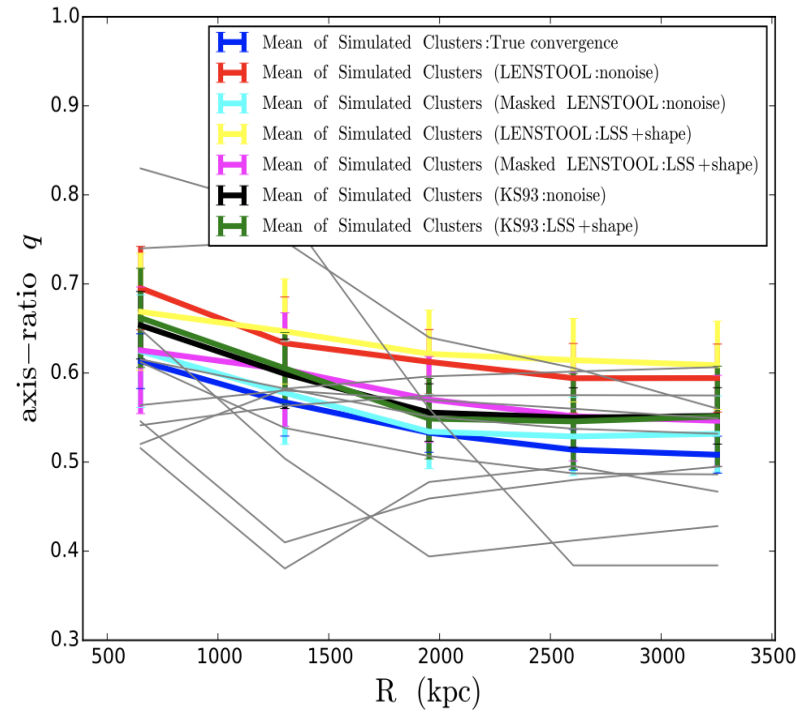
⇒ Hybrid-Lenstool joint SL+WL modeling can help

observations

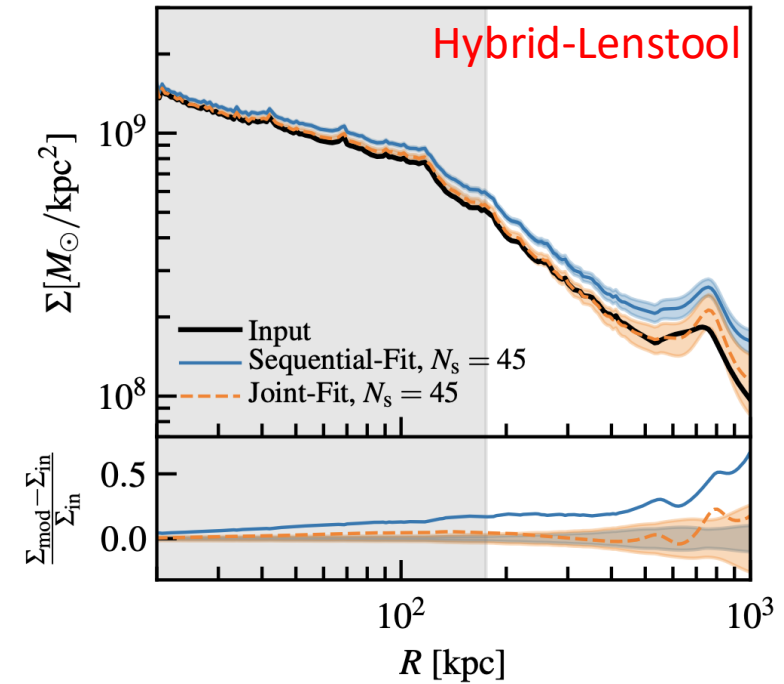
Harvey et al. 2020



Tam et al. 2020

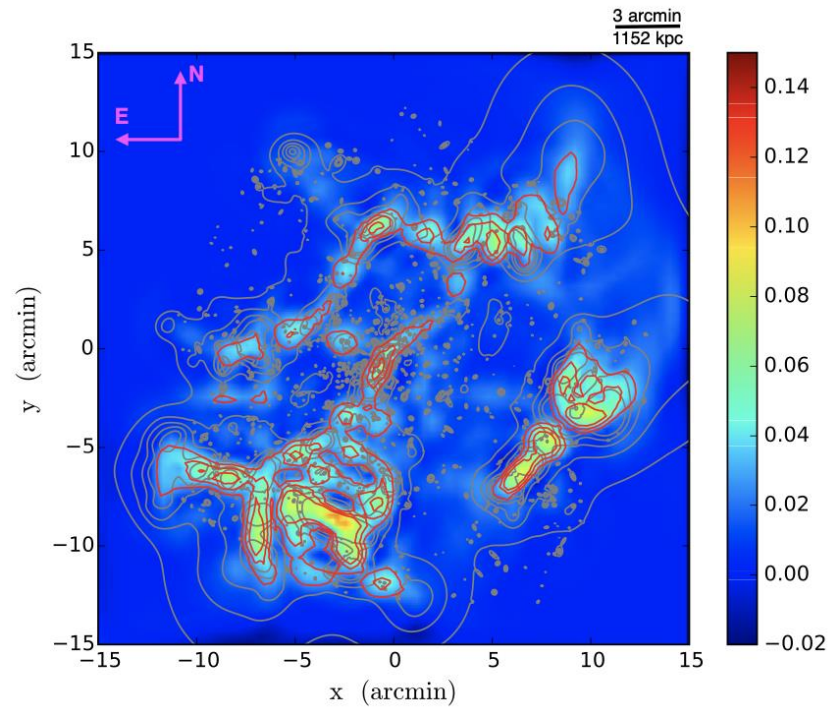


Niemiec et al. 2020

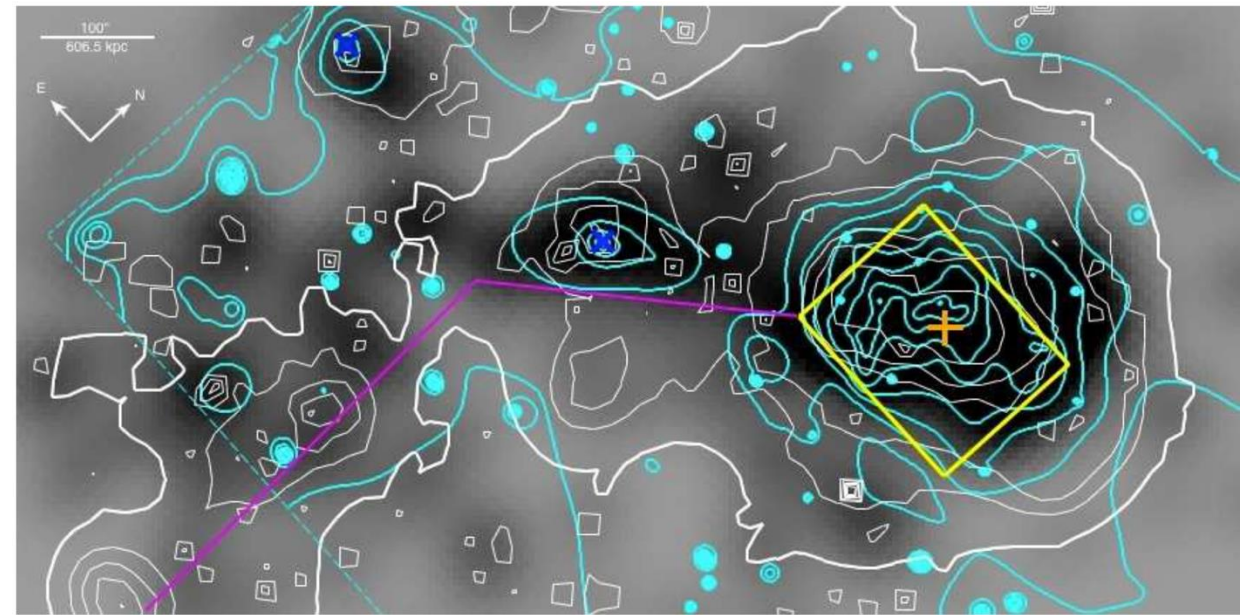


# And filaments

Tam et al. 2020  
Direct detection of filaments



Jauzac et al. 2012



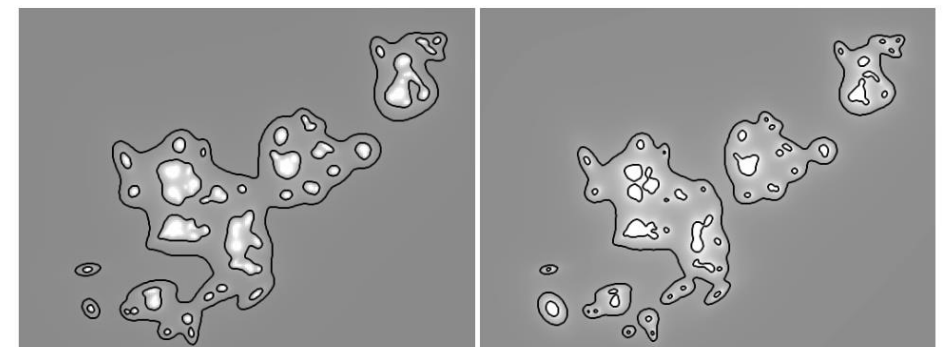
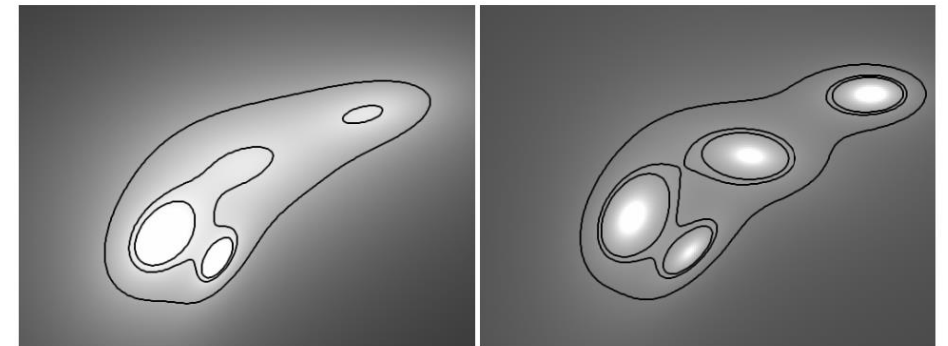
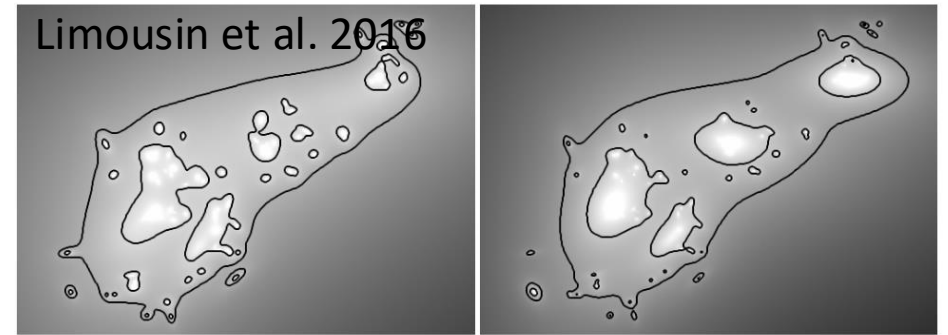
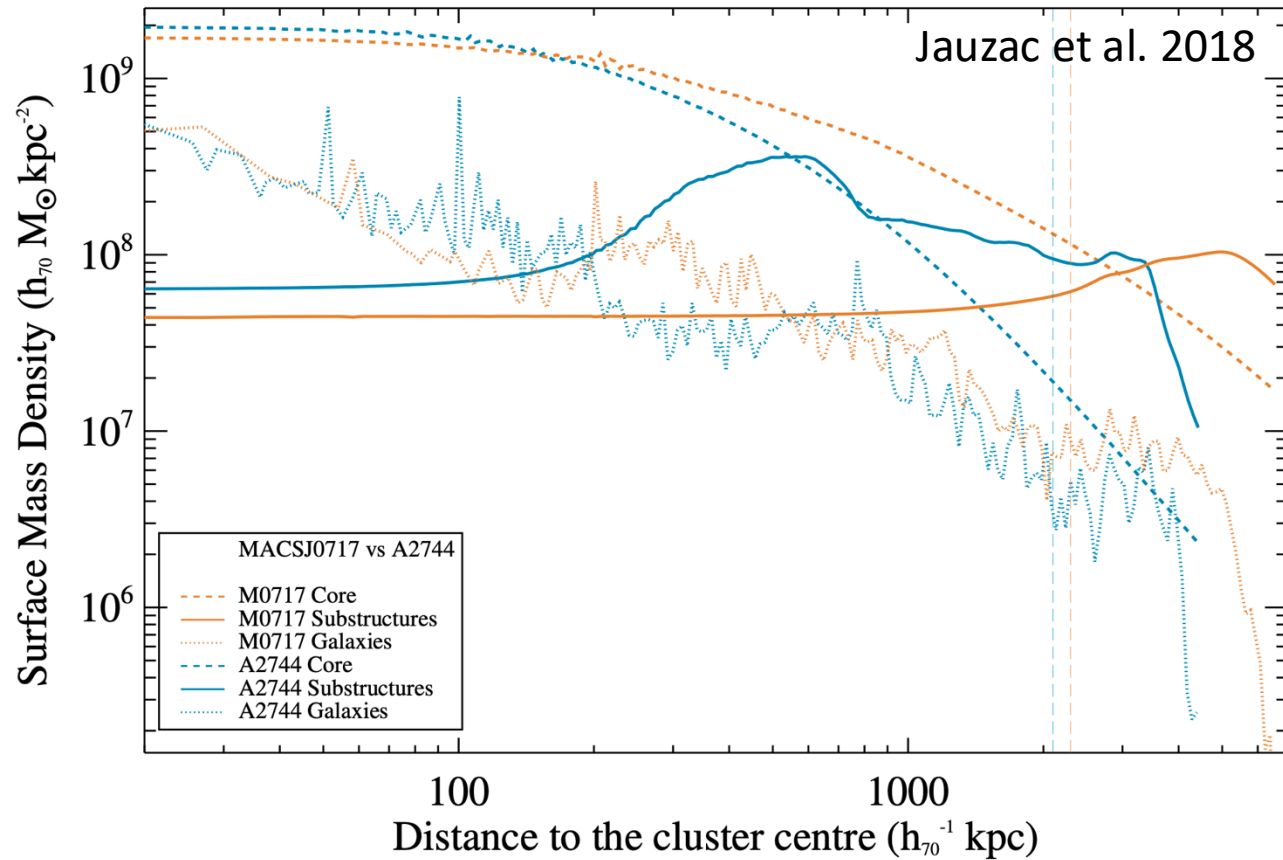
6x3 HST ACS mosaic,  $\sim 50$  gal/arcmin<sup>2</sup>

⇒ WL stacking in Euclid / CSST?

$$Q \equiv \alpha_0 Q^{(0)} + \alpha_1 Q^{(1)} + \alpha_2 Q^{(2)},$$

Aperture Multipole Moments (Schneider & Bartelmann 1997)

# Cluster Substructures



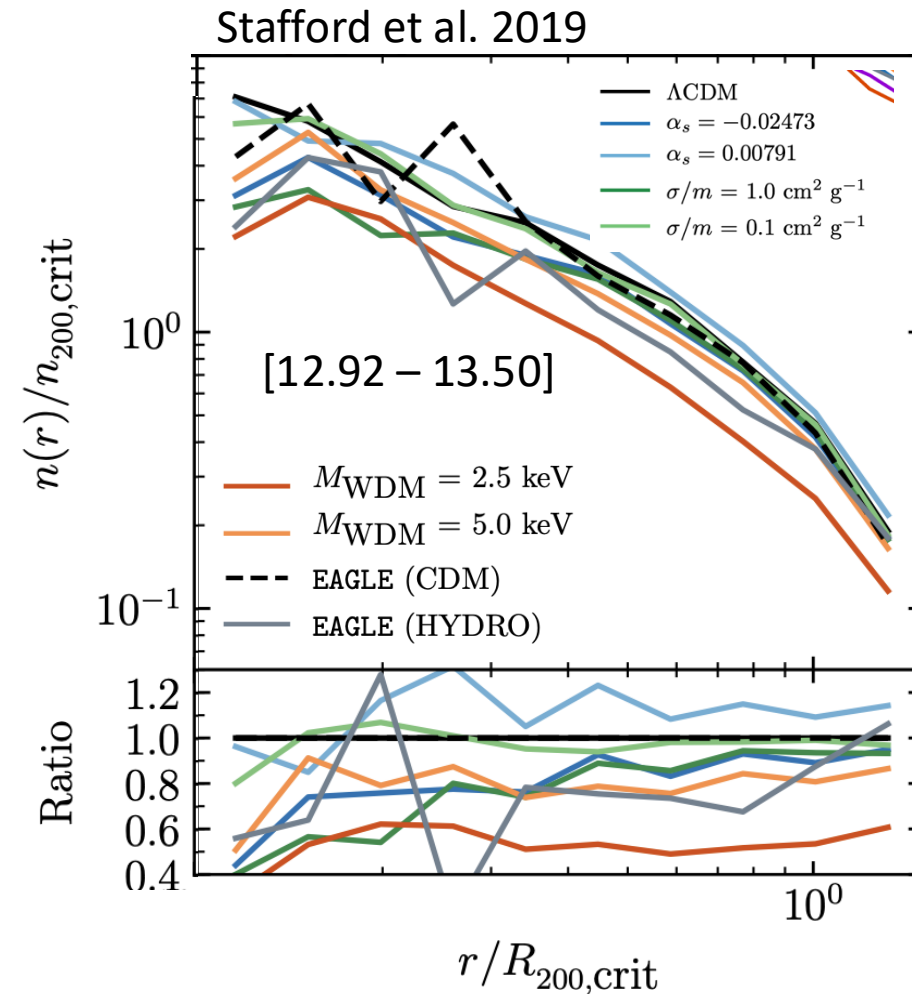
=> Forward modeling can give insight on DM and baryon components

=> Degeneracy between subhalos and host



# Cluster SubStructures

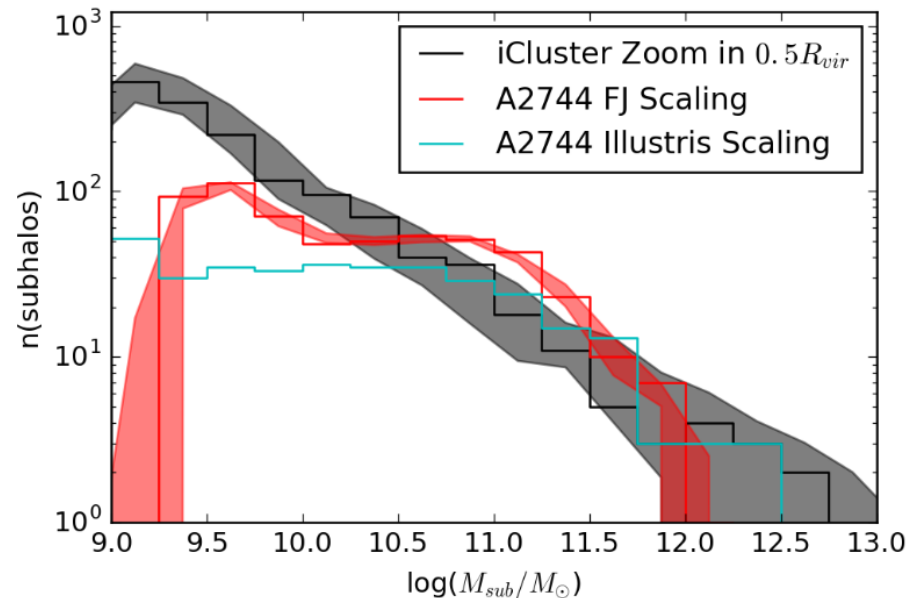
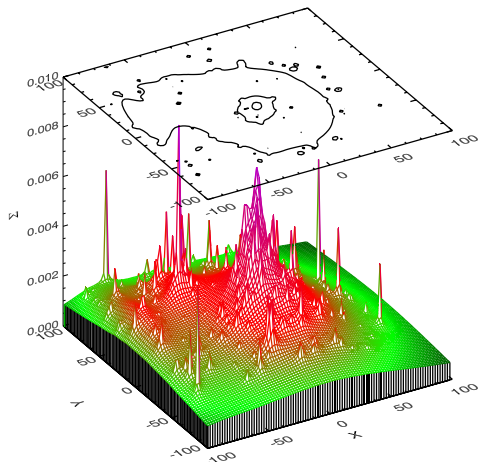
- Light 2.5keV WDM has the lowest number counts, because this model has less low mass subhalos
- $\sigma/m = 1.0 \text{ cm}^2/\text{g}$  SIDM has low counts at small radius because of heat transfer between 'hot' host DM, and 'cool' subhalo DM + enhanced tidal stripping because of cored density profile of subhaloes
- f(R) cosmology could also impact the mass segregation function (Arnolds & Li, 2019), because f(R)-gravity increases the number of low-mass halos (not screened)



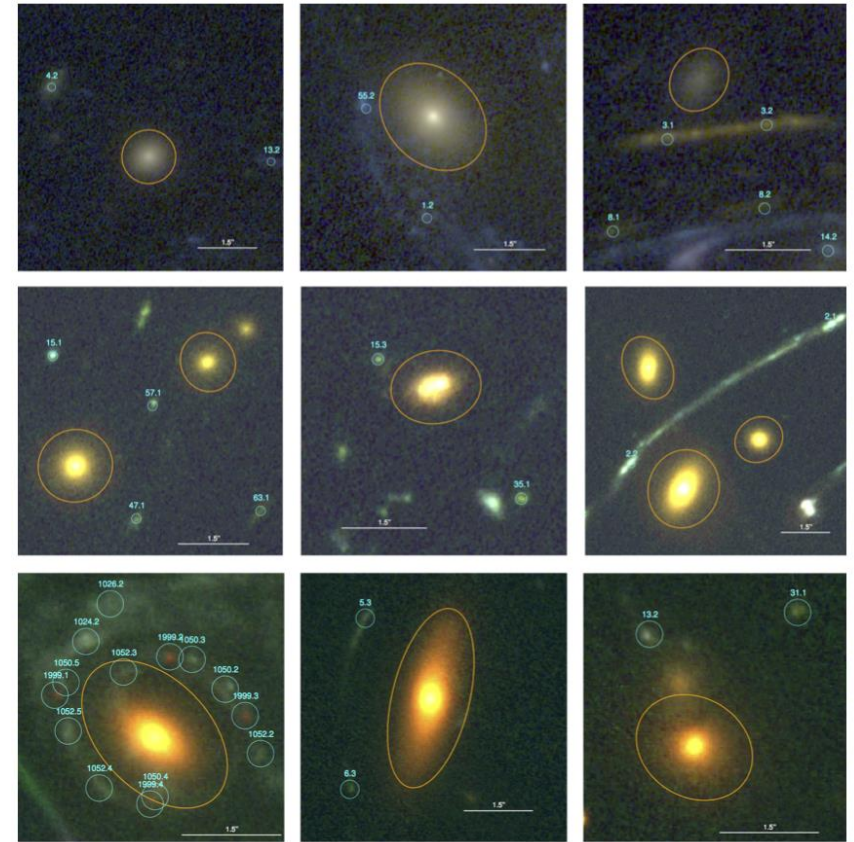
# DM tidal stripping

## *Strong-Lensing in galaxy clusters*

- Modeling of DM distribution with strong-lensing constraints
- Comparison of subhalo mass function with hydro-simulations

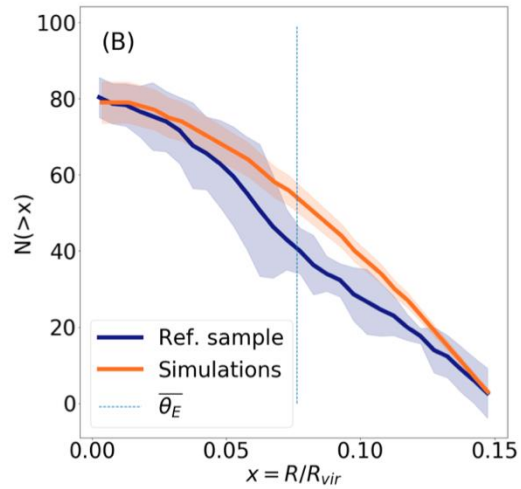


Natarajan et al. 2017

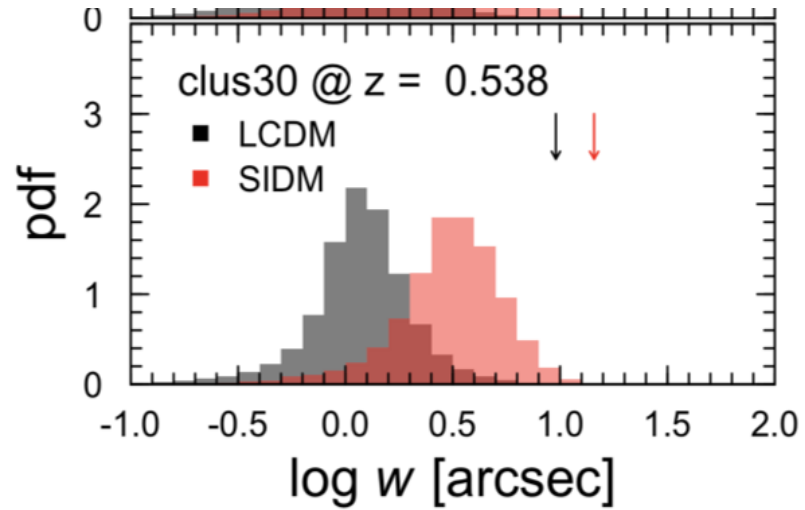


# Cluster Substructures

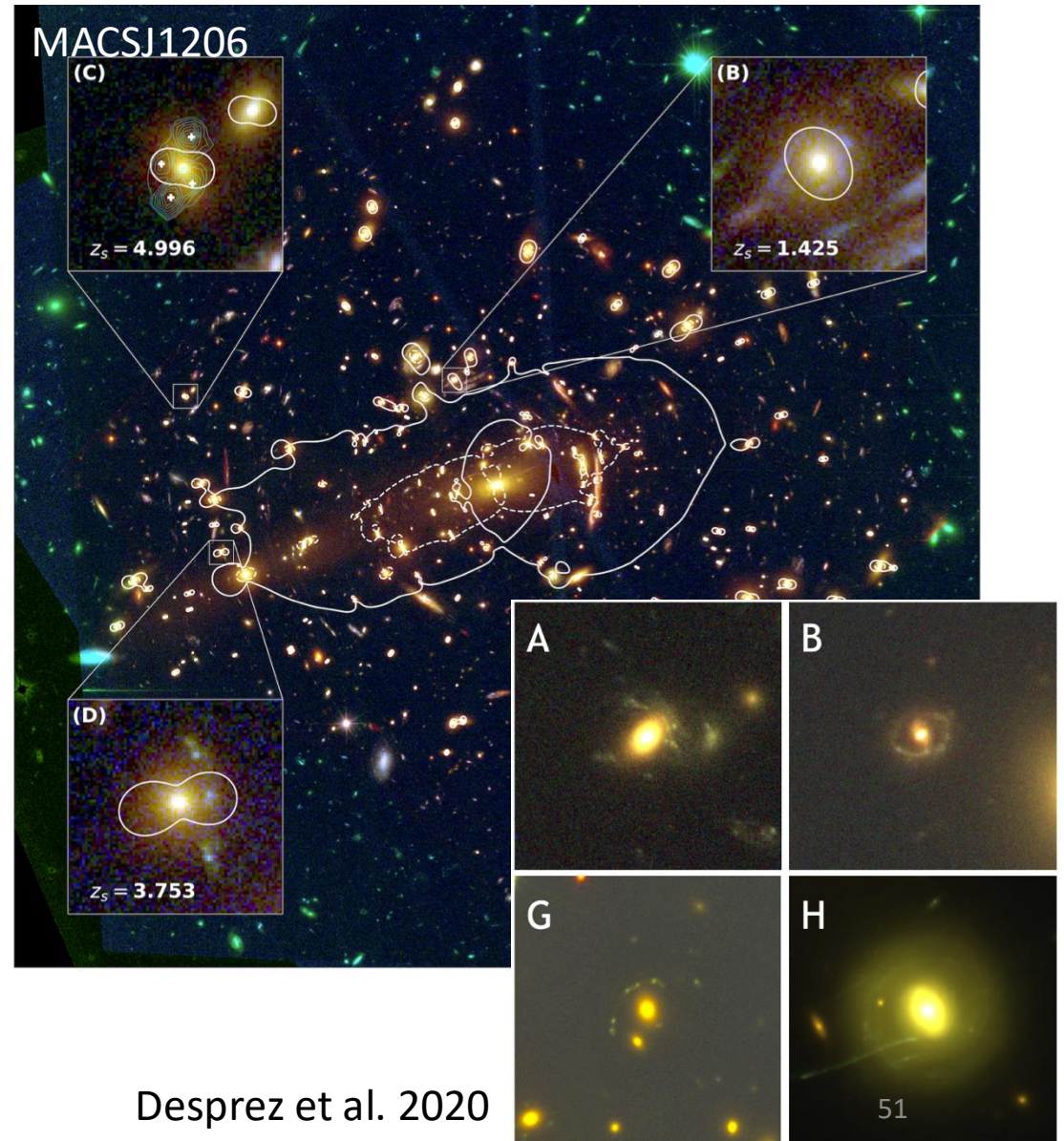
Meneghetti et al. 2020



Vega-Ferrero et al. 2020



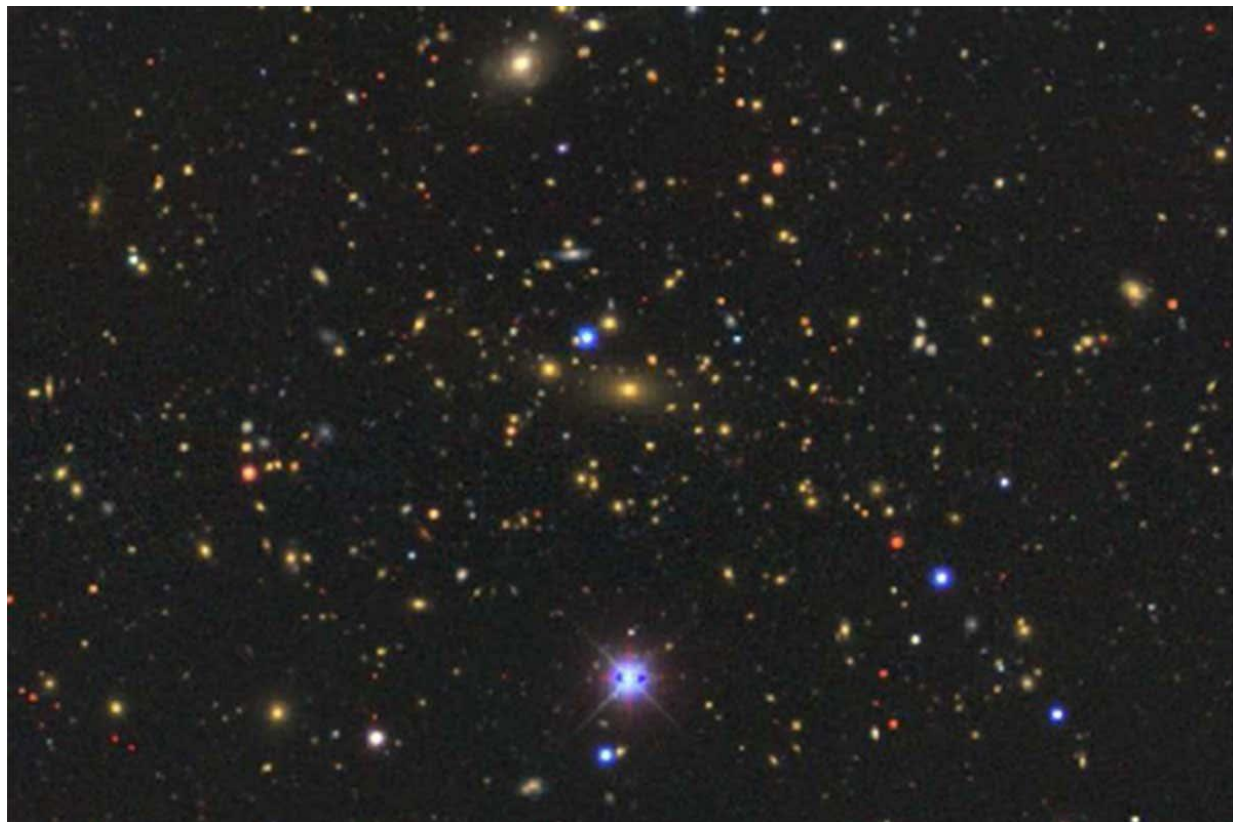
- ⇒ Enhancement of substructures at small radius
- ⇒ Substructures are more compact ( $v_{disp}$  is larger than in simulations)
- ⇒ More tidal stripping? Cored profiles? SIDM?
- ⇒ SIDM produces less arcs but they are more magnified



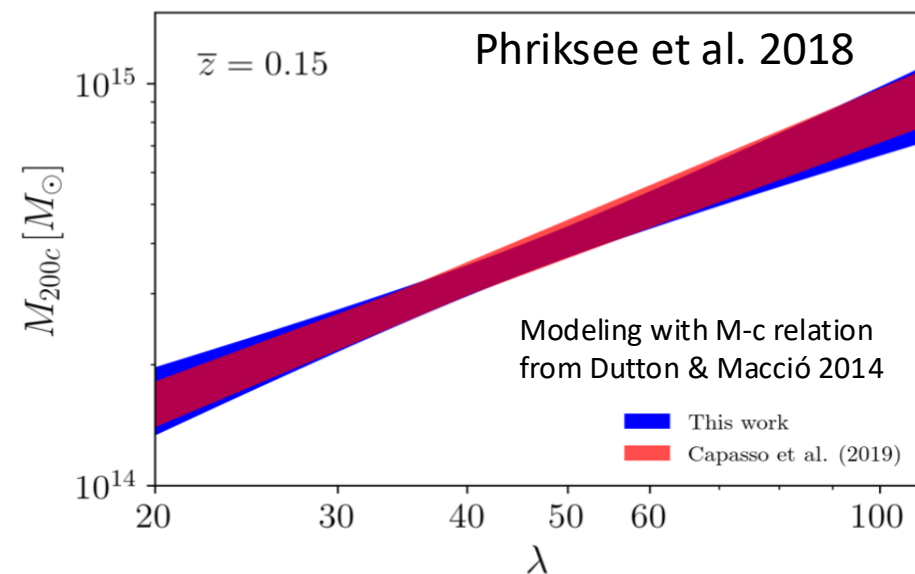
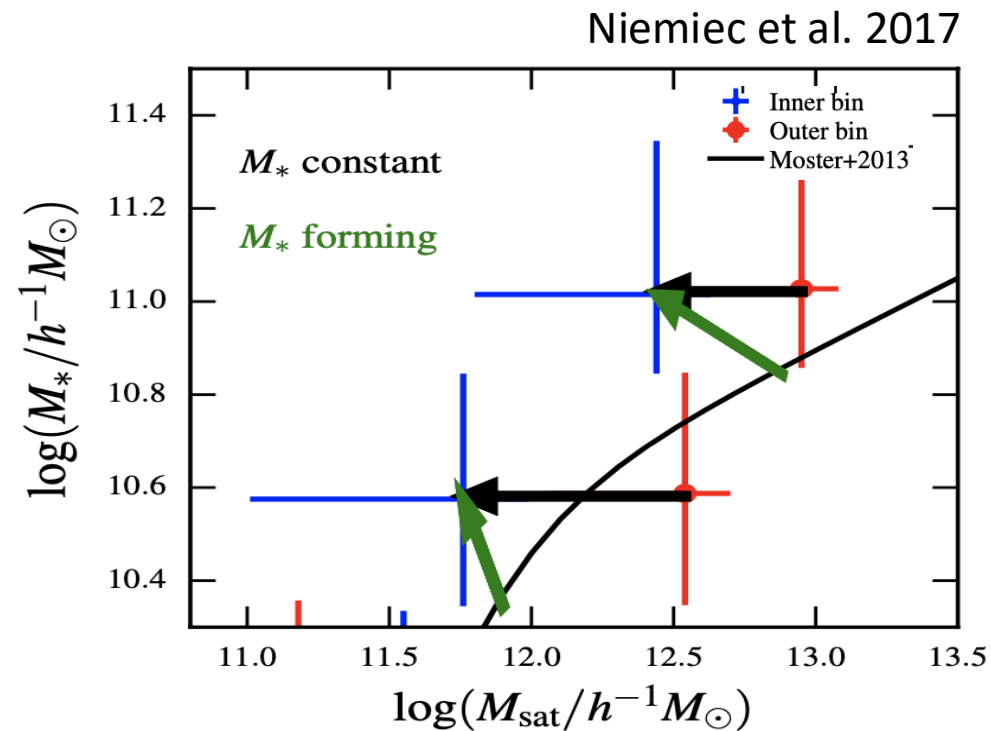


# DM tidal stripping & M-c relation

## *Stacking of weak-lensing in galaxy-clusters*

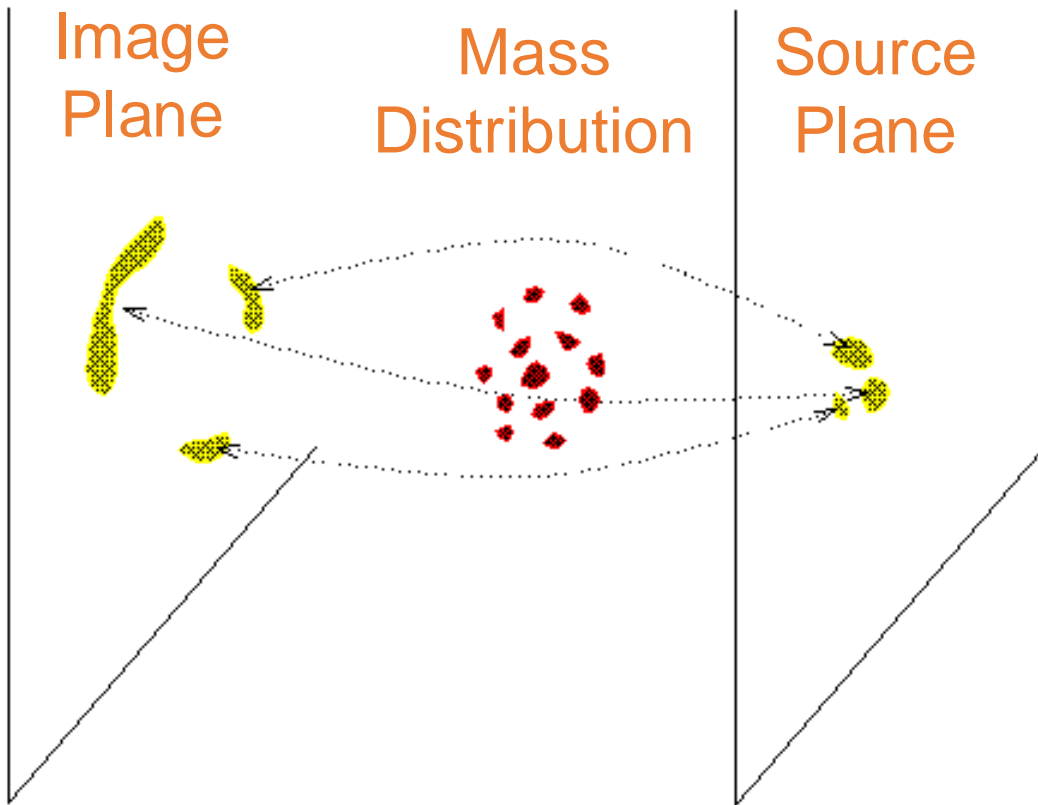


Credit: Supercluster Saraswati (DECaLS, Bagchi et al. 2017)



# Strong Lensing

Principle of “inversion” of multiple images



# Dark Matter mapping

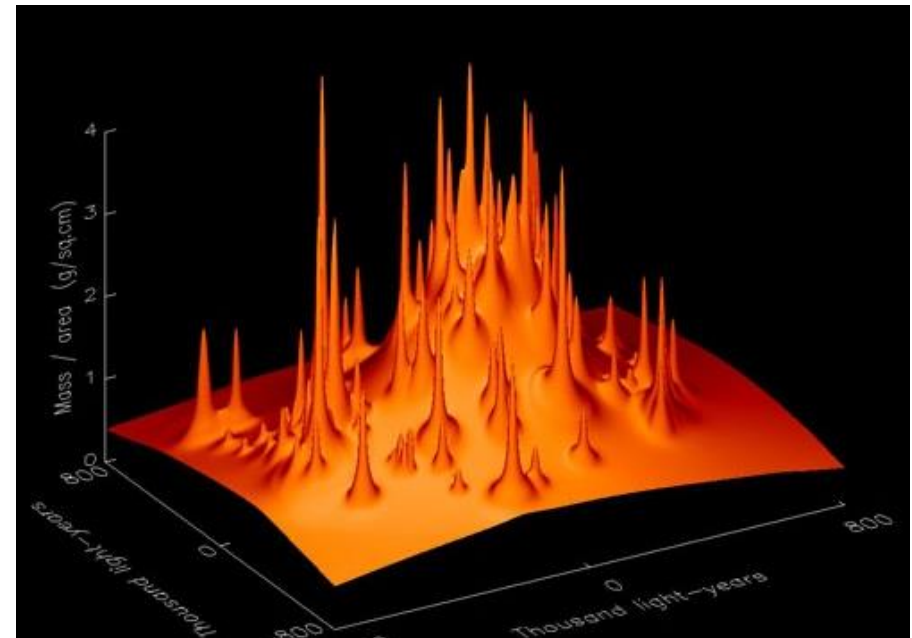


Credit: Colley & Turner (Princeton), Tyson (Lucent Technologies), HST, NASA

A background galaxy appears multiple times

Matter in galaxy clusters is distributed with a density peak in the center  
→ Dark matter + baryons

Credit: Kochanski, Dell'Antonio and Tyson (Bell Labs)





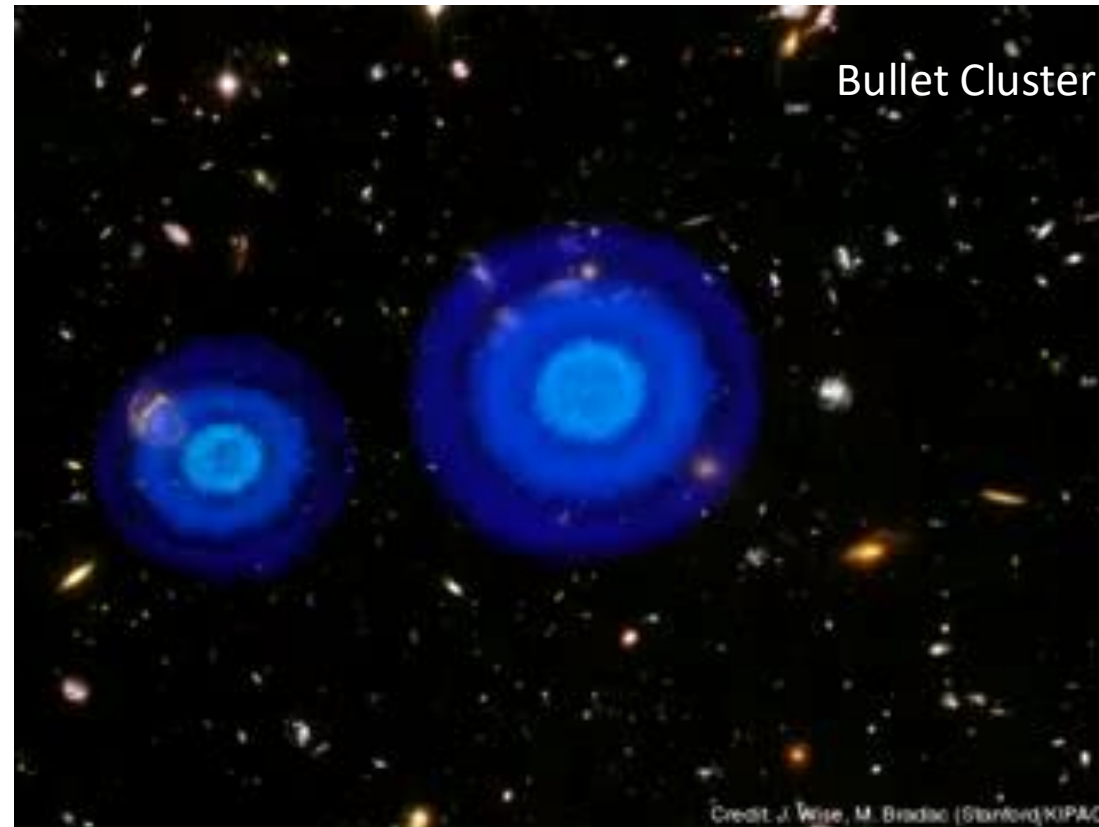
# Galaxy clusters content

## A galaxy cluster contains

- 80% dark matter
- 15% hot gas ( $\sim 10^7$  K)
- 5% stars in galaxies

## Observable

SL/WL  
Xray/SZ  
Kinematics



Credit: X-ray: NASA/CXC/CfA/M.Markevitch et al.; Optical: NASA/STScI; Magellan/U.Arizona/D.Clowe et al.  
Lensing Map: NASA/STScI; ESO WFI; Magellan/U.Arizona/D.Clowe et al; Movie: KIPAC/J. White/M. Bradac

# Properties of galaxies in clusters

*Galaxies evolve in clusters in the same way  
They have similar formation history*

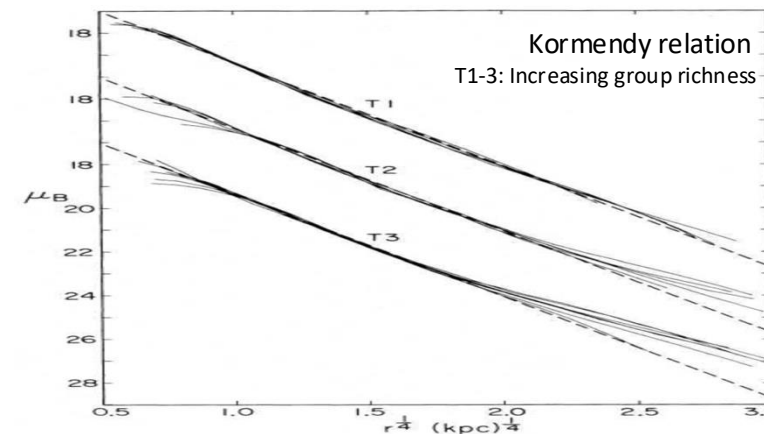
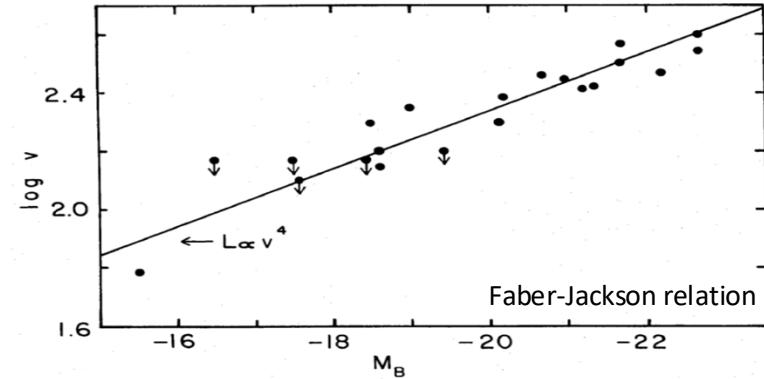
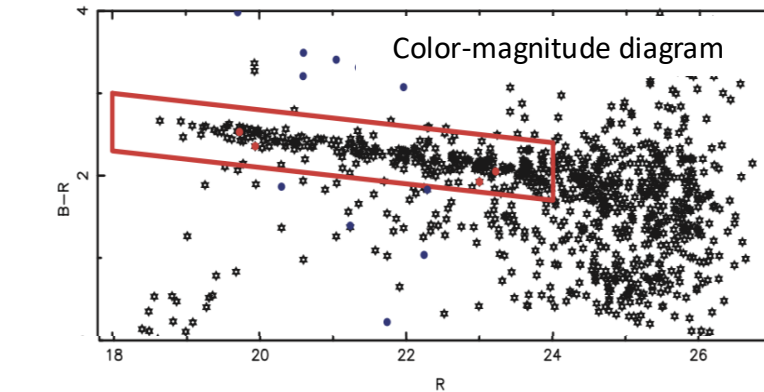
Cluster galaxies have similar colors

⇒ color-magnitude diagram

Cluster galaxies follow:

- Faber-Jackson(1976) relation between velocity and luminosity
- Kormendy(1977) relation between size and luminosity

⇒ Fundamental plane (eg. Djorgovski & Davis, 1987)



# Strong lensing modeling strategy

## Observationally motivated models

- Decomposition into halos
- Few constraints (multiple image positions)

$$\phi_{tot} = \phi_{cluster} + \sum_i \phi_{halos}^i$$

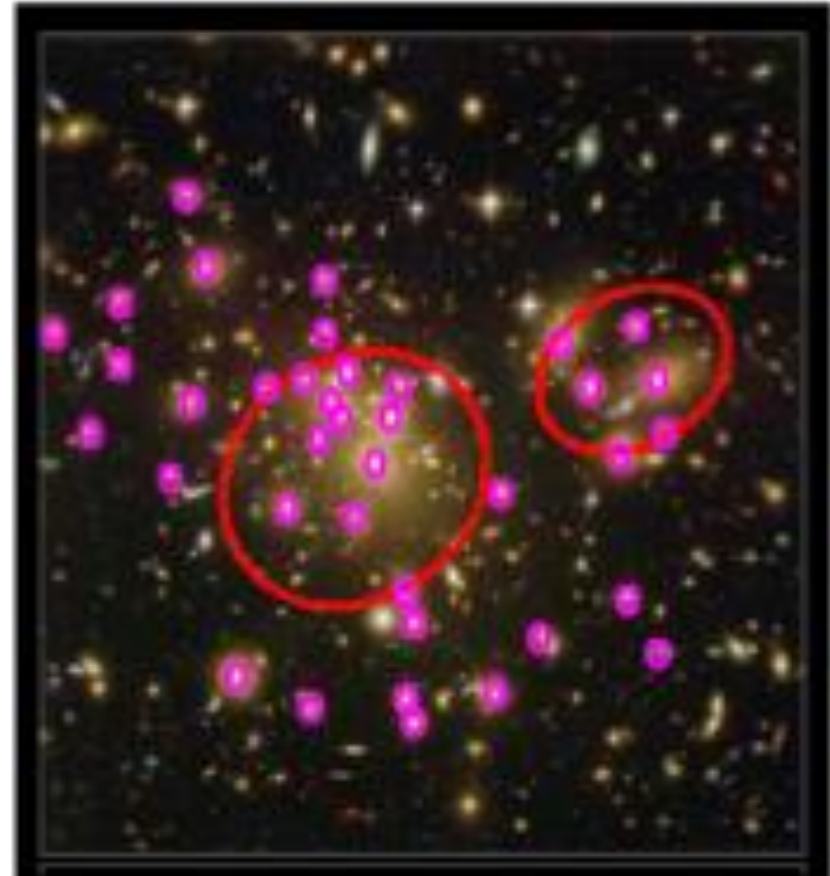
Need to scale the galaxy halo components with galaxy luminosity to limit the number of free parameters:

$$\sigma = \sigma_* \left( \frac{L}{L_*} \right)^{1/4} \quad r_{cut} = r_{cut}^* \left( \frac{L}{L_*} \right)^\eta$$

$$\frac{M}{L} \propto L^{\eta-1/2}$$

$$\eta = 1/2 \quad \text{Constant M/L}$$

$$\eta = 0.8 \quad \text{FP scaling}$$





# usual matter density profiles

Isothermal sphere

$$\rho = \rho_0 / \tilde{R}$$

$$\rho_0 = \frac{\sigma^2}{2\pi G}$$

PIEMD (Kassiola, 1993)

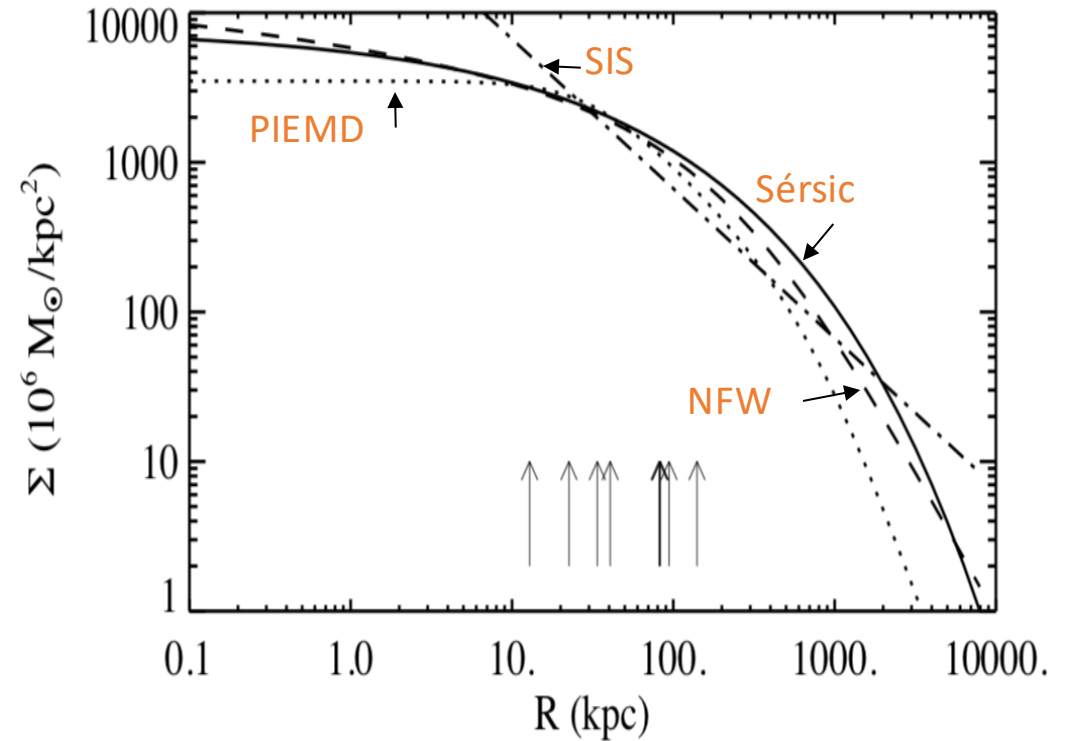
$$\rho = \frac{\rho_0}{\left(1 + \frac{\tilde{R}^2}{r_c^2}\right) \left(1 + \frac{\tilde{R}^2}{r_{cut}^2}\right)}$$

$$\rho_0 = \frac{\sigma_\infty^2}{2\pi G r_c^2}$$

Navarro, Frenk, White (1996)

$$\rho = \frac{\delta_c \rho_c}{\frac{\tilde{R}}{r_s} \left(1 + \frac{\tilde{R}}{r_s}\right)^2}$$

$$\delta_c = \frac{200}{3} \frac{c^3}{\ln(1+c) - c/(1+c)}$$

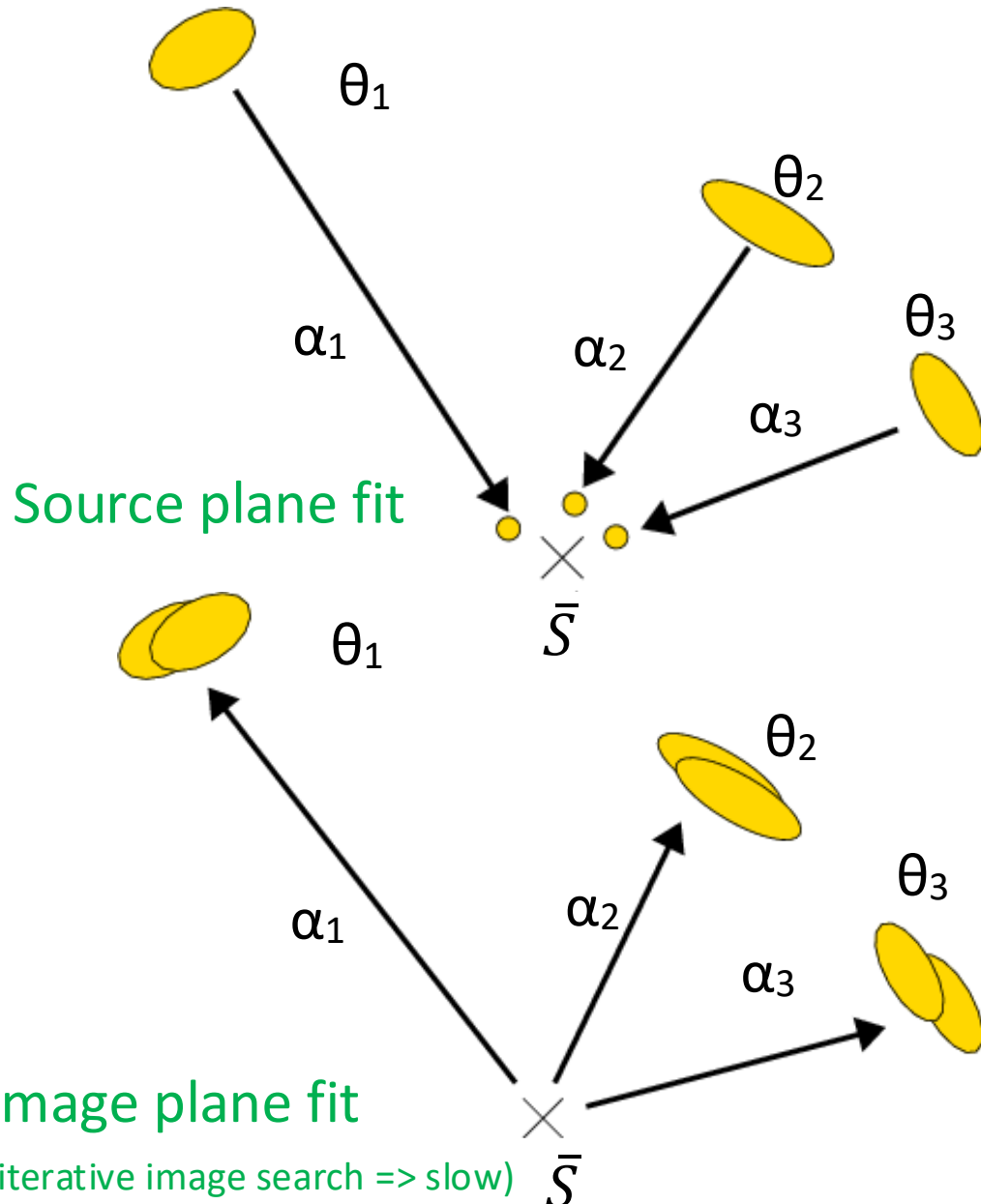


Sérsic (1963)

$$\ln \left( \frac{\Sigma}{\Sigma_e} \right) = -bn \left[ \left( \frac{\tilde{R}}{R_e} \right)^{\frac{1}{n}} - 1 \right]$$

$$bn \simeq 2n - \frac{1}{3} + \frac{4}{405n} + \frac{46}{25515n^2} d$$

# Strong lensing fit of a single source



- The model is validated when predicted and observed images fall at the same location
- In practice, a RMS  $\sim 0.5''$  for about 20-100 multiple images is usual
- Source plane fit: a few computing days

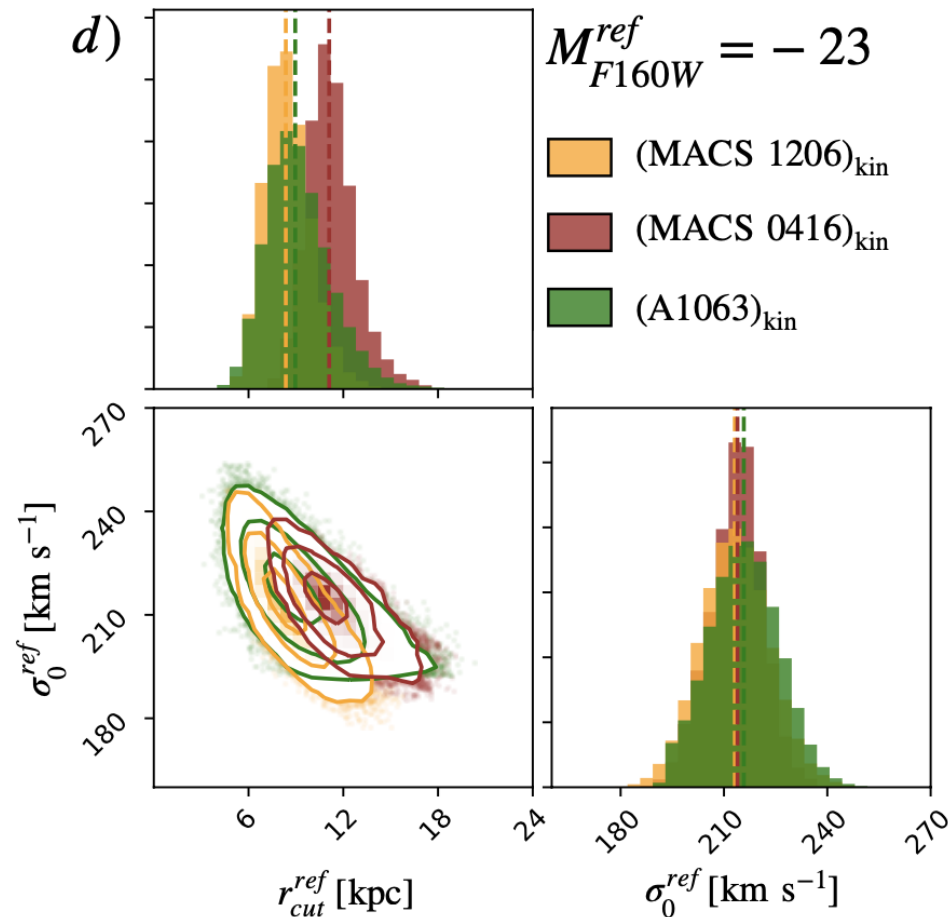
$$\chi^2 = \sum \left( \frac{S_i - \bar{S}}{\sigma} \right)^2$$

- Image plane fit:  $\sim 1$  week

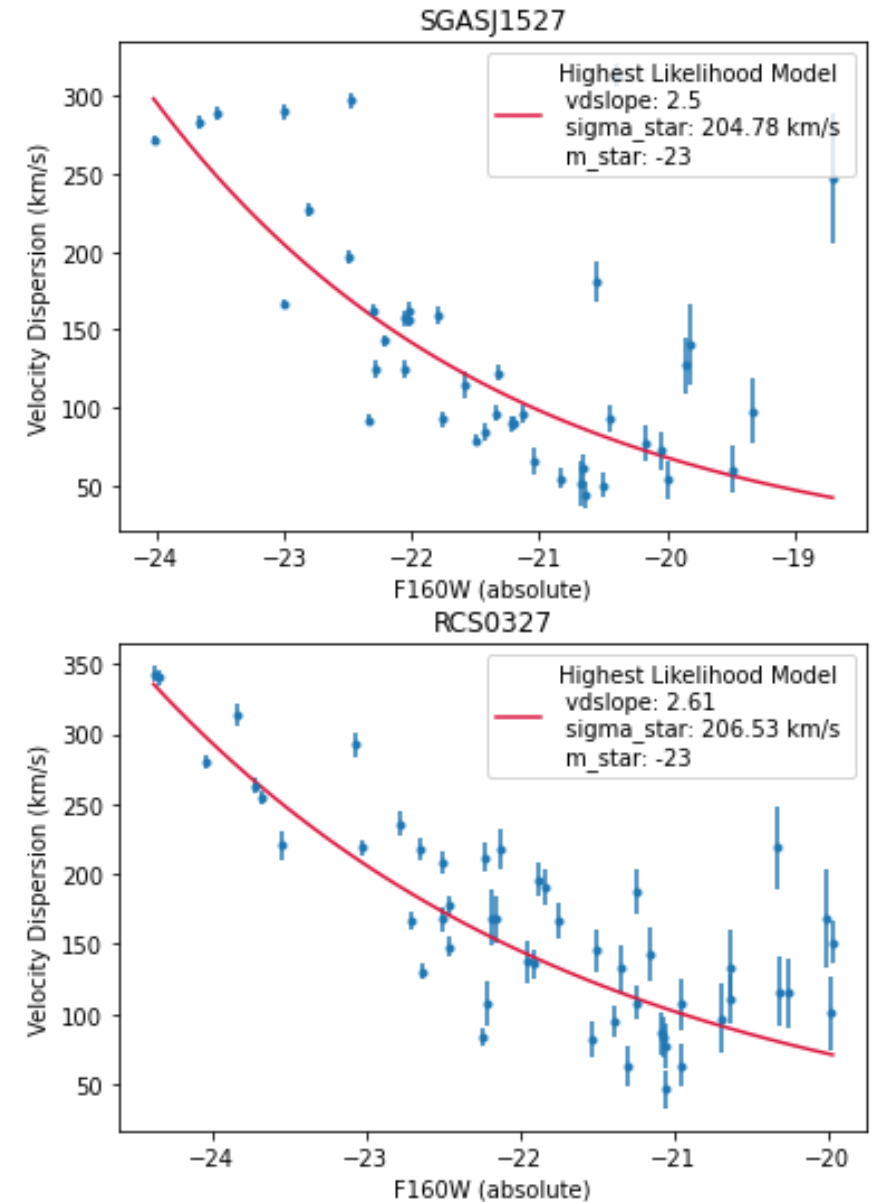
$$\chi^2 = \sum \left( \frac{\theta_i^{obs} - \theta_i^{pred}}{\sigma} \right)^2$$

# How to best use data?

=> Calibration of the mass / luminosity relation



=> Galaxies in clusters are self-similar also in terms of DM halo size?

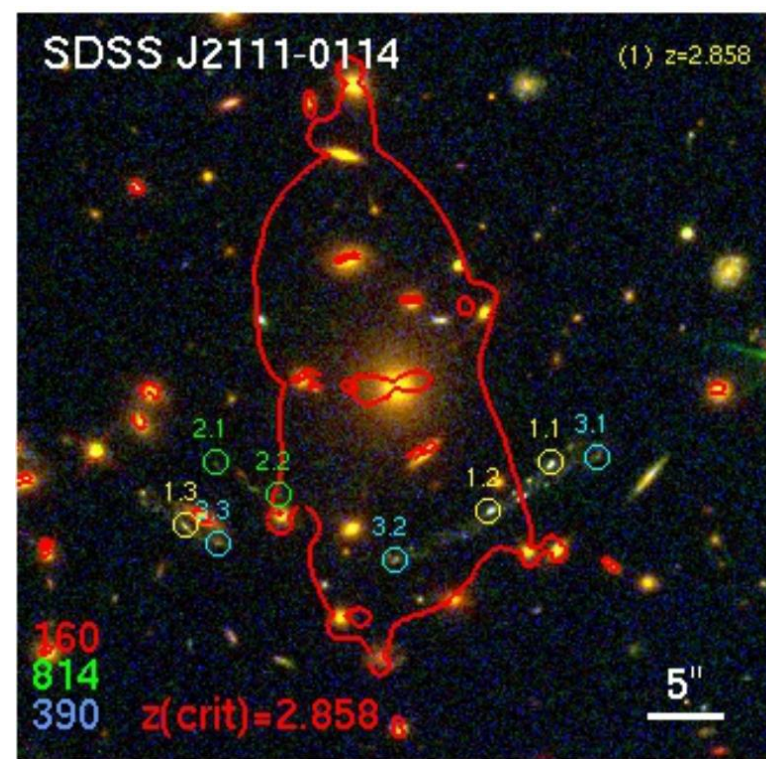
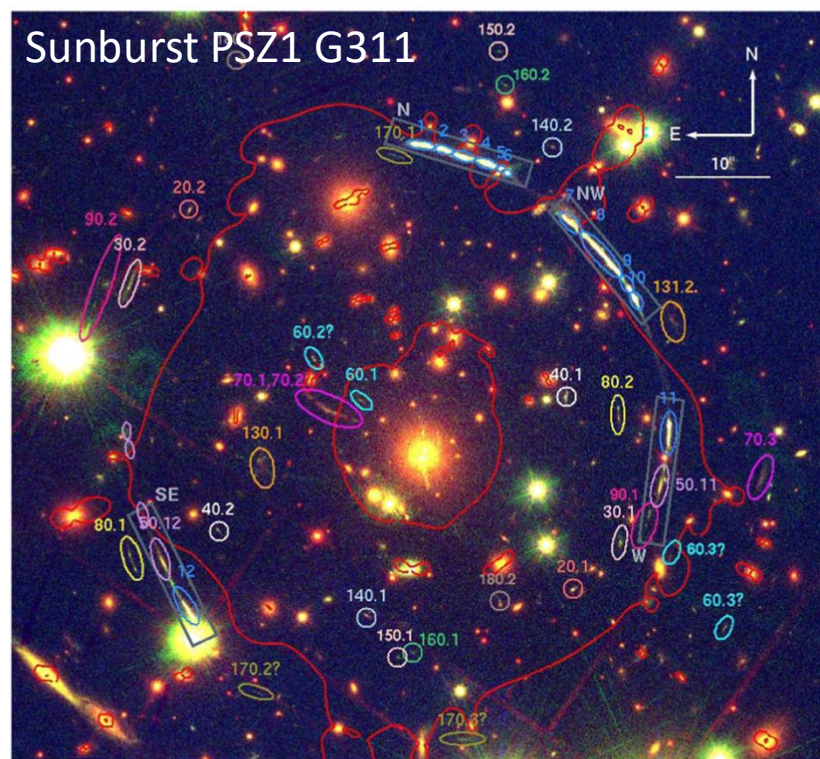
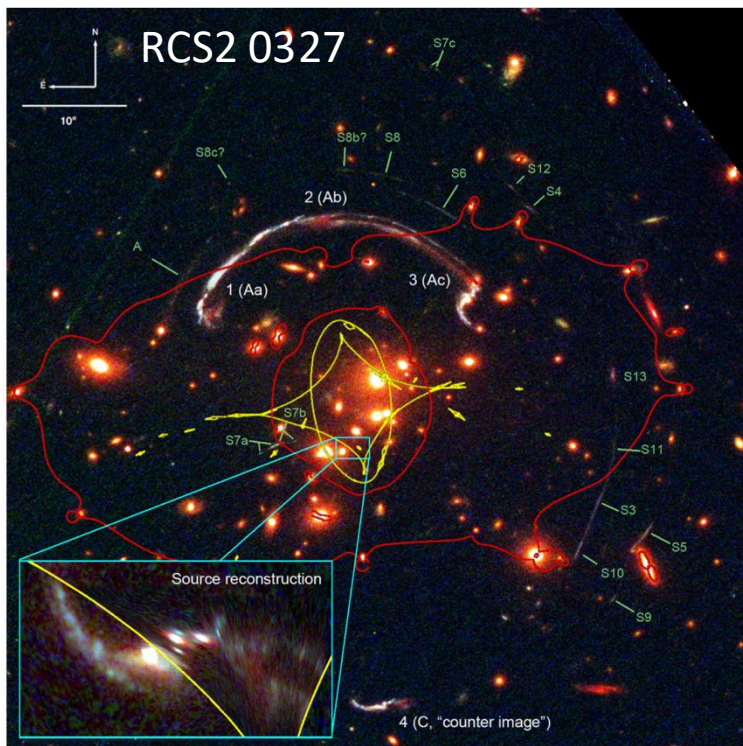


Credits: Joaquin Hernandez & Giuseppe D'Ago

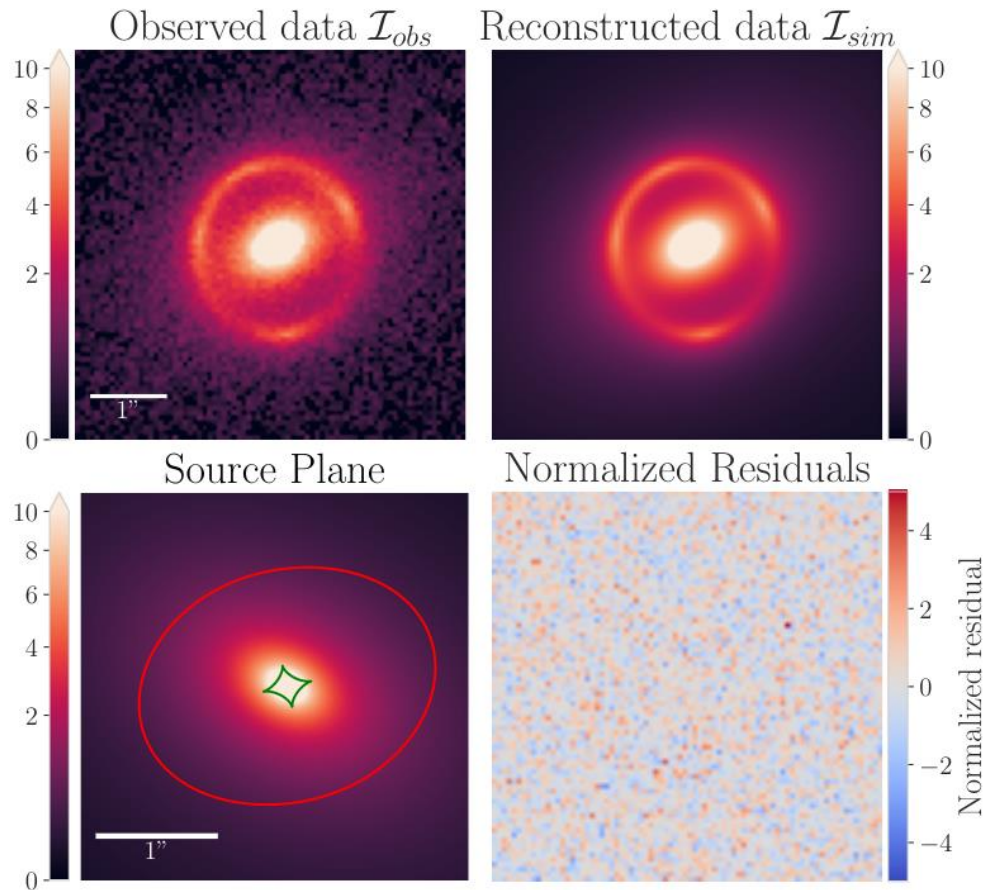


# The Arctomo cluster sample

Cluster	Redshift	$N_{\text{spec}}$	$N_{\text{vdisp}}$	$N_{\text{src}}$	$E_{\text{B}-\text{V}}$
SGAS J1226+2152	0.437	51	22	0.0185	
PSZ1 G311.05-18.48	0.443	59	32	0.0926	
RCS2 032727-132609	0.565	70	32	0.0672	
SGAS J211119.34-011423.5	0.638	38	29	0.0714	



# Strong lensing modeling alternative



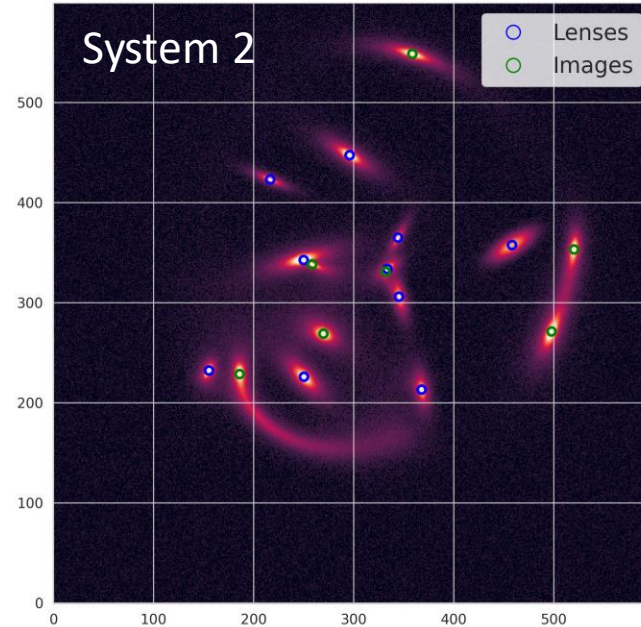
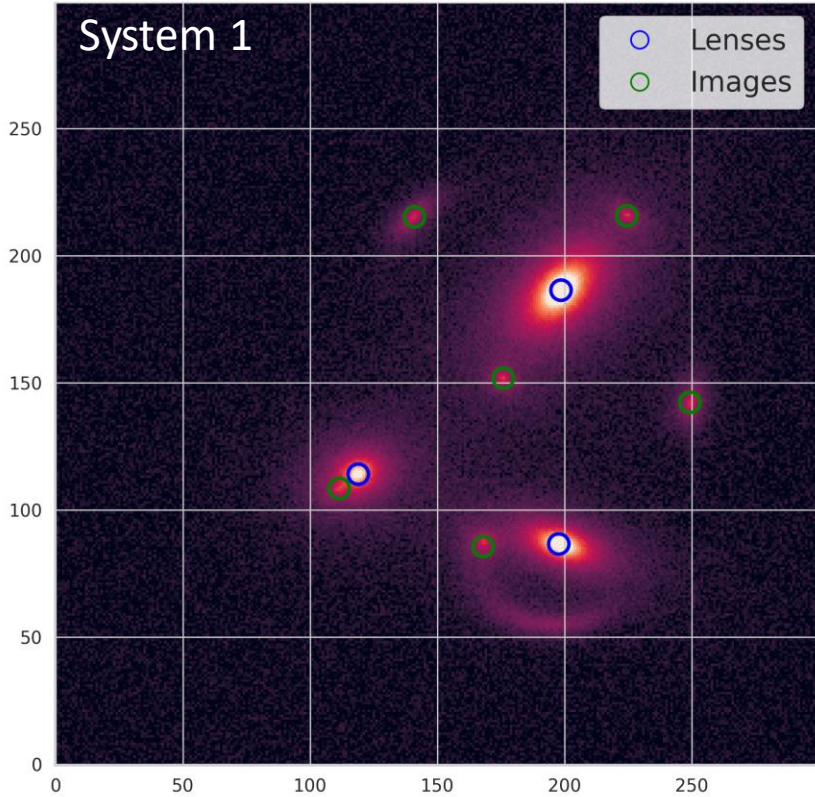
- GIGA-Lens uses GPU and machine learning tools for modeling strong gravitational lensing by Bayesian inference
- The likelihood is given by pixel-to-pixel residual
- It is intended mainly for galaxy-galaxy lensing
- Does not include the redshift

Gu, A., et al. *arXiv preprint arXiv:2202.07663* (2022).

Credits: Felipe Urcelay



# SL modeling with alternative techniques



Credits: Felipe Urcelay

=> Well designed for ground-based observation (ex: LSST)

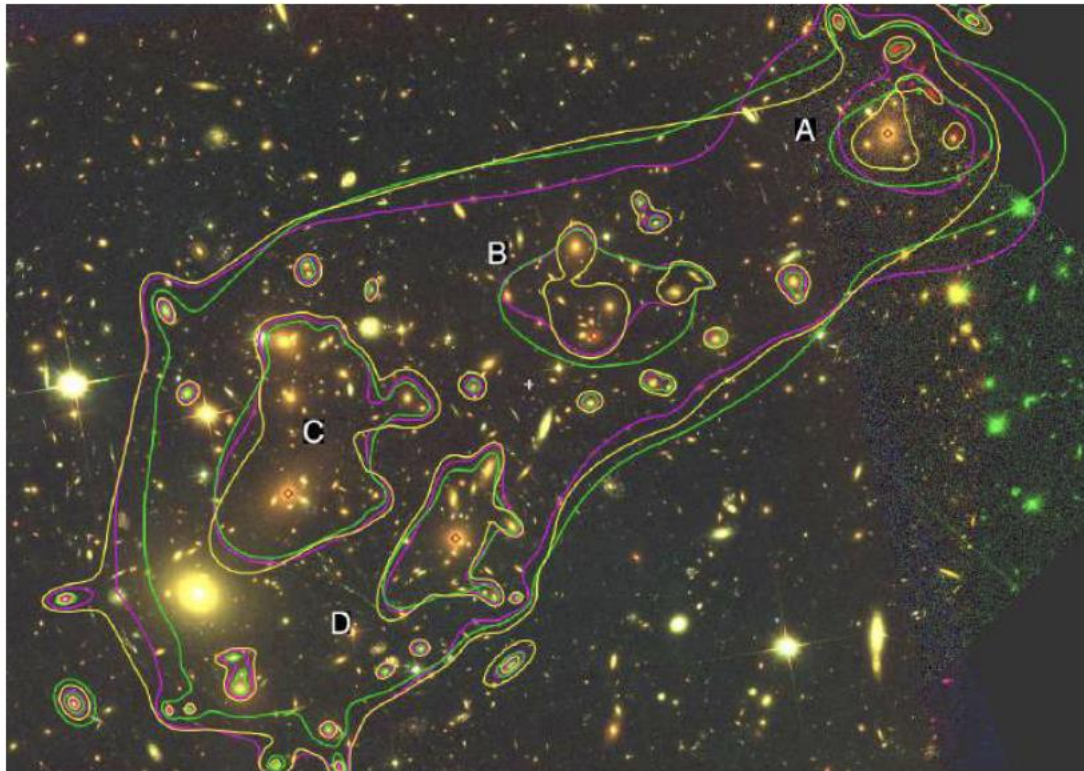
	System 1: 3 lenses		System 2: 10 lenses	
	Source plane positions	Pixels	Source plane positions	Pixels
<b>GIGA-Lens</b> P100 GPU	40s	140s	120s	9min 20s
<b>Lenstool</b> i7 CPU 8 threads	6s	230s	30s	1h



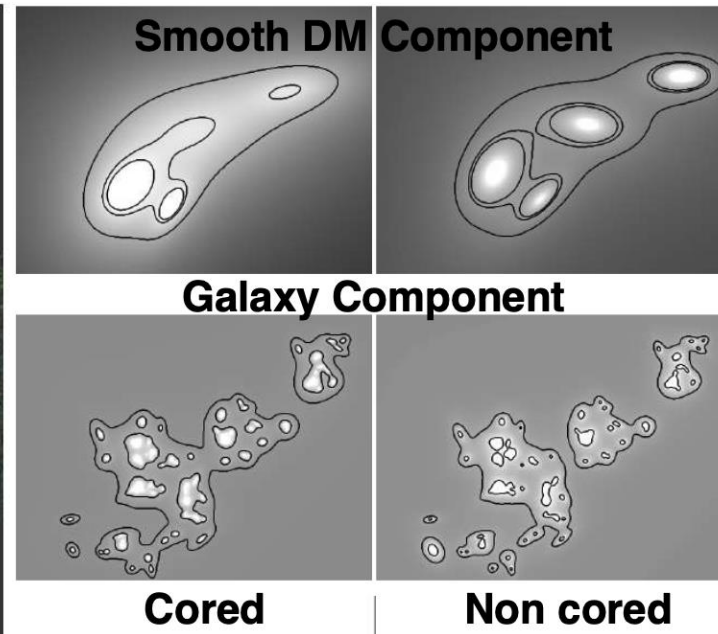
# Strong lensing recent progress

Better modelling thanks to

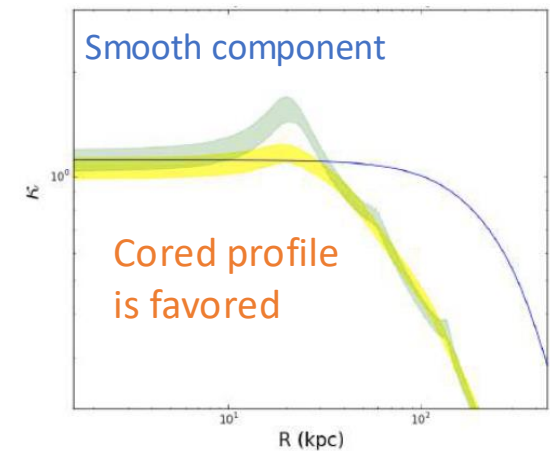
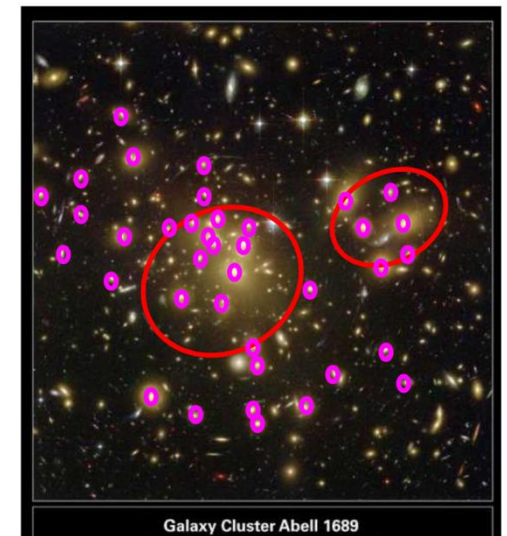
- More multiple images constraints with deep HST observations (HFF program, JWST)
- Integral field spectroscopy data to constrain galaxy kinematics (MUSE)



Limousin et al. 2017



=> Self-Interacting DM can produce a cored inner profile



Limousin et al. 2022

# Strong Lensing simulation challenge

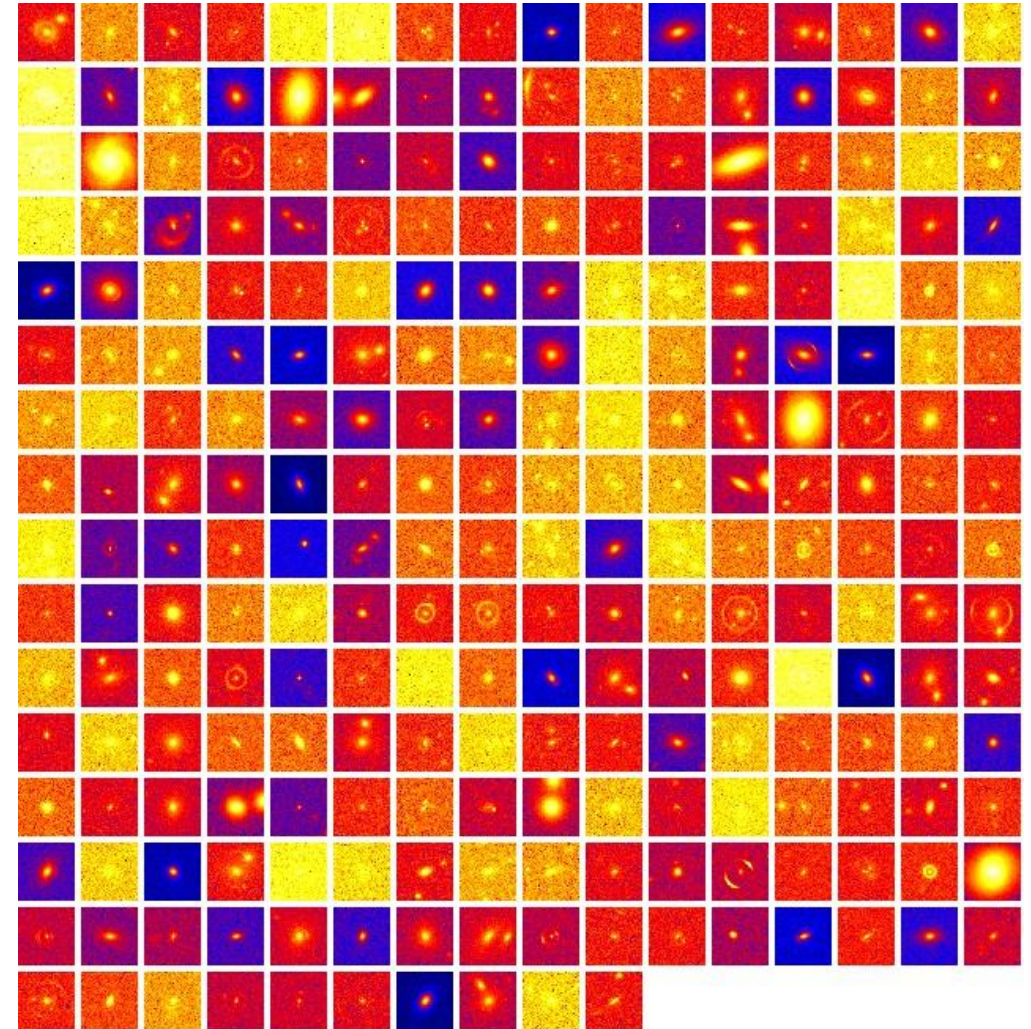
Simulation setup:

- 100,000 candidates to classify
- 4-bands ground-based (GB) images (KiDS-like)
- Single band space-based (SB) images (Euclid-like)

Challenge details:

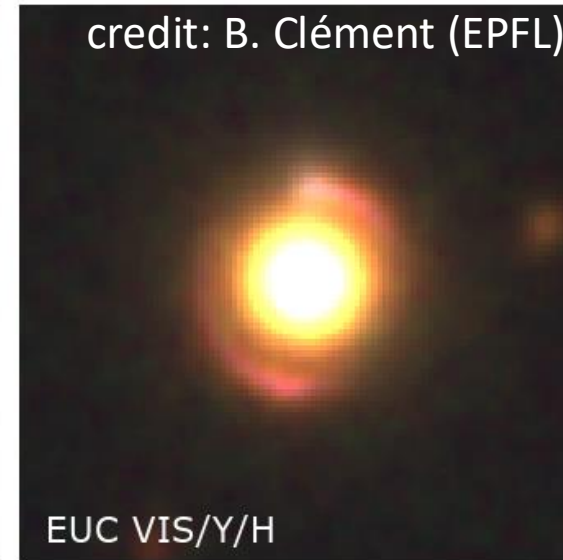
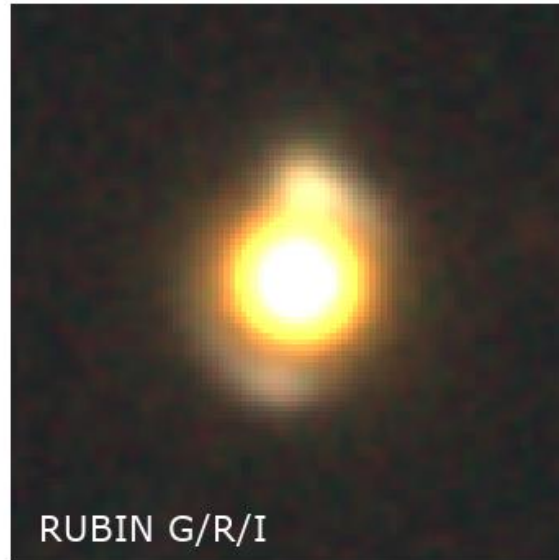
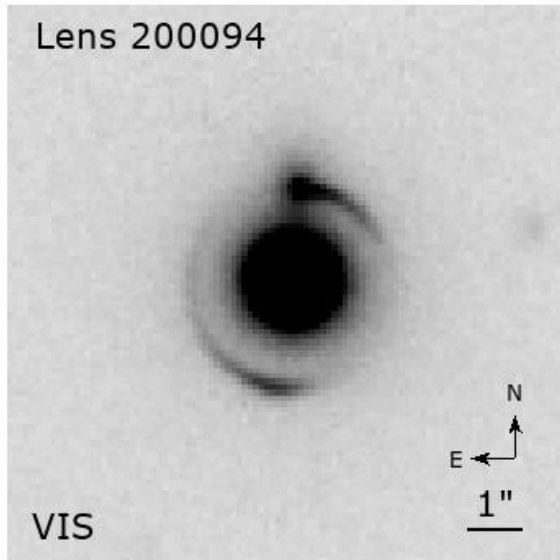
- 48h to upload classification of all candidates
- 24 participating teams
- Mostly ML approach (e.g. SVM, CNN) but also human inspection (

Metcalf et al. 2016





# Euclid SCIENTIFIC challenge 8 (SC8)



## Simulated area: $150\text{deg}^2 + 5\text{deg}^2$

- 200 SL systems + galaxies + high-z QSO + LBG + stars
- Set of 31-bands + 2 grism images
- Simulation: 4435 CPU x 2 days, 46TB
- Reduction storage: TBD

Future plans: Add QSO lensing

## Goal of SC8

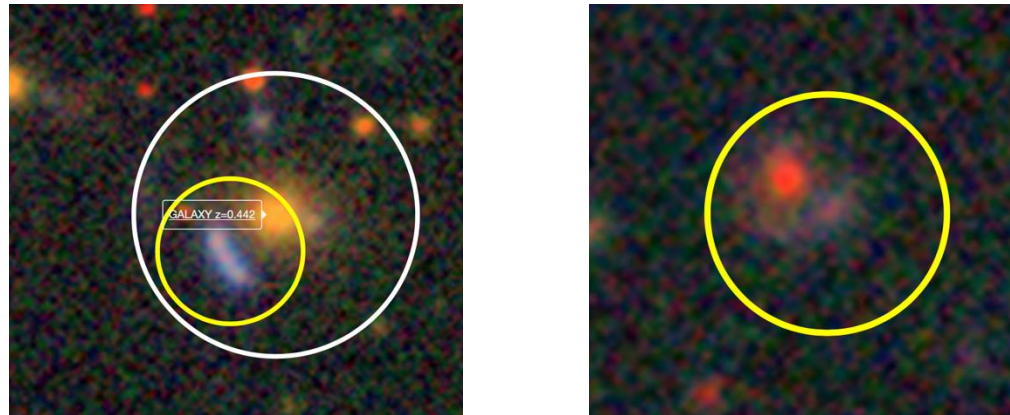
- Run the data reduction pipeline to the end
  - Pipeline validation, computing & storage assessment
- Get noise properties to prepare next SL challenge
  - Include all instrument noise calibrated on lab measurements
  - Include all pipeline data reduction noise



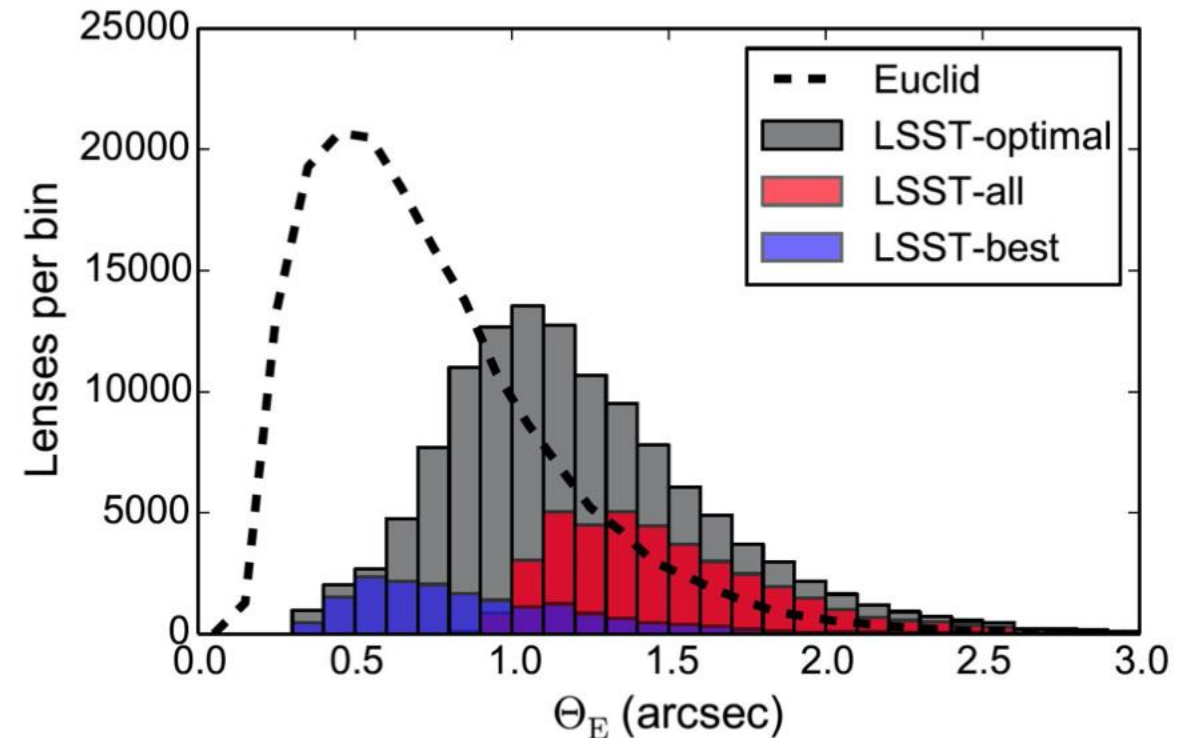
# Next STEP: spectroscopy

- DESI

- Already discovered  $\sim 1500$  SL systems in *grz* imaging survey (Huan XC et al. 2021)
- Declination  $> -20$ , mag  $\sim 23.5$
- Expected  $\sim 400$  new SL spectroscopic redshifts



4MOST Proposal (PI: Collett)



- 4MOST proposal for SL systems

- $R < 24$  & 10,000 spectroscopic redshifts
- 5000 velocity dispersion measurements
- Decision in Dec 2021

# Project objective (3 years)

Interdisciplinarity: Combining diverse scientific disciplines to foster creativity and achieve a common goal through different approaches

Common goal: to characterize the nature of dark matter

Approach 1: Gravitational lensing in cosmology

- Able to measure density profile and number of subhalos in galaxies

Approach 2: Direct and indirect detection in (astro-)particle physics

- Able to distinguish DM particles

Project Milestones

=> Show that the micro nature of DM (WIMP or axion) modifies macro observables (analogy with baryonic feedback)

# Quality and Ambition of the project

- 2 well-established CPPM & LAM teams: Recognized for their analysis expertise
  - Tools: Lenstool Jullo et al. 2007, Clumpy Nezri et al. 2012, RAMSES Nuñez et al. 2021
- CPPM & LAM involved in international projects
  - WIMP: **KM3NET**: Extend ANTARES telescope 12 lines -> 115 lines (2021-)
  - **DarkSide**: proven technology with innovative design → DS-20k (2025-)
  - Axion: **MadMax**: innovative concept → prototyping phase for validation (2021-25)
  - **Euclid, HST+JWST**: High Resolution Detection and Imaging of Gravitational Lenses
  - **VLT & ELT-HARMONI**: Gravitational lens spectroscopy (redshifts)
- Ambition:
  - Challenge simulations: impact of micro DM physics at the macro level. Analogy with baryon physics (Nuñez et al. 2021)
  - Lens profile measurement (Limousin et al. 2016, 2022) + detection of substructures in gravitational lenses (Natarajan et al. 2017)



# Implementation modality

- **WP1: Common language for modeling DM halos, tidal effects, tidal streams**

=> The halo of DM halos is the common object of the DM search & gravitational probe communities

=> Implementation of consistent models in Lenstool & Clumpy

=> Analysis of lens systems and measurement of density profiles and number of subhalos

- **WP2: Impact of baryons+DM on the morphology and evolution of (sub)halos**

=> Run of hydrodynamic cosmological simulations with the same properties of DM and baryon physics

**Challenge:** Find consistent recipes despite the different simulation scales (Mpc → sub-pc)

- **WP3: Using WP1 and WP2 results to estimate uncertainties in detections**

=> Prediction of direct & indirect detection rates from models (MD+baryons), simulation results, observational results